Structural Behaviour of Unreinforced and Reinforced Cement Stabilised Rammed Earth Columns under Axial Compression

A thesis submitted for the degree of

Doctor of Philosophy

By

Deb Dulal Tripura

Department of Civil Engineering
Indian Institute of Technology Guwahati
Guwahati – 781 039, India

Declaration

I do hereby declare that the work presented in this thesis entitled ***"Structural Behaviour of Unreinforced and Reinforced Cement Stabilised Rammed Earth Columns under Axial Compression"*** for the award of the Degree of **Doctor of Philosophy** and submitted in the Department of Civil Engineering, Indian Institute of Technology Guwahati, India, is an authentic record of my own work. The study was carried out under the supervision of ***Dr. Konjengbam Darunkumar Singh***, Associate Professor, Department of Civil Engineering, Indian Institute of Technology Guwahati, India, during the period from December 2011 to March 2015.

The results presented in the thesis is neither submitted nor under consideration for submission to any other University/Institute for the award of any degree or diploma.

(Mr. Deb Dulal Tripura)

Reg. No. 11610428

Date:

Place: IIT Guwahati

Certificate

This is to certify that the thesis entitled ***"Structural Behaviour of Unreinforced and Reinforced Cement Stabilised Rammed Earth Columns under Axial Compression"*** submitted by **Mr. Deb Dulal Tripura** to the Indian Institute of Technology Guwahati, India, for the award of the degree of ***Doctor of Philosophy,*** is a record of bonafide research work undertaken by him. The study was carried out under my supervision during the period from December 2011 to March 2015.

The thesis work, in my opinion is worthy of consideration for the award of the degree of ***Doctor of Philosophy*** in accordance with the regulation of the institute.

(Dr. Konjengbam Darunkumar Singh)
Associate Professor
Department of Civil Engineering
Indian Institute of Technology Guwahati, India

Date:

Place: IIT Guwahati

Dedicated to

My dearest parents, family and to the downtrodden people

Message

"When your heart is filled with discontentment, look into the eyes of the poorest of the poor, then everything seems to melts away"

Acknowledgement

"How big or small the mission may be, it is never accomplished unless a seen or unseen hand plays a role"

At the very outset, let me thank the Almighty, for giving me such a wonderful mentor, friend and philosopher in the form of ***Dr. Konjengbam Darunkumar Singh.*** His simplicity and positive attitude have truly inspired and motivated me in accomplishing the present mission. In times of weariness his words of inspirational and moral support ***"Don't worry, everything will be alright"***, enabled my perseverance for the pursuit of excellence. His words and deeds will ever be cherished in every endeavour of my life.

I am very much thankful to *Prof. B.V.Venkatarama Reddy*, Department of Civil Engineering, Indian Institute of Science Bangalore, for answering my queries in times of needs. His work on alternative building materials and technologies, have really motivated me to carry out the present study.

I also express my sincere thanks to *Prof. Subashisa Dutta* - the Head, faculties and staffs of Civil Engineering Department, IIT Guwahati for their kind support during the entire period of my study.

Indeed, I am very glad in having the company of *Sachidananda*, *Sonu* and *Gishan* as my fellow scholars, who really made the work impossible to possible even in my absence. I will ever relish their friendship.

I gratefully acknowledge the sincere uncomplaining help rendered by my beloved students, *Pratik, Bandana, Ranjit, and Souvik* of NIT Agartala during the entire process of experimental work. I also thank *Subhankar, Manik, Bilton* and *Amar,* and other staffs and workers of the Structural Engineering Laboratory of NIT Agartala for their valuable support while carrying out the experiments.

I am also obliged to *Pinku, Nikhil, Subendu, Stephen, Arup* and *Sujit,* and all other staffs of the Mechanical workshop, Smithy and Carpentry workshops of NIT Agartala for their untiring support in fabricating the equipments required.

I am indebted to my youngest uncle *Mr. Birendra Tripura,* who showed me the path of better education and my brother in-law *Mr. Shanti Kr. Debbarma,* who helped me in realizing my dream. I shall never forget their contribution.

I am grateful to my sisters *Suchitra, Nancy, Menaka, Binata*, and *Monika (niece)* for their patient support to my family in times of needs and particularly during my absence.

I also express my deepest gratitude to all my well-wishers.

Acknowledgement will be incomplete if I do not mention the names of my beloved wife *Chameli* and my lovely son *D. Kwthar* for their patient understanding and immense support during the entire journey of my study. I shall always be indebted to them.

I am extremely indebted to my mother who in spite of every difficulty since childhood until today acted as a guardian angel in excelling higher education.

Finally, the completion of the study is possible by the ample love and blessings received from my adored parents *Late Chandra Mani Tripura* and *Mrs. Chukaiti Tripura;* and my in-laws *Mr. Swadesh Debbarma* and *Mrs. Binita Debbarma.*

Thank God for everything.

Deb Dulal Tripura

Abstract

The present study aims to determine the suitability of locally available soil (Agartala, India) for the production of cement stabilised rammed earth (CSRE) columns with a proposed CSRE specimen making technique, followed by investigations on the effects of (1) slenderness ratios on the axial column strengths of both unreinforced rectangular and circular CSRE columns, (2) cross-sectional aspect ratios on unreinforced rectangular CSRE columns, and (3) lateral steel reinforcement ratios for CRSE columns longitudinally reinforced with steel and bamboo splints.

The properties of locally available soil and its suitability was determined in terms of density, strength, compaction energy and durability in both cured and uncured conditions using the proposed block-making equipment and technique. Test result shows that the average characteristic strength of cured samples is about two times higher than that of uncured samples. The compressive strength and density of CSRE blocks (with 10% cement content) is quite sensitive to the variations in compaction energy up to 16.94 kg-cm/cc. Increase in compaction energy from 7.26 to 16.94 kg-cm/cc tends to increase the compressive strength and density by about 23% and 11% respectively than that obtained at an energy level close to the standard Proctor effort. It is concluded that the local soil used for the production of CSRE blocks using the proposed block-making equipment and technique satisfy the design criteria outlined in various standards such as NZS 4297 (1998), IS 2110 (2002) and AS HB 195 (2002) in terms of compressive strength and density.

The influence of structural parameters such as slenderness ratio (λ), cross-sectional aspect ratio (width/thickness ratio, Φ), and cross-sectional shapes (circular, square and rectangular) on load-capacity (P_u), reduction factor (k), failure pattern etc., on concentrically loaded unreinforced CSRE columns are presented. Columns of cross-sectional sizes: 150 mm x 150 mm, 150 mm x 190 mm, and 150 mm x 230 mm for rectangular; 150 mm diameter for circular cross sections, with a height of 900 mm, 1200 mm and 1500 mm were considered for the experimental programme. Experimental results on ultimate compressive strength (σ_u) of columns were compared with the results obtained with Engesser's tangent modulus theory (Bleich, 1952); and the validity of using masonry design rules for the design of CSRE columns was

evaluated. Safety factors were determined based on stress reduction factors obtained from the study. Test result shows that the lateral and vertical deformation (at comparable load) increases with increasing values of λ. Typically, columns tested failed by formation of vertical cracks initially at the platen-column interface followed by shearing and splitting at the later stages of loading. The value of σ_u decreases with increase in λ. The values of k at λ = 8 and 10 were determined to be 0.92 and 0.84 for rectangular columns and 0.90 and 0.82 for circular columns respectively. At increasing values of Φ (keeping thickness constant at 150 mm) the values of P_u for rectangular columns increases. It was observed that when Φ is increased from 1.0 to 1.27 and 1.0 to 1.53, the values of P_u increased by about 20% and 40.5% respectively, for λ = 6, 8 and 10 of all the column sets, agreeing with the increase in cross-sectional area as Φ increases. The k values outlined in earthen standards such as NZS 4297 (1998) and AS HB 195 (2002), and masonry standard IS 1905 (2002) are in a close range to the experimental values by about ~4.0% at λ = 8 - 10. However, in the case of circular columns, the codal values are found to be higher by about ~7%, thus showing relatively un-conservative nature.

Structural behaviour of CSRE columns reinforced with steel (4 numbers of 8 mm diameter steel as longitudinal and two-legged 6 mm diameter as transverse reinforcements; Fe500 steel) under concentric axial loading, for a fixed column height of 1500 mm was assessed. Effects of key variables such as transverse reinforcement ratio, total reinforcement (i.e. combined longitudinal and transverse) ratio etc., were studied. Test result shows that the behaviour of CSRE columns reinforced with closer tie spacing (e.g. 50 mm) is characterized by gradual spalling of cover at the failure zone leading to a loss of axial capacity before the transverse confinement becomes effective. The values of P_{us} (ultimate load for steel reinforced column) for SR200, SR100 and SR50 (where SR = steel reinforced, and 50, 100, 200 represents tie spacing in mm) columns are about 4.6%, 16% and 33% higher than that of unreinforced CSRE (UCSRE) column, respectively. A linear increase in P_{us} is observed as the total reinforcement ratio was increased from 0% to 3.41%. A gradual increase in P_{us} has been seen when the total reinforcement ratio is increased from 0% (i.e. unreinforced) to 1.52%, 2.15% and 3.41% by about 4.5%, 16% and 36% respectively. As the transverse reinforcement is increased from 0.63% to 1.26% and

0.63% to 2.51%, P_{us} is found to increase by about 11% and 30% respectively. Axial deformation at peak load (δ_{uv}) increased by about 6.3% and 19.1%; whilst lateral deformation at 60 kN (δ_{l60}) (i.e., pre-peak/ultimate load) by about 13.6 % and 100%, when the tie spacing decreased from 200 mm to 100 mm and 100 mm to 50 mm respectively, suggesting an improved ductility with core confinement.

Structural behaviour of CSRE columns reinforced with bamboo-steel under concentric axial loading, for a fixed column height of 1500 mm was also assessed. In this study, the vertical reinforcement steels have been replaced by approximately rectangular bamboo splints (with an equivalent cross-sectional area as that of 8 mm diameter bar). It was found that P_{ubs} (ultimate load for bamboo-steel reinforced column) of bamboo-reinforced CSRE columns are about 3.7% to 15% higher than that of unreinforced CSRE column when total (bamboo and steel) reinforcement ratio is increased from 1.52% to 3.41%. An increase in P_{ubs} of about 6% to 12% has been seen when the transverse reinforcement ratio increased from 0.63% to 1.26% and 0.63% to 2.51% respectively. It was observed that P_{ubs} of SR50 column is about 17% higher than that of BSR50 (BSR = bamboo-steel reinforced), however only minor differences are seen for larger tie spacing, i.e. 200 mm. Similar failure patterns as those of steel reinforced CSRE columns are observed for bamboo-steel reinforced CSRE columns, except for post-ultimate snapping or breaking of buckled bamboo longitudinal reinforcement. A nearly linear increase in δ_{uv} and δ_{l60} have been observed i.e. around ~10% and 14% respectively when the tie spacing decreased from 200 mm to 50 mm, thus showing an improvement in ductility.

Contents

List of Tables

List of Figures

Notations

γ_d	Dry density
γ_f	Factor of safety for dead loads
γ_m	Material strength variations and workmanship factors
δ_l	Lateral deformation
δ_{l60}	Lateral deformation at 60 kN load
δ_t	Tensile deformation
δ_{uv}	Ultimate vertical deformation
δ_v	Vertical deformation
ε	Average compressive strain
ρ_l	Longitudinal reinforcement ratio (= A_{sl}/A_g)
ρ_w	Lateral reinforcement ratio (= A_v/as)
ρ_t	Total reinforcement (= $\rho_l+\rho_w$)
σ	Average compressive strength
σ_{cr}	Critical stress or buckling strength
σ_u	Ultimate compressive strength
Φ	Aspect ratio (= a/d)
Ψ_m	Reduction factor for strength of mortar
Ψ_u	Unit reduction factor for sample structural strength
a	Width of column cross-section
d	Depth/thickness of column
f_k	Characteristic compressive strength of columns
F_m	Mean of the maximum loads carried by test samples

h	Height of column
k	Reduction factor (= P_u / P_{u6})
l	Effective height of the column
l/r	Slenderness ratio
m	Moisture content of specimen
n	Number of compacted layer
r	Radius of gyration (= √(I/A))
s	Tie spacing
A	Cross-sectional area of specimen
A_g	Gross area of section
A_{sl}	Total longitudinal reinforcement
A_v	Transverse reinforcement area within tie spacing
BSR	Bamboo-Steel Reinforced
CSRE	Cement Stabilised Rammed Earth
E_c	Compaction energy
E_t	Tangent modulus at failure
H	Height of fall of rammer
I	Moment of inertia
ITM	Initial Tangent Modulus
L	Length of specimen
MDD	Maximum Dry Density
N	Number of blows per layer
OMC	Optimum Moisture Content
OPC	Ordinary Portland Cement
P	Axial load

P_{cr}	Buckling load
P_u	Ultimate load/ load-capacity of column
P_{u6}	Average ultimate load of column at λ equals to 6
P_{ubs}	Ultimate load of bamboo-steel reinforced CSRE column
P_{ur}	Ultimate load ratio (= $P_u \times k$)
P_{us}	Ultimate load of steel reinforced CSRE column
P_{us200}	Ultimate load of steel reinforced CSRE column at 200 mm tie spacing
P_{ubs200}	Ultimate load of steel reinforced CSRE column at 200 mm tie spacing
SR	Steel Reinforced
UCSRE	Unreinforced Cement Stabilised Rammed Earth
V	Volume of mould
W	Weight of Proctor rammer
W'	Weight of specimen
X_a	Average of a test series
X_1	Lowest result of a test series
X_s	Standard deviation of a test series

Chapter 1

Introduction

1.1 General

The present energy crisis resulting from rapid industrialization has given rise to a major concern about managing the energy resources still available and environmental degradation (Ghavami, 2005). As a result, there is an intense on-going search for alternative building materials, which will minimize the energy crisis as well as environmental degradation. In the recent past, rammed earth construction techniques have gained a renewed interest across the world, due to its varied sustainable benefits such as availability of local material (soil on site or near the site), low embodied energy, simple construction procedure, non-polluting etc., (e.g. Easton, 1982; Houben and Guillaud, 1994; Walker, 1995; Jayasinghe and Kamaladasa, 2007; Ciancio and Beckett, 2013; Reddy, 2014; Bui et al., 2014). Several studies have been made on suitability of soil, structural behaviour of unreinforced and reinforced rammed earth walls and columns (e.g. Easton, 1982; Walker, 1995; Hall, 2004; Jayasinghe and Kamaladasa, 2007; Maniatidis and Walker, 2008; Burroughs, 2008; Reddy and Kumar, 2010; Reddy and Kumar, 2011; Ciancio and Beckett, 2013; Bui et al., 2011; Lindsay, 2012; Ciancio and Augarde, 2013; Gupta, 2014) and many countries have developed standards, practice guidelines, handbooks etc., for earth construction that include various aspects such as soil selection, construction equipments and techniques, testing procedures, structural design guidelines etc., (e.g. NZS 4297, 1998; AS HB 195, 2002; 1S 2110, 2002; ASTM E2392/E2392M, 2010).

From the literature review, it has been observed that various types of soil such as laterite soil, sandy soil etc., have been found suitable for rammed earth constructions, and use of 4-12% cement for cement stabilised rammed earth (CSRE) constructions have been reported (e.g. Walker, 1995; Ngowi, 1997; Guettala et al., 2006; Jayasinghe and Kamaladasa, 2007; Reddy and Kumar, 2011). In CSRE constructions, the main ingredients are soil, sand, gravel, and cement. This technique involves dry mixing of soil, sand, gravel, and cement followed by addition of water. The wetted soil mixture

is then poured/placed into the formwork and compacted into progressive layers until the desired is achieved followed by dismantling of formwork and wet curing for specified period. Furthermore, structural behaviour (e.g. load and deformation capacities, load eccentricity effect) of unstabilised columns and unreinforced CSRE walls have been studied (Maniatidis and Walker, 2008; Reddy and Kumar, 2011). Gupta (2014) reported on the effect of using diagonal and horizontal stirrups on the load-capacity of steel reinforced CSRE columns.

However, to the best of author's knowledge a systematic study on the influence of structural parameters such as slenderness ratio (λ), cross-sectional aspect ratio (width/thickness ratio, Φ), and cross-sectional shapes (circular, rectangular etc.) on load-capacity (P_u), reduction factor (k), failure pattern, lateral reinforcement ratio etc., on axially loaded CSRE columns have not been presented. In addition, although, studies have shown that bamboo can be a potential substitute to steel in structural concrete elements such as beams and columns (e.g. Ghavami, 2005; Agarwal et al., 2014) and can improve ductility of rammed earth wall under horizontal load (Gao et al., 2009), no reports have been found in the literature on the use of bamboo as reinforcement for CSRE columns. Hence, in this research effort, suitability of locally available soil (Agartala, India) for the production of CSRE columns has been checked with a proposed CSRE specimen making technique, followed by investigations on the effects of (1) slenderness ratios on the axial column strengths of both unreinforced rectangular and circular CSRE columns, (2) cross-sectional aspect ratios on unreinforced rectangular CSRE columns, and (3) lateral steel reinforcement ratios for CRSE columns longitudinally reinforced with steel and bamboo bars. The objectives of the present study are enumerated in the following section.

1.2 Objectives of the investigation

Based on the literature review the following objectives have been identified for the present study:

1. To study the characteristic properties of unstabilised and CSRE blocks in terms of density, strength, compaction energy and durability in both cured and uncured conditions using locally available soil (Agartala, India).

2. To select and validate the block making equipment and technique that can be used for construction of rammed earth structures.
3. To evaluate the structural behaviour of axially loaded CSRE columns of square, rectangular and circular sections considering the effects of key parameters such as slenderness ratio, cross-sectional aspect ratio etc., on load-deformation, failure patterns etc.
4. To evaluate the structural behaviour of axially loaded steel and bamboo-steel reinforced CSRE columns of square sections considering the effects of structural parameters such as transverse reinforcement ratio, total reinforcement ratio etc., on the failure pattern; load-lateral deformation and load-axial deformation of columns.

1.3 Thesis organization

The thesis is presented into seven chapters.

1. Introduction
2. Literature review
3. Materials characterization
4. Structural behaviour of CSRE columns
5. Structural behaviour of steel reinforced CSRE columns
6. Structural behaviour of bamboo-steel reinforced CSRE columns
7. Conclusions and future scope of work

Chapter 1 introduces the research area and a brief account of every chapters of the present study.

Chapter 2 describes briefly the detailed literature review made on earth/rammed earth constructions. The literature review mainly focuses on the historical background of rammed earth constructions, suitability of soil, sustainability, structural behaviour of rammed earth walls/columns and codes of practice on rammed earth constructions.

Chapter 3 deals with determination of properties of locally available soil and its suitability as a construction material. The properties of unstabilised and CSRE blocks were studied in terms of density, strength, compaction energy and durability in both

cured and uncured conditions. All the test samples were produced using steel rammer and wooden mould, with an attempt to select and validate the block-making equipment and technique that can be used for rammed earth constructions. The test results such as compressive strength, density etc., were compared with the values outlined in many standards and guidelines.

Chapter 4 deals with a study on the load-capacity of CSRE columns under concentric axial compression. Tests on CSRE cylinders, prisms and columns of circular, square and rectangular cross-sections were performed. Effects of slenderness ratio and aspect ratio on the column strength, deformation and capacity reduction factors were assessed. A comparative study was made between the ultimate compressive strength (σ_u) of columns determined using Engesser's tangent modulus theory and experimental results. Furthermore, validity of using masonry design rules for the design of CSRE columns was evaluated and safety factors of columns were determined to assess the possibility of constructing a single storey load bearing houses. Experimental results such as reduction factors, slenderness effects etc., were compared with the values proposed in literature, standards and guidelines; and a failure mechanism of column has been proposed.

Chapter 5 investigates the behaviour of steel reinforced CSRE columns of square cross-section under concentric axial compression. Both longitudinal and lateral reinforcement were provided with steel. Effects of structural parameters such as total reinforcement ratio, lateral reinforcement ratio, etc., on the failure pattern; load-lateral deformation and load-axial deformation of columns were studied. Compaction technique and failure pattern of columns are discussed.

Chapter 6 presents an experimental study on the behaviour of CSRE column reinforced with bamboo (longitudinal) and steel (lateral) under concentric axial compression. Effects of structural parameters such as total reinforcement ratio, lateral reinforcement ratio etc., on the failure pattern; load-lateral deformation and load-axial deformation of columns were studied. Comparative study was made between the test results of steel and bamboo-steel reinforced CSRE columns.

Finally, in **Chapter 7** summary of major conclusions from the thesis and future scope of work have been presented.

Three appendices are added at the end of the thesis. **Appendix A** shows (a) compaction energy calculation equivalent to standard Proctor effort, (b) compaction energy calculation for wooden cube mould and (c) estimation of compaction energy in terms of number of blows and mass of soil required for column of size 150 mm x 150 mm x 900 mm. **Appendix B** shows (a) determination of tangent modulus for columns from the stress-strain curve of prism, (b) determination of stress/capacity reduction factor and (c) determination of factor of safety. **Appendix C** shows (a) estimation for longitudinal reinforcement and (b) estimation for lateral reinforcement.

Chapter 2

Literature Review

This chapter presents a review of literature relating to rammed earth constructions. The literature review has been presented broadly into five sections: (i) historical background on rammed earth constructions; (ii) suitability of soil; (iii) sustainability; (iv) structural behaviour of rammed earth walls/columns, and (v) codes of practice on rammed earth constructions.

2.1 Introduction

Rammed earth is an ancient construction technique, which has recently gained renewed interest due to varied sustainable benefits. In this technique, moisten soil (stabilised or unstabilised) is filled in a temporary formwork (wooden or steel) and compacted/rammed into successive layers of ~10 to 12 cm thick by means of rammer. After compaction of every couple of layers (equivalent to height of formwork), the formwork is raised (if necessary) at higher level and the process is continued until the desired construction is completed. Soil, sand, gravel and stabiliser (cement, lime, asphalt etc.) are the major constituents for unstabilised and stabilised rammed earth constructions. Some of the major advantages of rammed earth constructions are: (i) low cost of materials and locally available; (ii) low energy and transportation costs; (iii) low fire risk and non-combustible; (iv) durable; (v) flawless surface and flexibility in wall thickness and plan; and (vi) non requirement of high skilled workers etc. Its disadvantages include: (i) loss of strength on saturation; (ii) erosion due to rain impact; (iii) longer construction period and weather-dependent; and (iv) construction recommendation in hard soil and non-flooding areas etc. Notwithstanding these disadvantages, rammed earth construction has gained considerable research interests especially, because of its relatively sustainable and cost effective aspects (e.g. Jayasinghe and Kamaladasa, 2007; Reddy and Kumar, 2010; Bui et al., 2014; Reddy et al., 2014; Gupta, 2014). In this chapter, details of literature review on rammed earth constructions are presented with a special focus on unreinforced and reinforced rammed earth structural elements.

2.2 Historical background on rammed earth constructions

Until today, there is no consensus about the date when man first used earth as a building material. However, many researchers date back the early construction of earth buildings to 8000 – 4000 B.C. (Pollock, 1999; Minke, 2000; Berge, 2009). Evidences of earth constructions can be traced in all the main cradles of civilizations: Indus valley civilization, Chinese civilization, Mesopotamian civilization, Tigris-Euphrates civilization etc., (Kumar, 2009). Moulded, rammed earth, cob walls, adobe, poured earth represents some of the common earth construction techniques used in the past (Houben and Guillaud, 1994). The early used of rammed earth technique dates back to 500 – 200 B.C. with the construction of the Great Wall of China (Fig. 2.1) being the first of its kind (Easton, 1982; Jiyao and Weitung, 1990; Houben and Guillaud, 1994). Since then, the technique spread in various parts of the world (Fig. 2.2) (Jaquin et al., 2008).

Besides, the Great Wall of China, the rammed earth walls surrounding Horyuji Temple in Japan built in 707 A.D., (Jaquin, 2008) is another fascinating example of ancient rammed earth structure in Asia sub-continent (Fig. 2.3). During 1300 - 1600 A.D., constructions of rammed earth structures were undertaken in Ladakh, Bhutan and Tibet using simple wooden moulds (Chayet et al., 1990, Jaquin, 2008, see Fig. 2.4). Further spread of rammed earth technique during 18th century to mid of 19th century in Asia sub-continent can be seen from the examples of rammed earth buildings in the city of Shibam in Yemen and Gujarat in India, etc. (Figs. 2.5 and 2.6) (Helfritz, 1937; Kumar, 2009).

In Europe, General Hannibal first introduced rammed earth technique with the construction of rammed earth watchtowers during 300 B.C. (Easton, 1982). The Alhambra fortress of Granada in Spain built in 889 A.D., is one of the most exciting examples of rammed earth construction in Europe (Fig.2.7) (Jaquin, 2008). During 1600 – 1900 A.D., a good number of rammed earth constructions were built in Switzerland (Kleespies, 2000), Weilburg in Germany (Schick, 1987) and southern England (Figs. 2.8 and 2.9) (Walker et al., 2005). The Church of Holy Cross in Stateburg, South Carolina built in 1857 A.D., with plain rammed earth is one of the most striking examples of historic rammed earth constructions in USA (Fig. 2.10)

(Easton, 1982). Furthermore, the rammed earth technique also spread to South America and Australia (see Fig. 2.11) through the migration of European people in 16th and 19th century A.D., respectively (Jaquin, 2008).

In the recent past rammed earth construction technique has gained renewed interest due to its varied sustainable benefits such as low cost, low embodied energy etc. Figs. 2.12 to 2.14 show some of the modern rammed earth buildings in India and steel reinforced CSRE columns.

2.3 Suitability of soil for rammed earth constructions

According to Houben and Guillaud (1994), there is no direct answer to the question, "Is this soil suitable for construction?" The earth used for making rammed earth generally refers to sandy loam subsoil. The topsoil is unsuitable for construction due to considerable presence of organic matter that biodegrades, absorbs water, and is highly compressible, and it must be limited to 1 or 2% of the total mass of soil if allowed at all (King, 1996). These inherent deficiencies may be overcome by stabilising soil with chemical binders, such as cement or lime, followed by mechanical compaction (Walker, 1995). Many Researchers have investigated the physical properties of soil particularly with reference to gradation, Atterberg limit, density, strength and some aspects of durability that define the suitability of soil for rammed earth constructions (e.g. Patty, 1936; Patty and Minium, 1945; Verma and Mehra, 1950; Easton, 1982; Houben and Guillaud, 1994; Heathcote, 1995; Walker, 1995; Lilley and Robinson, 1995; Keable, 1996; King, 1996; Rauch and Kapfinger, 2001; Hall and Djerbib, 2004; Bahar et al., 2004; Walker et al., 2005; Jayasinghe and Kamaladasa, 2007; Maniatidis and Walker, 2008; Burroughs, 2008; Bui et al., 2009; Bui et al., 2011; Reddy and Kumar, 2011; Milani and Labaki, 2012; Tripura and Sharma, 2013; Miccoli et al., 2014; Bui et al., 2014). Some of the important conclusions on properties of soil and recommendations made by various researchers and standards are highlighted in Tables 2.1 and 2.2 respectively. It can be observed from Tables 2.1 and 2.2 that there exist a wide range of values for clay, silt, sand and gravel fractions of the soil used for rammed earth constructions. Clay, silt, sand and gravel content ranges from 5 – 40%, 0 – 30%, 20 – 75% and 10 – 62% respectively. Wide range of values exists for Atterberg limits – the liquid limit (LL) and plasticity

index (PI) ranges from 15.4 – 49% and 2 – 30% respectively. The density achieved for rammed earth is in the range of 1700 – 2200 kg/m^3. However, it may be noted that in most of the studies information on the type of density being measured e.g. dry density, air-dry density or bulk density with some moisture in it, are not readily available, although density is one of the important factors for achieving higher strength in rammed earth constructions. Wide variations in the compressive strength values achieved for rammed earth, such as wet and dry compressive strength of stabilised rammed earth is in the range of 0.7 – 2 MPa and 1.4 – 27 MPa respectively, on the other hand compressive strength of unstabilised rammed earth range from 0.62 – 6.8 MPa. Cement content ranging from 4 – 12% have been used for stabilisation. The compressive strength values specified in earth standards for unstabilised and stabilised soil range from 1.3 – 3 MPa and 1.4 – 5 MPa respectively, whereas these values in other literatures (e.g. Verma and Mehra, 1950; Easton, 1982; King, 1996; Walker et al., 2005; Bui et al., 2007; Burroughs, 2008; Reddy and Kumar, 2011) vary from 1 – 6.8 MPa and 1.82 – 27 MPa respectively. This shows that the codal values are more conservative. New Zealand standard NZS 4298 (1998) recommends that to achieve the correct level of compaction the handle of a 6.5 kg hand rammer should 'ring' when dropped from a height of 300 mm on the wall material when the moisture content is not more than 4% dry of optimum or 6% wet of optimum. This technique seems to be quite ambiguous as it is not always possible to judge the level of compaction, and as such not very helpful for a scientific control of quality and strength. Similarly, many of the studies did not explain clearly on the compaction technique and formwork used for rammed earth constructions.

2.4 Sustainability of rammed earth constructions

According to Ghavami et al., (1999), next to the food shortage, the housing shortage is one of the most crucial problems on earth and to improve this situation and make it possible to build more houses, particularly for low-income families, locally available materials such as soil, bamboo, etc., can be used. Nowadays rammed earth construction is attracting renewed interest due to its green characteristics in the context of sustainable development (Bui et al., 2014). The use of rammed earth construction material in remote regions or under-developed countries is suggested as a

viable alternative to other more common building materials like concrete and steel (Ciancio and Beckett, 2013). Rammed earth house possesses attractive appearance and present advantageous living comfort due to substantial thermal inertia and the "natural regulator of moisture" of rammed earth walls (Bui et al., 2014). Several researchers have studied thermal characteristics of rammed earth (e.g. Taylor and Luther, 2004; Maniatidis et al., 2007; Taylor et al., 2008 etc.). Based on a case study, Taylor and Luther (2004) observed that the overall thermal property of rammed earth building is improved above that expected by consideration of thermal resistance values alone.

Due to availability of local material (soil on site or near the site), rammed earth constructions have low embodied energy (Reddy and Jagadish, 2003; Reddy, 2004; Jayasinghe and Kamaladasa, 2007; Bui et al., 2014). Reddy and Kumar (2010) carried out a study on embodied energy in CSRE walls. A comparison has been made between energy content of cement and energy in transportation of materials, with that of the actual energy input during rammed earth compaction in the actual field conditions and the laboratory. Based on the study it was concluded that the embodied energy in CSRE walls is only about 15–25% of the embodied energy in burnt clay brick masonry. Very recently, Reddy et al., (2014), made a case study on low embodied energy cement stabilised rammed earth building, in Bangalore, India. The study dealt with the construction aspects, structural design and embodied energy analysis of a three-storey load bearing school building complex (Fig. 2.12). An analysis of the embodied energy revealed that the embodied energy of CSRE building is ~1.15 GJ/m^2, which is considerably less than that of the embodied energy of conventional burnt clay brick building (3–4 GJ/m^2) and reinforced concrete framed structure building (4–10 GJ/m^2). The case study also demonstrated the scope for reducing the carbon emissions in the construction sector by using low embodied energy materials such as CSRE walls and alternative floor/roof systems.

2.5 Structural behaviour of rammed earth walls/columns

2.5.1 Unreinforced rammed earth

Unstabilised rammed earth has been used for building for quite a long time (e.g. Patty, 1936; Patty and Minium, 1945; Schick, 1987; Houben and Guillaud, 1994; Lilley and

Robinson, 1995; Hall, 2002; Maniatidis and Walker, 2003; Hall and Djerbib, 2004; Maniatidis and Walker, 2008; Miccoli et al., 2014a), and successful use of CSRE for load-bearing walls can be seen across the world (Verma and Mehra, 1950; Easton, 1982; Hall, 2002; Walker et al., 2005; Kotak, 2007; Jayasinghe and Kamaladasa, 2007; Reddy and Kumar, 2009a; Reddy and Kumar, 2011; Kandamby and Jayasinghe, 2011; Ciancio and Gibbings, 2012; Beckett and Ciancio, 2013).

Several studies have been carried out on the performance of rammed earth walls and buildings analytically (e.g. Maiti and Mandal, 1985; Maniatidis and Walker, 2008; Ciancio and Augarde, 2013), experimentally (e.g. Yamin et al., 2004; Maniatidis and Walker, 2008; Gomes et al., 2011; Bui et al., 2011; Reddy and Kumar, 2011) and numerically (e.g. Yamin et al., 2004; Jaquin, 2008; Liang et al., 2011; Nowamooz and Chazallon, 2011; Gomes et al., 2011; Bui et al., 2011; Miccoli et al., 2014b). Besides studies under static loading (e.g. Maniatidis and Walker, 2008; Reddy and Kumar, 2011), dynamic studies were also carried out on the performance of rammed earth walls and buildings (Yamin et al., 2004; Gomes et al., 2011; Bui et al., 2011). Maniatidis and Walker (2008) studied the structural capacity of unstabilised rammed earth columns of square cross-section (300 mm x 300 mm) of 1.8 m, 2.4 m and 3 m heights under concentric and eccentric compression loading; focusing on the effect of load eccentricity and slenderness ratios (= 6, 8 and 10). The load-capacity of concentrically loaded columns was determined to be 46.7, 65.8 and 58.1 kN for slenderness ratio equals to 6, 8 and 10 respectively. It is observed that the load values are higher at higher slenderness ratios, which is quite ambiguous. Generally, it is expected that the load-capacity of column drop with increasing slenderness ratio. Reddy and Kumar (2011) investigated the structural behaviour of story-high CSRE walls. The test comprised of prism, wallette and wall of sizes: 150 × 150 × 300 mm, 600 × 155 × 720 mm and 750 × 152 × 3000 mm (width × thickness × height) respectively. The average compressive strengths of prism, wallette and wall were determined to be 6.50, 5.47 and 3.91 kN respectively. It was observed that the wall strength decreases with increasing slenderness ratio and there was nearly a 30% reduction in strength as the slenderness ratios increased from 4.65 to 19.74. At higher slenderness ratios, there was a close agreement between the experimental and predicted values using the Engesser's tangent modulus theory (Bleich, 1952).

2.5.2 Reinforced rammed earth

In the recent past, steel have been introduced as reinforcing materials in order to attain higher strength of rammed earth elements for innovative applications. It has been observed that rammed earth beams reinforced with steel improves the load-capacity by about 383% to 570% and flexibility of the soil beams substantially (Gaind and Char, 1983). Bond property of steel bars (12 mm diameter) embedded in rammed earth, gave a reasonable bond strength of 1.08 to 19.52 kN (Walker and Dobson, 2001). A very few literatures could be found on steel reinforced rammed earth walls and columns. Lindsay (2012) briefly described the use of structural steel elements (steel bars) within stabilised rammed earth walling. It was recommended that steel reinforced columns should be placed either at the very end of the wall or at least 20% of the total wall length from end of the wall. Gupta (2014), conducted test on two full-scale composite (i.e., steel reinforced) rammed earth columns made of horizontal and diagonal stirrups. It was observed that the column with diagonal stirrups was much stiffer i.e., carry significantly higher load of about 167% more than the column with horizontal stirrups.

Besides steel, bamboo has also gained popularity as a reinforcing material. Extensive studies on the performance of bamboo as reinforcement in structural concrete elements showed that bamboo can substitute steel satisfactorily and the structural elements developed and studied (i.e. bamboo reinforced concrete) could be used in many building constructions (Ghavami, 2005). Investigation on the behaviour of chemically treated bamboo reinforced concrete columns showed that the load-capacity of column reinforced with 8% bamboo is equivalent to 0.89% steel reinforced column and thus concluded that bamboo has the potential to substitute steel as reinforcement for structural members like column (Agarwal et al., 2014). However, a very limited study has been reported for bamboo reinforced rammed earth constructions. Studies on rammed earth wall reinforced with bamboo cane under monotonic horizontal load have been shown to improve the yield load, i.e., the vertical bamboo ribs improved ductility of the rammed earth wall (Gao et al., 2009). Studies on bond behaviour of bamboo strips embedded in CSRE blocks produced reasonable bond strength ranging from 1.01 to 3.45 MPa (Tripura and Sharma, 2014).

2.6 Codes of practice on rammed earth constructions

In the last few decades a good number of earth building codes, standards and guidelines have been developed by various countries across the world e.g. Australian earth building handbook; California historical building code; Chinese building standards; Ecuadorian earth building standards; German earth building standards; Indian earth building standards; International building code / provisions for adobe construction; New Mexico earth building materials code; New Zealand earth building standards and Peruvian earth building standards (as mentioned in ASTM E2392/E2392M, 2010). Among all these standards, New Zealand standards (NZS 4297, 1998) and Australian earth building handbook (AS HB 195, 2002) are most widely referred in the literature. According to Maniatidis and Walker (2008), New Zealand earthen standard (NZS 4297, 1998) is the most well known structural design standard for earth building at present. The NZS 4297 (1998) deals with structural and durability design of earth buildings. Table 2.3 shows capacity reduction factors (k) for various values of slenderness ratios based on earthen (NZS 4297, 1998; AS HB 195, 2002) and masonry (AS 3700, 1988; BS 5628, 1992; IS 1905, 2002) standards. It can be observed that k values for earthen standards are adopted from masonry standard AS 3700 (1988). The k values listed in AS 3700 (1988) are relatively lower than those in IS 1905 (2002) and BS 5628 (1992) standards. It is seen that the prevailing earthen standards do not adequately address the structural design requirements for earthen buildings and hence design rules developed for masonry construction are generally followed (Maniatidis and Walker, 2008). In the study made by Maniatidis and Walker (2008) on axially loaded 'unreinforced' and 'unstabilised' rammed earth columns, an attempt was made to validate the application of masonry standard design provisions to earthen walls/columns. It was concluded that for small load eccentricities (up to 10%), existing codes/guidance (such as NZS 4297, 1998; AS HB 195, 2002) provided a good estimate of the measured experimental performance.

2.7 Summary and conclusions

Literature review on historical background of earth construction, suitability of soil, sustainability, structural behaviour of rammed earth walls/columns and codes of

practice on rammed earth constructions has been carried out. Based on the literature review the following conclusions have been drawn:

1. Rammed earth construction technique have been in use since 500 B.C. and in the recent past this technique have gained renewed interest due to its varied sustainable benefits such as low cost, low embodied energy etc., compared to other conventional building materials like burnt clay bricks, steel etc.
2. Various types of soil have been found suitable for rammed earth constructions. Clay, silt, sand and gravel content of the soil used ranges from 5 – 40%, 0 – 30%, 20 – 75% and 10 – 62% respectively.
3. For cement stabilised rammed earth constructions use of 4 – 12% cement have been reported.
4. Structural behaviour of unstabilised and cement stabilised rammed earth walls and columns have been studied. However, a systematic study of the influence of structural parameters such as slenderness ratio, cross-sectional aspect ratio, and cross-sectional shapes on load-capacity, reduction factor, failure pattern etc., on concentrically loaded CSRE columns have not been reported.
5. A limited study on reinforced rammed earth column, for example, the effect of diagonal and horizontal stirrups on the load-capacity of steel reinforced CSRE columns has been reported. However, the effect of stirrups spacing (lateral reinforcement ratio) has not been presented so far.
6. Studies have shown that bamboo can be a potential substitute to steel in structural concrete elements such as beams and columns. Bamboo reinforcement was found to improve the ductility of the rammed earth wall under horizontal load.
7. Most of the rammed earth standards use capacity reduction factors from masonry standards without sufficient validation. An experimental study (Maniatidis and Walker, 2008) on unreinforced and unstabilised rammed earth column showed that for small load eccentricities (up to 10%), existing codes/guidance provided a good estimate of the measured experimental performance.

Table 2.1. Highlights of important conclusions and recommendations from literatures.

Authors/ standards	Composition of soil and recommendations	Compressive strength (MPa)	Density (kg/m^3)	Linear Shrinkage (%)	Equipment used for making compression test samples
Patty and Minium (1945)	Sand: 40 – 75%; optimum: 75%; addition of 6 mm aggregates up to 45% to increase strength	0.65 – 2.77 (dry)	1730 – 2160	----	----
Verma and Mehra (1950)	Sand: >35%; LL: <25%; and PI: 8.5 – 10.5	> 2.8 (dry)*	1940 – 2000	----	Wooden formwork, metal rammer
Easton (1982)	Clay: 30% and sand : 70%	2 (dry)	1950	----	----
Lilley and Robinson (1995)	Clay: 11 – 21%	1.8 – 2.0 (dry)	----	----	----
King (1996)	----	10 – 27 (dry)*	2070	----	----
Keable (1996)	----	1.5 – 2 (dry)	----	----	----
Rauch and Kapfinger (2001)	----	2.40 (dry)	----	----	----
Clark and Walker (2003)	Gravel: 39%; silt: 12% and clay:11%	1.1 – 2.2 (dry)	1870 – 2020	0.25 – 1.6	----
Hall et al. (2004)	----	3.5 (dry)*	----	----	----
Earth Building Association of Australia (2004)	----	> 2.8 (dry) after 28 days	----	<5	----
Walker et al. (2005)	Sand and gravel: 45–80%; silt: 10–30%; clay: 5–20%; cement: 4–12%; LL: <45%; and PI: 2–30%	>1		<5	----
Bui et al. (2007)	----	1.0 (dry)		----	----

*Stabilised rammed earth.

Table 2.1. Highlights of important conclusions and recommendations from literatures (contd.).

Authors/ standards	Composition of soil and recommendations	Compressive strength (MPa)	Density (kg/m^3)	Linear Shrinkage (%)	Equipment used for making compression test samples
Jayasinghe and Kamaladasa (2007)	(i) Sandy soil: - gravel: 32.2%; sand: 59.4%; clay and silt: 8.4%. (ii) Hard laterite: - gravel: 56%; sand: 29.6%; clay and silt: 14.4%. (iii) Clayey: - gravel: 50.5%; sand: 30.4%; clay and silt: 19.1%. Fines (clay and silt) content <20%.	1.82 –3.71 (dry)*	1800 – 2000	----	Steel rammer, steel form work
Maniatidis and Walker (2008)	Gravel: 30%; sand: 45%; silt: 13%; clay: 12%; LL: 49%; and PI: 24%.	0.62 – 0.97 (dry)	1760 – 2030	----	Plywood-faced concrete formwork; pneumatic rammer,
Burroughs (2008)	Clay/silt: 21–35%; gravel: 13–62%; sand: 30–70%; LL: ≤35%; PL: 16–19%; PI: <15% and sand: <16%.	>2 (dry)*	----	----	----
Reddy and Kumar (2011)	Sand: 72.6%; silt: 11.6%; clay: 15.8%; LL: 26.9% and PL: 17.5%.	6.19 – 6.80	1980 (unstabilised); 2030 (8% cement stabilised)	----	Metal mould and steel rammer
Ciancio et al. (2013)	(i) For unstabilised soil:- gravel: 10–20%; sand: 20–50%; silt: 0–25%; clay: 5–40%; LL:15.6–34.5% and PI: 3.1–18.4%. (ii) For cement-lime stabilised soil:- gravel:20–45%; sand: 20–60%; silt: 0–25%; clay: 5–30%; LL:15.4–38.5%; and PI: 4–23.3%.	>2 (dry)	1740 – 2160	Unstabilised :0–7.1 Cement stabilised: 0.2–7.1	Not specified
Middleton (1992)	Relatively low clay content.	>2 (dry)*	98% of Proctor standard	----	----

Table 2.2. Highlights of important conclusions and recommendations from standards/guidelines.

Standards/ guidelines	**Composition of soil and recommendations**	**Compressive strength (MPa)**	**Density (kg/m^3)**	**Linear Shrinkage (%)**	**Equipment used for making test samples**
NZS 4298 (1998)	----	>1.3	----	----	Hand/mechanical rammer; formwork not clearly specified
IS 2110 (2002)	Sand: ≥ 35%; LL: ≤ 27%; and PI: 8.5 – 10.5%.	≥ 1.4 (dry)* ≥ 0.7 (wet)*	≥ 1800	----	Metal rammer, timber formwork
AS HB195 (2002)	Soil for cement stabilisation: Sand and gravel: 45–80%; silt: 15–30%; clay: 0–25%; LL: <40% and PI: 2–22%; cement: 4–12%. For rammed earth: Sand and gravel: 45–75%; silt: 10–30%; clay: ≤ 20%; LL: <40% and PI: <2–22%; cement: 4–12%.	>1* 1– 15 (dry-rammed earth)	1700 – 2200 (rammed earth)	10–60 mm	Plywood, timber planks, mild steel or aluminium.; metal/timber rammer; pneumatic rammer.
Lehmbau Regeln (2009)	----	2 – 3 (dry) 3 – 5 (dry) *	1700 – 2200	----	----

*Stabilised rammed earth.

Table 2.3. Reduction factors (k) for various values of slenderness ratios (λ).

Slenderness ratio (λ)	Reduction factor (k)				
	Eccentricity to thickness ratio (e/t_w) ≤ 0.05				
	Earthen standard		Masonry standard		
	NZS 4297 (1998)	AS HB 195 (2002)	IS 1905 (2002)	AS 3700 (1988)	BS 5628 (1992)
6	1.00	1.00	1.00	1.00	1.00
8	0.94	0.94	0.95	0.94	1.00
10	0.88	0.88	0.89	0.88	0.97
12	0.82	0.82	0.84	0.82	0.93
14	0.76	0.76	0.78	0.76	0.89
16	0.70	0.70	0.73	0.70	0.83
18	0.64	0.64	0.67	0.64	0.77
20	_	0.58	0.62	0.58	0.70

Fig. 2.1. The Great Wall of China (constructed ~3000 years ago) (*Source:* Patriciagrayinc).

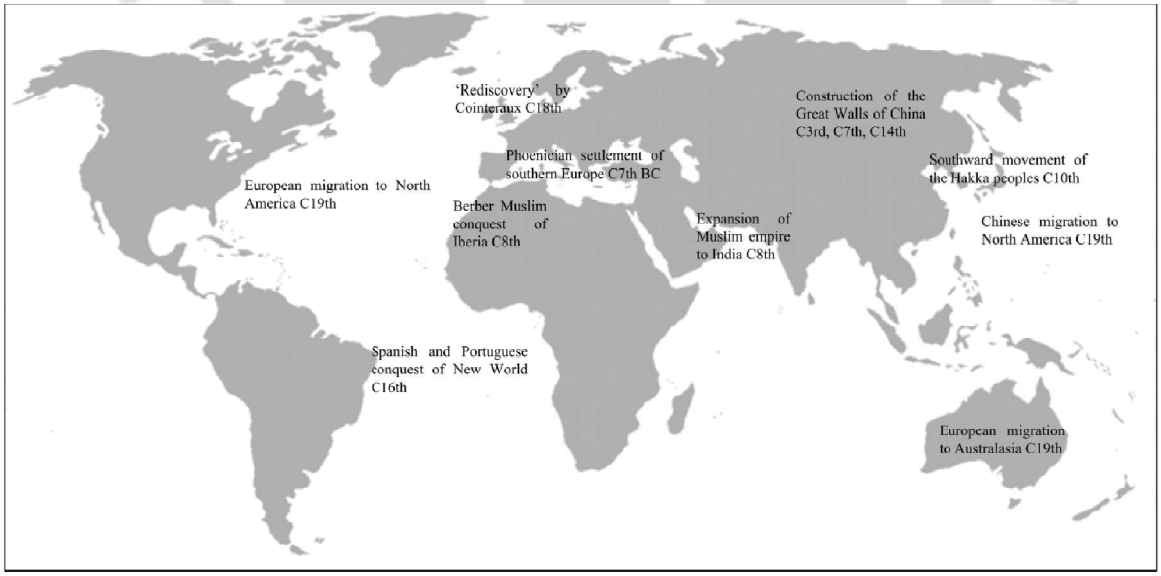

Fig. 2.2. Map of the major movements of the rammed earth technique (*Source:* Jaquin et al., 2008).

Fig. 2.3. Rammed earth walls surrounding Horyuji Temple, Japan (constructed ~1300 years ago) (*Source:* Henman, 2004).

Fig. 2.4. Basgo fort, India (constructed before ~1357 A.D.) (*Source:* Jaquin, 2006).

Fig. 2.5. Cement stabilised rammed earth buildings in Gujarat, India (*Source:* Kumar, 2009).

Fig. 2.6. Mud clay ancient palace in Tarim city, Yemen (constructed ~300 years ago) (*Source:* Helfritz, 1937).

Fig. 2.7. Alhambra Fortress of Granada, Spain (constructed in 889 A.D.) (*Source:* Alhambra).

Fig. 2.8. Unstabilised rammed earth building in Weilburg, Germany (constructed in 1826 A.D.) (*Source:* Kumar, 2009).

Fig. 2.9. Rammed earth chalk building in Winchester, Hampshire, UK (*Source:* Kumar, 2009).

Fig. 2.10. The Church of the Holy Cross in Stateburg, South Carolina, USA (constructed in 1857 A.D.) (*Source:* Wikipedia).

Fig.2.11. Modern rammed earth building, Australia (*Source:* Favhomedecors).

Fig. 2.12. Rammed earth school building in Bangalore, India (*Source:* Reddy et al., 2014).

Fig. 2.13. Rammed earth building in Agartala, India.

(a) (b)

Fig.2.14. Steel reinforced CSRE columns (Source: Clifton, 2015)

Chapter 3

Materials Characterization

This chapter deals with the determination of properties of locally available (Agartala, India) soil and its suitability as a construction material. The properties of unstabilised and cement stabilised rammed earth (CSRE) blocks are studied in terms of density, strength, compaction energy, and durability in both cured and uncured condition. An attempt has also been made to select and validate the block-making equipment and technique that can be used for construction of rammed earth structures.

3.1 Introduction

Most of the naturally occurring soils such as fine-grained soils (e.g. silts and clays), highly organic soils (or peat), etc. lack in strength, dimensional stability, density and durability required for building construction. As mentioned in Section 2.3, top soil is generally not preferred for construction as it contains organic matter, and King (1996) suggested that the organic content should be limited to ~1-2 % by mass for construction purposes. Although, it is difficult to provide a straight forward criteria demarcating the type of soil suitable for construction, sandy loam sub-soil is predominantly regarded as suitable 'earth' for making rammed earth (Houben and Guillaud, 1994). In the literature (see Tables 2.1 and 2.2) several types of soil have been researched to check their suitability for earth construction, in their natural state or with stabilisation (with chemical binders such as cement, lime etc.) procedures (e.g. Walker, 1995; Bahar et al., 2004; Jayasinghe and Kamaladasa, 2007). As discussed in Chapter 2**,** there exists a wide range of values for clay (5-40%), silt (0-30%), sand (20-75%), gravel (10-62%) , Atterberg limits (LL:15.4 – 49% and PI: 2 – 30% respectively), density (1700 – 2200 kg/m^3), compressive strength (0.7– 27 MPa) etc., that are reported to be suitable. In addition, stabilisation with 4 – 12% cement have also been reported for rammed earth studies (e.g. Verma and Mehra, 1950; Easton, 1982; King, 1996; Walker et al., 2005; Bui et al., 2007; Reddy and Kumar, 2011). However, it may be noted that in most of the studies details of the type of mould,

rammer etc. needed for the production of rammed earth blocks are not mentioned precisely. Therefore, in the present chapter the properties of locally available soil at Agartala, India and its suitability as a construction material are studied, followed by an attempt to select and validate block making equipment and technique that can be used for construction of rammed earth structures. The properties of unstabilised and stabilised (with cement) rammed earth blocks in terms of density, strength and durability are presented. The properties of CSRE blocks with varying cement content under cured and uncured conditions as well as under constant (close to standard Procter effort) and varying compaction energy.

3.2 Experimental programme

3.2.1 Materials

Soil sample used in the present study was collected from a depth of 0.5 -1.5 m from National Institute of Technology (NIT) Agartala campus, India. Table 3.1 outlines the properties of the soil and Fig. 3.1 shows its gradation curve. The properties of soil was determined as per Indian standards - IS 2720 Part 4 (1995), IS 2720 Part 5 (1995) and IS 2720 Part 7 (2002). Wet sieve analysis was used for classification of granular material and sedimentation for the cohesive material. Ordinary Portland cement of 43-grade conforming to IS 8112 (1989) was used in the experimental investigations. The initial and final setting time of cement is 40 and 180 minutes respectively, with a specific gravity of 3.09.

3.2.2 Determination of optimum moisture content and maximum dry density

The water content at which a specified compactive force can compact a soil mass to its maximum dry unit weight is known as optimum moisture content (OMC). Based on tests on stabilised soil, Bahar et al. (2004) obtained OMC values of ~9.5–11.0% with a corresponding dry density of ~2000 kg/m^3. It was observed that if too little water is present, the soil cannot achieve the same level of compaction due to a greater degree of friction between the soil particles, whereas if excess water is present then capillary water occupies the soil pore spaces, reducing the level of achievable compaction and increasing the level of porosity upon drying of soil. New Zealand Standard NZS 4298 (1998) states that for rammed earth production the moisture

content range should not be more than 4% dry of optimum or 6% wet of optimum, and this practice was strictly observed during the present sample production scheme. To determine OMC and maximum dry density (MDD), the soil was first oven-dried to a constant mass at a temperature of 105–110°C for 24 hour and pulverized into a coarse powder manually. Moisture values were also occasionally determined by rapid moisture meter for a quick check. Then a standard Proctor test was carried out for both unstabilised and cement stabilised soils. The remaining soil samples were sun-dried. Fig. 3.2 shows the maximum dry density vs. moisture content relations of various soil–cement proportions. The bulk density of soil mixed with 10% cement is about 2100 kg/m^3.

3.2.3 Equipment for production of rammed earth blocks

A mild steel rammer weighing about 5.6 kg with a solid handle of 25 mm diameter and 1.02 m length attached with a 95 × 95 mm mild steel ramming face of thickness 20 mm, was used for compacting manually. A wooden cube mould of 100 × 100 × 100 mm (inner dimension) and 20 mm wall thickness was used to assist the direct comparison of rammed earth blocks with more familiar standard concrete cubes of height/width ratio 1. A 97 × 97 mm mild steel collar guide of 300 mm height and 0.5 mm wall thickness was used to facilitate the location of the hand rammer into the cube mould. Fig. 3.3 shows the details of equipment used for making blocks and Fig. 3.4 shows the schematic diagram of block-making equipment.

3.2.4 Production of test samples

Five categories of rammed earth block production in terms of cement content (i.e., 0%, 4%, 6%, 8% and 10% cement by dry mass of soil) were undertaken. The moisture content of the sun-dried soil was determined by rapid moisture meter before production of rammed earth blocks, thus ensuring an additional level of standardization. The soil was thoroughly mixed with 4% cement and subsequently with 6–10% cement, respectively, followed by addition of water up to OMC in separate batches of 6 kg such that it is sufficient to produce two 100 mm cube samples.

The inner surface of the cube mould was painted with form oil, and the moistened soil was compacted in three separate layers. About 900–1000 g of soil amounted to approximately one third the height of the cube mould when compacted. According to Bahar et al. (2004), mechanical stabilisation by dynamic compaction appears to give better results as compared with a static or vibro-static compaction. In the present study dynamic compaction method was adopted with a rammer height of fall 300 mm in accordance with IS 4332 Part 5 (2006b) and ramming equipment as described above. It was observed that unlike NZS 4298 (1998), the handle of the rammer starts ringing initially within three to four blows followed by non ringing sound then ringing sound just at the point of achieving the maximum compaction. Compaction energy (~5.6 kg-cm/cc) close to standard Proctor value was adopted throughout the production run to achieve the required compaction level. Fig. 3.5 shows a typical rammed earth cube.

Part of the CSRE blocks were cured for 28 days under wet burlap then dried in ambient temperature prior to testing. The remaining samples were kept uncured in the laboratory at the same temperature. Samples were also produced to study the effect of age of curing on compressive strength at varying cement contents. Table 3.2 shows the production details of the test samples.

3.2.5 Effect of compaction energy

The 10% CSRE (i.e. with 10% cement) blocks were used to study the effect of compaction energy on density and strength. The samples were produced at constant OMC but at varying levels of compaction energy at the rate of eight samples per level of compaction energy. Table 3.3 shows the details of compaction energy applied. The compaction energy/ effort was calculated using the formula given in ASTM D–698–12 (ASTM 2012) as follows:

$$E_c = \frac{nNWH}{V} \tag{3.1}$$

where E_c = compaction energy (kg-cm/cc); n = number of compacted layer; N = number of blows per layer; W= weight of rammer (kg); H = height of fall of rammer (cm); and V = volume of mould (cm^3).

3.2.6 Test procedure

The surfaces of all the test samples were cleaned prior to testing. Three specimens were randomly selected from each category of rammed earth blocks, and two strain gauges were attached to each of these specimens perpendicular to each other to determine lateral and longitudinal strains simultaneously along with determination of compressive strength as per IS 4332 Part 5 (2006b). The remaining samples were tested to determine compressive strength only. The test specimen was placed in between two 16 mm thick steel plates resting on a hydraulic jack with a 250 kN load cell mounted on it. Both strain gauges and load cell were connected to a data acquisition system as shown in Fig. 3.6. All the test equipments were calibrated prior to testing. The moisture content on a representative sample of fragments taken from the interior of the tested specimens was determined in accordance with IS 4332 Part 2 (2006a). The same method was adopted to determine the wet strength of cured samples immersed in water for two days prior to testing, following the work of Heathcote (1995). More discussion on durability test is shown in Section 3.3.6.

3.3 Experimental results and discussions

3.3.1 Density

The consistency of sample production was assessed in terms of density. Table 3.2 illustrates a typical production run of rammed earth blocks. The CSRE blocks produced were approximately 100 × 100 × 100 mm in size. The dry density of rammed earth blocks were determined using the formula given in IS 4332 Part 5 (2006b) as follows:

$$\gamma_d = \frac{100\ W'}{AL\ (100 + m)} \tag{3.2}$$

where W' = weight of specimen (g); A = cross-sectional area of specimen (cm^2); L = length of specimen (cm); and m = moisture content of specimen (%).There was a less variation in OMC (1–9%) and MDD (2–4%) values as the cement content varies between 0 and 10% as shown in Fig. 3.2. Thus, OMC and MDD are relatively less sensitive to the variation in cement content of the mix. This finding is in agreement

with the work of Kumar (2009). Typical values of dry density were between 1660 and 2000 kg/m^3 (Tables 3.4 and 3.5). The dry density variations of cured CSRE blocks were between 12–15.7% and uncured blocks were between 2.3–12.8% with compaction energy close to standard Proctor value. In both cured and uncured conditions, the values of dry density are quite consistent and slightly greater than standard Proctor values except for unstabilised blocks. The densities obtained thus satisfy the design values specified in Middleton (1992), NZS 4298 (1998), AS HB 195 (2002), IS 2110 (2002), and Lehmbau Regeln (2009). On visual observation, samples with high cement content exhibited visible shrinkage cracks but were smooth and had a hard surface finish. The samples with no or the least stabilizer were very stable with no visible cracking.

3.3.2 Effect of cement content and density on compressive strength

To further assess the reliability of sample production as well as to compare rammed earth blocks to conventional masonry materials, a compressive strength test was conducted as per IS 4332 Part 5 (2006b). Tables 3.4 and 3.5 show the details of the test results. The characteristic unconfined compressive strength was calculated using the formula given in NZS 4298 (New Zealand Standard, 1998) as follows:

$$f_k = \left[1 - 1.5\frac{Xs}{Xa}\right] X_1 \tag{3.3}$$

where f_k = characteristic unconfined compressive strength (MPa); X_s = standard deviation of a series, X_a = average of a series; and X_1 = lowest result.

The characteristic compressive strength of cured and uncured samples is in the range of 3.74–6.43 MPa and 0.87–4.14 MPa, respectively, for cement variation from 4-10%. Fig. 3.7 shows the increase in characteristic compressive strength with increasing cement content. The characteristic compressive strength of cured samples is about 2 times higher than uncured samples. This can be attributed to the hydration of cement on curing and filling of its product in the pores of the matrix thereby enhancing the rigidity of its structure by forming a large number of rigid bonds connecting sand particles. The strength of samples at 10% cement content is almost double the strength at 4% cement content, and the wet strength is about half the strength of cured samples. Lower values of characteristic compressive strength for wetted specimens as

compared to cured specimens may be related to the softening of soil due to water absorption (higher moisture content will lead to lower MDD and hence lower compressive strength). The differences in characteristic compressive strengths between uncured and wetted specimens are found to be small, for the two days of wetting period adopted for this study; however, it may be expected that wet compressive strength is likely to drop with further water absorption i.e. with more days of wetting.

It was observed that all the test samples satisfy the design criteria outlined in various standards except the strength of unstabilised, where the compressive strength is ~1.1 MPa (see Table 2.2). The coefficient of correlation between the strength of the test blocks is very strong irrespective of cured, uncured, and wet samples as the strength increases linearly with increasing cement content as shown in Fig. 3.7.

For a given compaction effort, the variations in dry density due to soil–cement proportion type is directly related to the characteristic unconfined compressive strength of the samples in both cured and uncured conditions as shown in Figs. 3.8 and 3.9, respectively. This may be attributed to the best packing density achieved for the soil– cement mixture corresponding to 4–10% cement content compacted under a given OMC. The strength of cured 4% and 10% CSRE blocks increases by about 79 to 31% higher than the strength of corresponding uncured samples with just an increase of 9% and 3% density, respectively. Further, it was observed that the compressive strength was sensitive to dry density, and OMC was insufficient to achieve the maximum dry density when the soil is stabilised with cement.

3.3.3 Effect of age of curing on compressive strength

A typical production run of CSRE blocks is shown in Table 3.2. The samples were tested after every seven days of curing interval and drying for 10 days (after curing) prior to testing. The effect of age of curing on compressive strength is shown in Fig. 3.10. It can be seen from Fig. 3.10 that there is a linear increase in the compressive strength when the age of curing is increased from 7 to 28 days, for cement content ranging from 4% - 10%. However, it can be observed that the increase in compressive strength is ~50% for higher cement content (i.e. 8 and 10%), whereas it is relatively

lower ~37% for 4% and 6% cement content. This may be related to the increased scope of hydration for CSRE higher with cement content. At 28 days curing the strength gained by 10% CSRE blocks was about 130% higher than 4% CSRE blocks. The rate of increment of strength was about 0.7–1.3 MPa per seven days of curing.

3.3.4 Effect of cement content on stress-strain characteristics

Influence of cement content on the stress-strain properties were studied on unstabilised and cured CSRE blocks. Table 3.4 outlined the details of test results and the stress–strain relationships are shown in Fig. 3.11. The compressive stress values are the outcome of the average results of three samples. The following important points were drawn from the test results:

1. The stress-strain relationships are linear initially followed by the nonlinear portion until peak stress value. After the peak (i.e., post peak), significant straining (or deformation) can be seen before the material fails. In some cases, the post peak response shows considerable deformation beyond the peak stress. The improvement in strength and ductility with cement content as compared to unstabilised condition may be attributed to the presence of cement in the soil mix, which contributes to the strength, and controls the deformation of specimens (by binding the soil grains, thus delaying the failure or formation of cracks in the soil mass as in unstabilised samples.) under compression in dry condition.
2. The strain at peak stress tended to increase with increasing cement content and dry density for 0–6% CSRE blocks with corresponding strain values of 0.008–0.03. No similar trend could be observed for 8–10% CSRE blocks with strain values of 0.02–0.023.
3. Initial tangent modulus (ITM) values were obtained to be in the range 0.1–2 GPa for unstabilised and stabilised rammed earth blocks. This value for CSRE blocks was higher than unstabilised blocks by about 130–1900% and it increases from 160 to 770% as the cement content increases from 4 -10%. Similarly, ITM increases from 0.1 to 2 GPa as the compressive strength and cement content increases from 1.1 to 9.73 MPa and 0 to 10%, respectively.

4. The modulus of elasticity (i.e. ITM) of CSRE blocks is about 1/10 the modulus of elasticity of concrete (say ~25 GPa for M25 grade concrete, IS 456 (2000)).

3.3.5 Effect of compaction energy on compressive strength and density

Details of compaction energy test results are shown in Table 3.3. The influence of varying compaction energy on strength and density is plotted in Fig. 3.12. The following observations were drawn from the test results:

1. Compressive strength and density increases with increasing compaction energy as shown in Fig. 3.12. The compressive strength increases from 6.43 to 10.18 MPa, respectively, with the increase in compaction energy from 4.84 to 16.94 kg-cm/cc.
2. From Fig. 3.12, it can be seen that the rate of increase in compressive strength is relatively higher (~50%) for compaction energy ~≤ 7.26 kg-cm/cc, then flattens (or very low increase rate i.e. ~ 5%) for compaction energy ~≥ 7.26 kg-cm/cc. This may be due to the best packing density achieved for the soil–cement mixture compacted under specific OMC with varying compaction energy. This pattern of increase in compressive strength is consistent with the pattern of density increase, where the density increased from 1710 - 1920 kg/m^3 for compaction energy ~≤ 7.26 kg-cm/cc; and 1920 - 1990 kg/m^3 for higher compaction energy (i.e. ~≥ 7.26 kg-cm/cc). Thus, it is seen that an optimum compaction is achieved at compaction energy close to 7.26 kg-cm/cc.
3. However, in the present study, compaction energy close to standard Proctor test ~ 5.6 kg-cm/cc (~ 22% lesser than 7.26 kg-cm/cc compaction effort) is adopted for all subsequent tests (Chapters 4-5), as Proctor compaction energy is relatively easier to relate as a standard and no definite consensus exists among researchers working in rammed earth.
4. The increase in density with increasing compaction energy can be divided into three parts: (a) a steeper rate (~12%) of increase at lower compaction energy (~≤ 7.26 kg-cm/cc), (b) stable or very low rate (~0.5%) of increase at moderate compaction energy (7.26 - 12.10 kg-cm/cc), and (c) low rate

(~3.1%) of increase with stabilisation for higher compaction energy (~≥ 12.10 kg-cm/cc). It is interesting to note that whilst the initial steeper increase and subsequent flattening of density at lower or moderate compaction energy levels can be related to improved densification due to readjustment of the constituent material compositions. The low increase rate of density at higher compaction energy may be associated with disintegration of constituent grain sizes (resulting in poor particle bonds) because of over compaction.

5. The variation of compressive strength with increasing dry density is shown in Fig. 3.13, where it can be seen that rate of increase of compressive strength with increasing density is relatively higher at lower density levels, however, the rate of increase drops down as the density increases.

3.3.6 Durability test

The durability of a CSRE block can be determined with the help of wet-to-dry strength ratio as was proposed by many researchers. According to Heathcote (1995), the ratio of wet-to-dry strength is an indicator of durability of earth wall components. The ratio of wet-to-dry strength of 0.33–0.50 may be regarded as suitable depending on the severity of the rainfall. Guettala et al., (2006) states that walls constructed with 5–8% cement soil blocks having a wet-to-dry strength ratio of 0.58–0.69, respectively, shows no deterioration as observed in a comprehensive durability study of stabilised earth. Jayasinghe and Kamaladasa (2007) state that the wet-to-dry strength ratio of 0.46–0.64 for clayey and hard laterite soil type is adequate for rammed earth walls under adverse conditions. Therefore, to determine wet-to-dry strength ratio, both cured and uncured CSRE blocks were immersed in water for two days prior to testing. Tables 3.4 and 3.5 outlined the test results. The ratio varies between 0.30–0.49 and 0.54–0.71 for cured and uncured samples respectively. The result shows that the ratios are within the range as proposed by many researchers (e.g. Heathcote, 1995; Jayasinghe and Kamaladasa, 2007), except uncured 4% CSRE blocks did not fall within the specified range (see Section 3.3.2). Furthermore, it was observed that the ratios are higher in case of uncured CSRE blocks, which may be due to extra hydration of cement that was unable to hydrate fully due to an insufficient

amount of water during compaction. The wet strength test was discarded for unstabilised soil blocks owing to negligible saturated strength.

3.3.7 Effect of cement content on tensile strength

Variation of splitting tensile strength with cement content for cured specimens is shown in Fig. 3.14. It can be observed that the tensile strength increases with increasing cement content, with the rate of increase showing relatively higher at higher cement content. As the cement content is increased by 10% (from 0% or unstabilised condition), the tensile strength improved by ~345%, thus it can be seen that there is a significant increase in the tensile strength with the introduction of cement as stabiliser. It is reported that the increase in tensile strength slows down beyond 10% cement (Bahar et al., 2004), but for the present range of cement content (up to 10%) it is not possible to make a comparison. Further, it is observed that the tensile strength of specimen with 10 to 0% cement content is about 2200 to 1000% lesser than their compressive strength respectively.

3.4 Summary and conclusions

This chapter deals with determination of properties of locally available soil and its suitability as a construction material. The properties of cement stabilised and unstabilised rammed earth blocks were studied in terms of density, strength, compaction energy, and durability in both cured and uncured condition. All the test samples were produced using steel rammer and wooden mould, with an attempt to select and validate the block-making equipment and technique that can be used for construction of rammed earth structures. From the detailed test results and analysis the following conclusions are drawn:

1. Regardless of cured or uncured condition the compressive strength and density of CSRE blocks increases with increasing cement content. The average characteristic strength of cured samples is about 2 times higher than uncured samples. On 21 to 28 days curing, the CSRE blocks can attain the compressive strength up to 37–50% higher than those cured for 7 days.

2. For a given compactive effort, the variations in dry density due to soil–cement proportion type is directly related to the characteristic unconfined compressive strength of the CSRE blocks in both cured and uncured conditions.
3. At optimum moisture content, it is not possible to achieve the maximum dry density and compressive strength of CSRE blocks although the compaction energy is increased beyond the standard Proctor effort. Use of cement content greater than 4% and curing of CSRE blocks is recommended to achieve higher values of density, strength, and durability.
4. The strength and density of CSRE (10% cement) blocks is quite sensitive to the variations in compaction energy up to 16.94 kg-cm/cc. Increase in compaction energy from 7.26 to 16.94 kg-cm/cc tends to increase in strength and density up to 1.2 times and 11% higher than that obtained at an energy level equivalent to the standard Proctor test. The compaction energy/effort beyond 3 times the Proctor value may cause a detrimental effect on the strength and density of the test specimen. Moisture content ranging between 1.79 and 2.65% of the test specimens during the test has negligible effect on strength and density.
5. The modulus of elasticity of CSRE blocks are sensitive to variation in compressive strength as well as cement content, and it is possible to have desired modulus value by adjusting the compressive strength and cement percentage.

Therefore, the soil used for production of CSRE blocks using the proposed block-making equipment and technique satisfy the design criteria outlined in various standards, such as NZS 4298, 1998; AS HB 195, 2002; IS 2110, 2002; and many researchers in terms of strength, density and durability.

Table 3.1. Properties of soil.

Property	Parameters	Details
Atterberg limits	Liquid limit, W_L	31.7 %
	Plastic limit, P_L	22.9 %
	Plasticity index, I_P	8.8 %
Grain size distribution	Sand	79 %
	Silt	13 %
	Clay	08 %
Proctor test	Optimum moisture content	19 %
	Maximum dry density (kg/m^3)	1760

Table 3.2. Production details of test samples.

% cement	No. of uncured samples for		No. of cured samples (28 days) for		Drying period (days) prior to testing		Effect of age of curing on compressive strength		Ambient Temperature during production	Relative humidity during production
	Dry test	[a]Wet test	Dry test	[a]Wet test	Uncured samples	Cured samples	Total samples	No. of sample tested at 7 days interval		
0	10	–	–	–	38	10	–	–		
4	10	10	10	10	38	10	24	6		
6	10	10	10	10	38	10	24	6	27-35 ^{0}C	70-80%
8	10	10	10	10	38	10	24	6		
10	10	10	10	10	38	10	24	6		

[a]*Immersed in water for two days prior to wet strength test.*

Table 3.3. Details of compaction energy.

No. of blows per layer	Total no. of blows	Compaction Energy (kg-cm/cc)	Dry density (kg/m^3)	Avg. Moisture content during test (%)	Avg. comp. strength (MPa)	Compaction equipment
25	75	5.60	1710	–	–	Standard Proctor
25	75	5.60	1710	1.65	8.21	Proctor rammer
10	30	4.84	1750	2.07	6.43	Rammer
15	45	7.26	1920	1.79	9.65	Rammer
20	60	9.68	1930	1.82	9.83	Rammer
25	75	12.10	1930	2.04	9.90	Rammer
30	90	14.52	1980	2.65	10.03	Rammer
35	105	16.94	1990	2.19	10.18	Rammer

Table 3.4. Summary of test result of cured samples.

% cement	Average wet compressive strength (MPa)[a]	Characteristic wet compressive strength (MPa)[b]	Average dry compressive strength (MPa)[c]	Characteristic dry compressive strength (MPa)[d]	Ratio of wet to dry strength	Average calculated dry density (kg/m^3)	Dry density variation w.r.t. Proctor value	ITM (GPa)	Poisson's ratio
4	1.35	1.23	4.45	3.74	0.30	1930	12% >	0.23	0.27
6	2.47	2.18	6.51	5.06	0.38	1960	15% >	0.60	0.28
8	3.29	2.99	7.15	5.46	0.49	1990	15.7% >	1.20	0.39
10	4.15	3.68	9.73	6.43	0.41	2000	14% >	2.00	0.39

[a] *Average value of ten sample tests after 28 days of curing and drying for 10 days and then wetting for 2 days prior to testing.*
[b] *Value of ten sample tests after 28 days of curing and drying for 10 days and then wetting for 2 days prior to testing.*
[c] *Average value of ten sample tests after 28 days of curing and drying for 10 days.*
[d] *Value of ten sample tests after 28 days of curing and drying for 10 days.*

Table 3.5. Summary of test result of uncured samples.

% cement	Average wet Compressive strength (MPa)[a]	Average dry Compressive strength (MPa)[b]	Standard deviation (MPa)	Characteristic compressive strength (MPa)[c]	Ratio of wet to dry strength	Average calculated dry density (kg/m^3)	Dry density variation w.r.t. Proctor value
0	–	1.10	0.31	0.30	–	1660	5.7% <
4	1.35	2.48	0.69	0.87	0.54	1750	2.3% >
6	2.47	3.46	1.17	1.08	0.71	1820	7% >
8	3.29	6.16	1.61	2.80	0.53	1900	10.5% >
10	4.15	7.42	1.33	4.14	0.53	1940	12.8% >

[a] *Average value of ten sample tests after 38 days of drying and wetting for 2 days prior to testing.*
[b] *Average value of ten sample tests after 38 days of drying in ambient temperature.*
[c] *Value of ten sample tests after 38 days of drying in ambient temperature.*

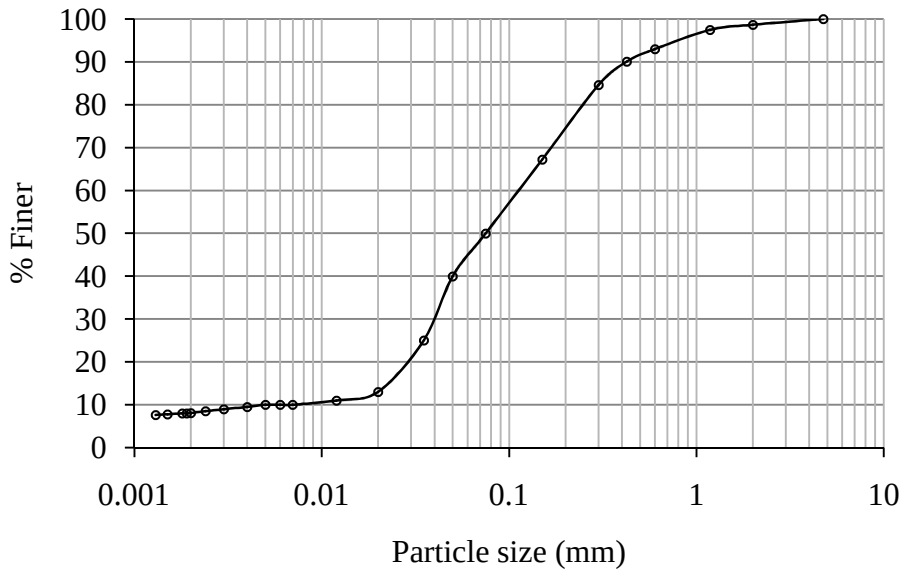

Fig. 3.1. Grain size distribution.

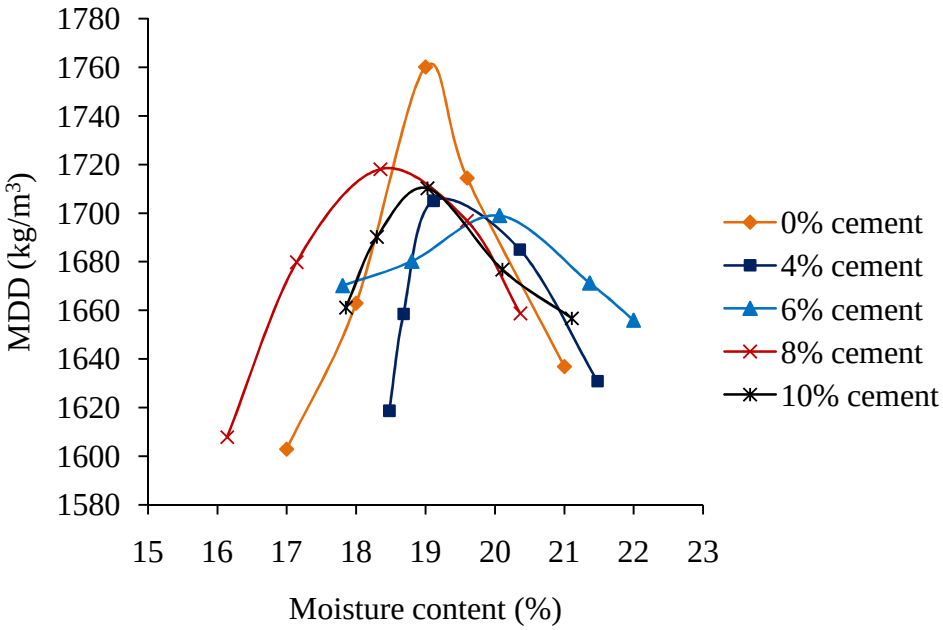

Fig. 3.2. Maximum dry density vs. moisture content.

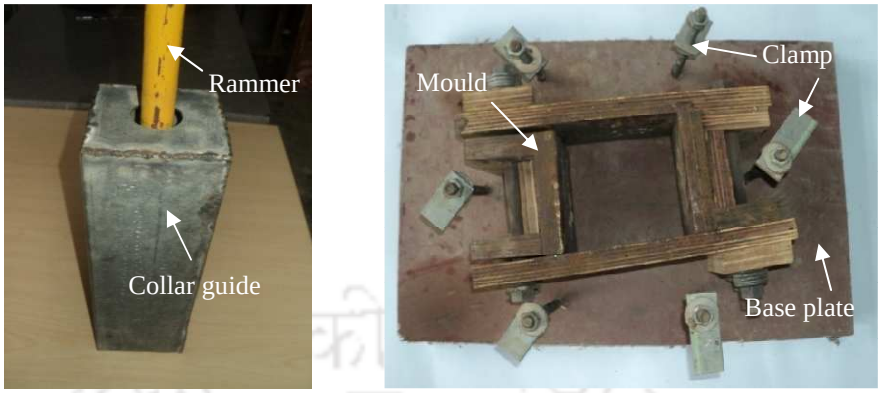

(a) Collar guide (b) Wooden mould

Fig. 3.3. Details of collar guide, rammer and wooden mould.

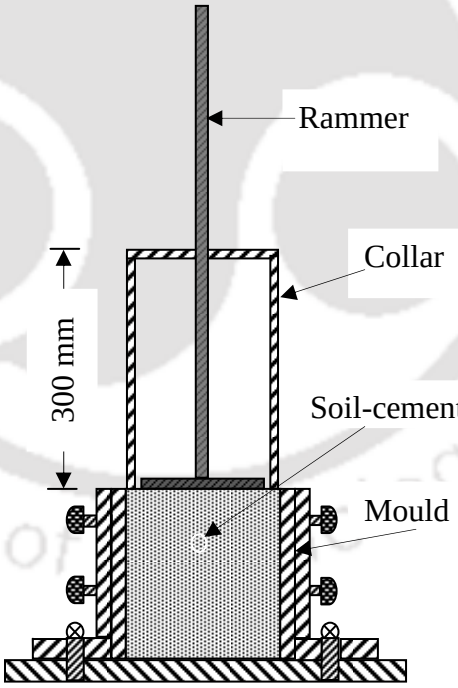

Fig. 3.4. Schematic diagram of block making equipment.

Fig. 3.5. Typical rammed earth cubes.

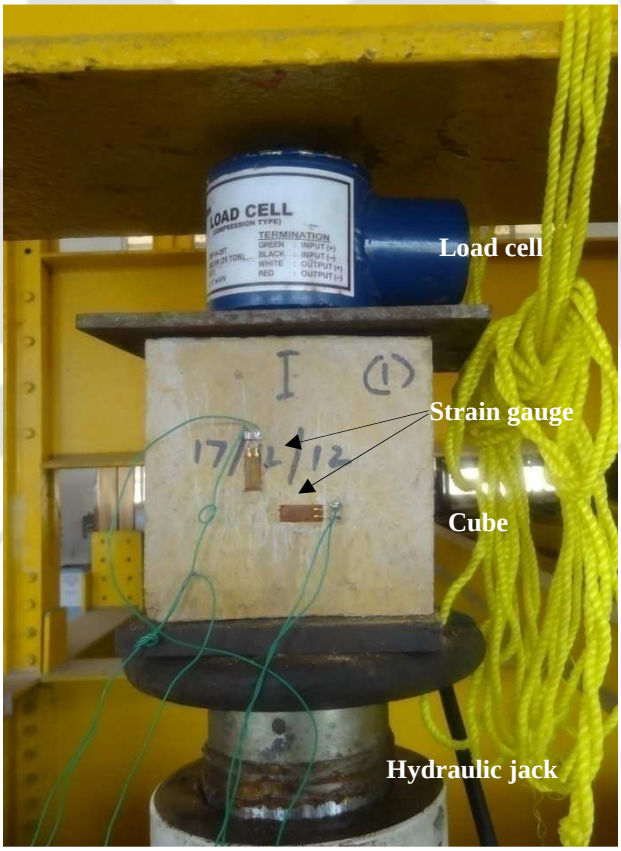

Fig. 3.6. Test setup.

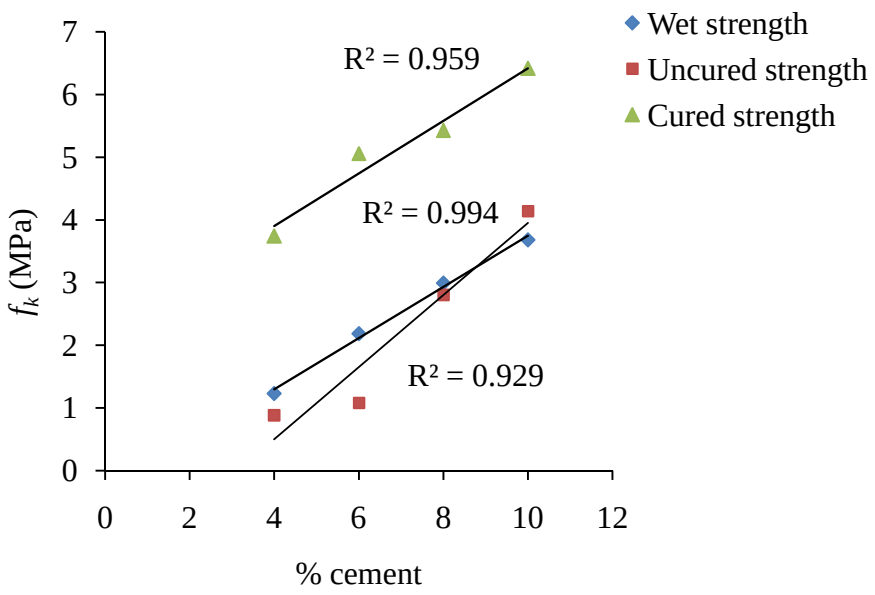

Fig. 3.7. Characteristic compressive strength vs. cement content.

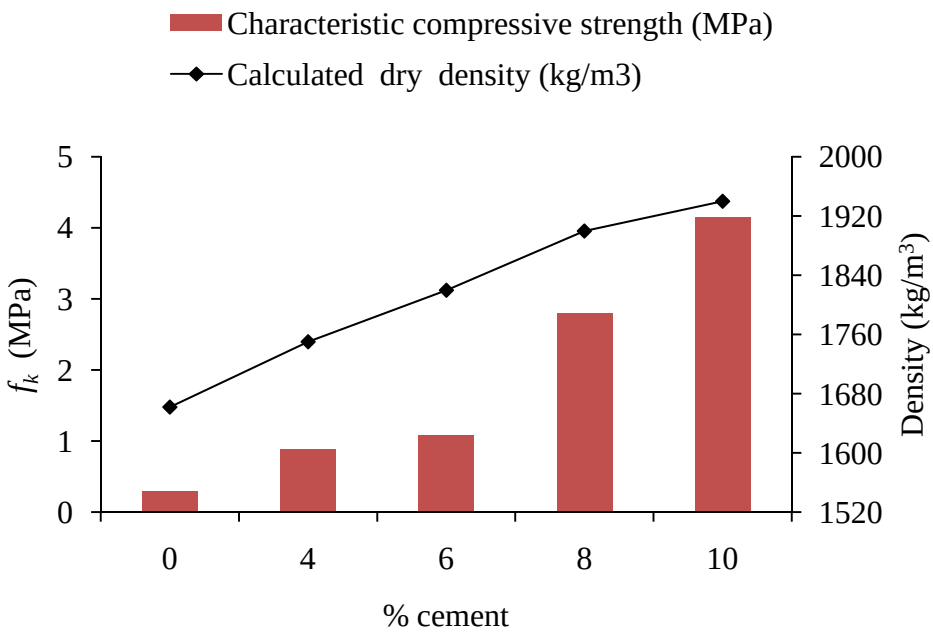

Fig. 3.8. Characteristic compressive strength, dry density of uncured samples vs. cement content.

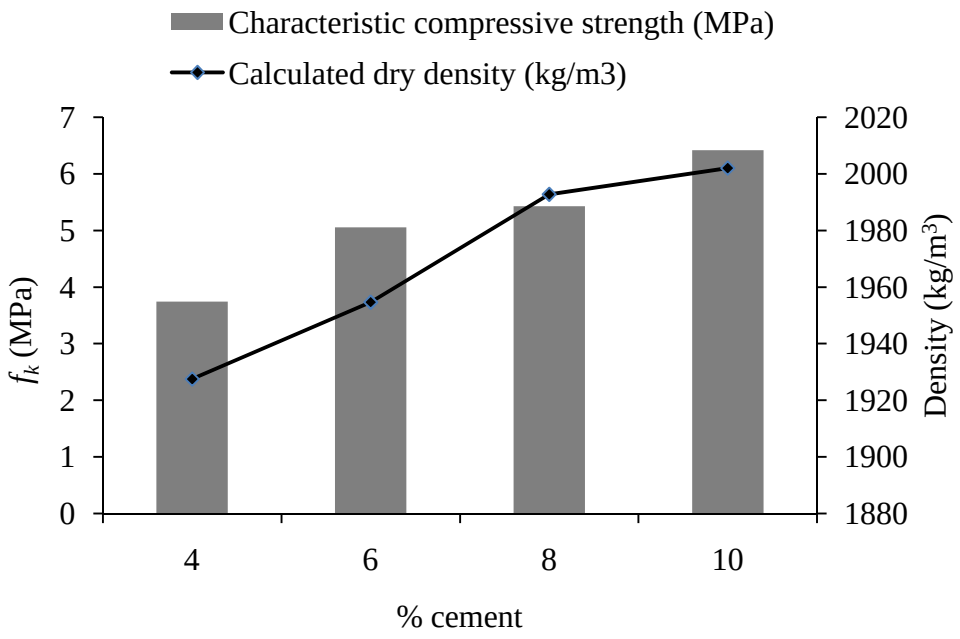

Fig. 3.9. Characteristic compressive strength, dry density of cured samples vs. cement content.

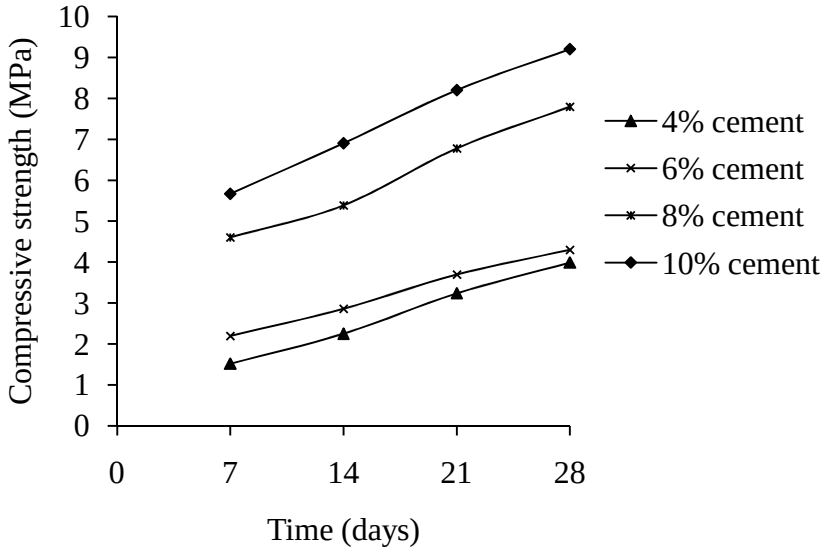

Fig. 3.10. Compressive strength vs. age of curing for varying cement contents.

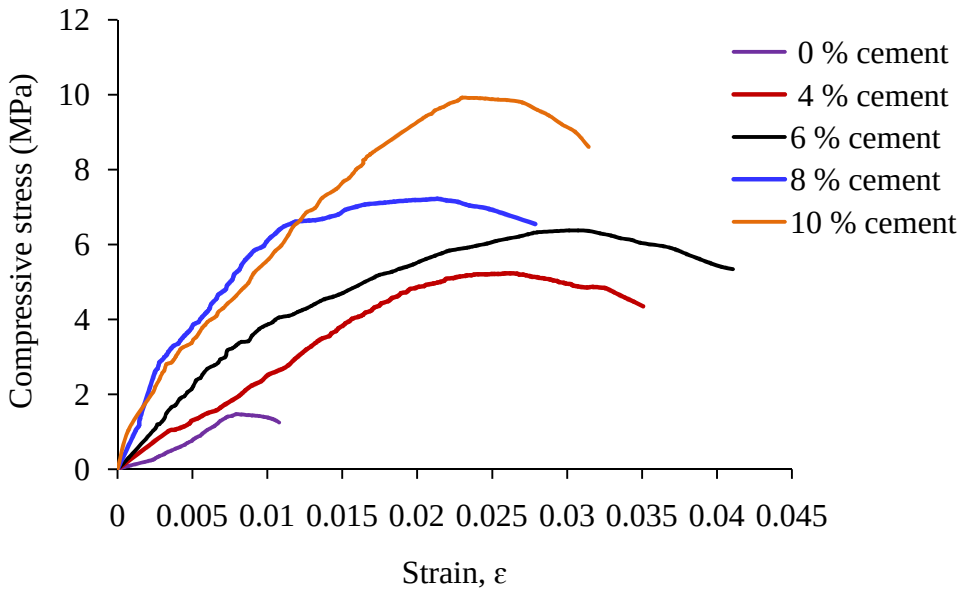

Fig. 3.11. Stress-strain curve of test samples, for varying cement contents.

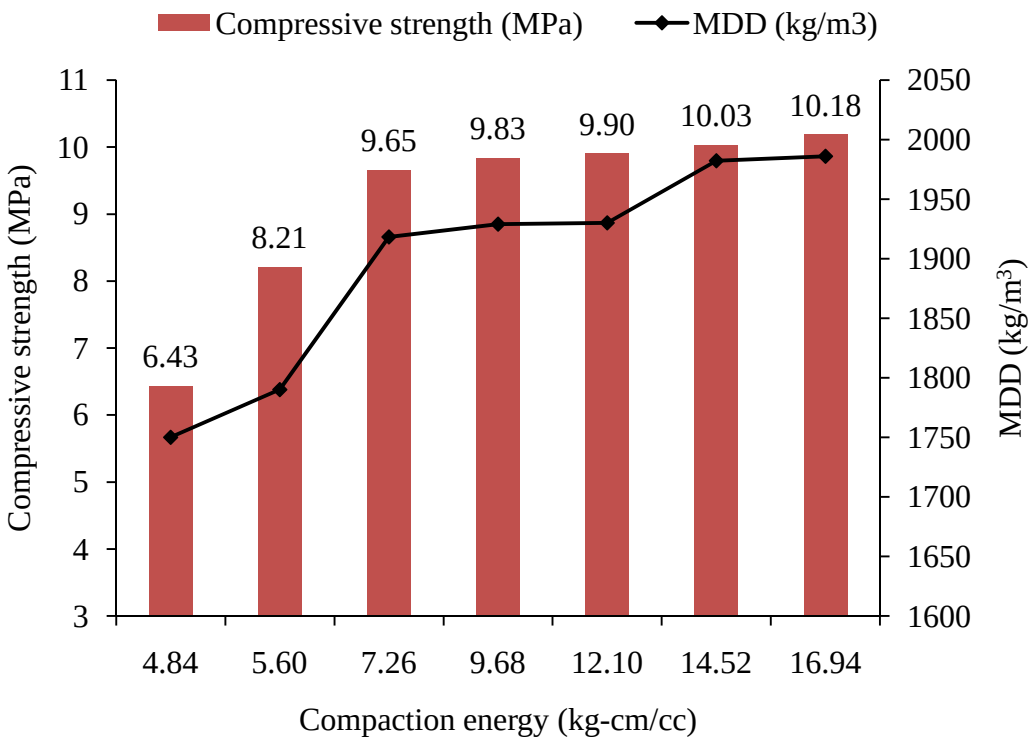

Fig. 3.12. Compressive strength, MDD vs. compaction energy.

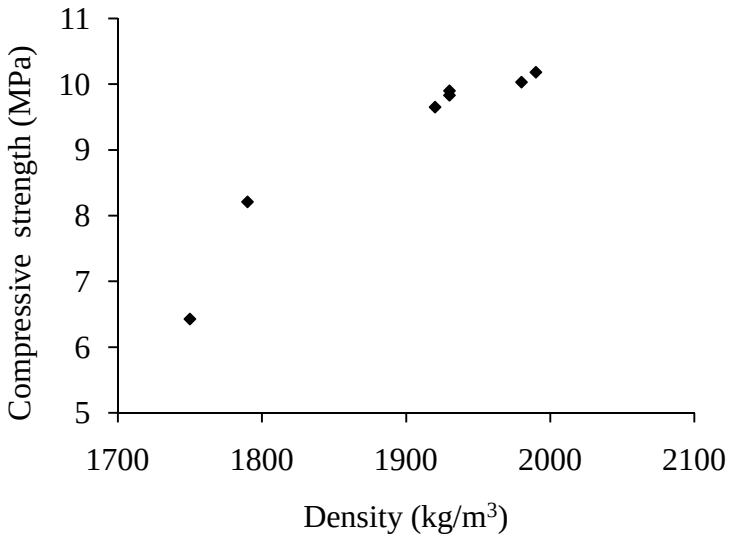

Fig. 3.13. Compressive strength vs. density.

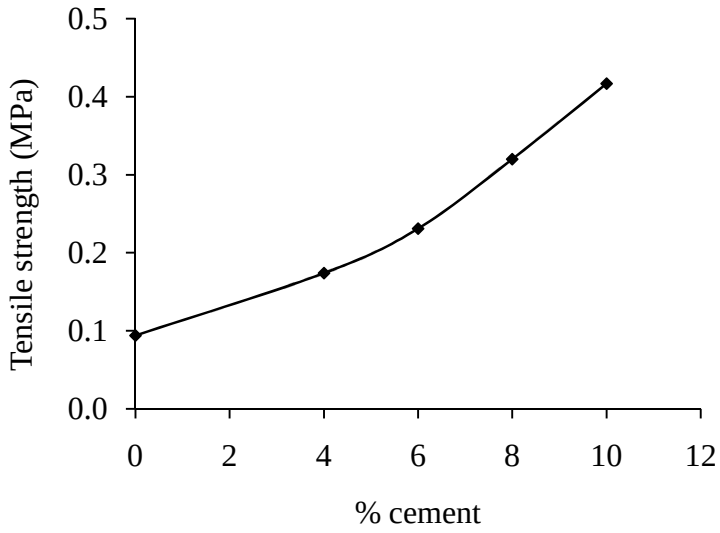

Fig. 3.14. Splitting tensile strength vs. cement content.

Chapter 4

Structural Behaviour of CSRE Column

This chapter deals with the study of axially loaded cement- stabilised rammed earth (CSRE) columns. Tests on CSRE prisms, cylinders and columns of circular (C), square (S) and rectangular (R) cross-sections were performed. Effects of slenderness ratio (λ) and aspect ratio (Φ) on the column strength, deformation and capacity reduction factors (k) were assessed. A comparative study was made on ultimate compressive strength (σ_u) of columns obtained from experimentation and Engesser's tangent modulus theory. Validity of using masonry design rules for the design of CSRE columns was evaluated.

4.1 Introduction

As discussed in the literature review (Chapter 2), in the recent past, rammed earth technique has gained renewed research interest (e.g. suitability of soil, structural behaviour of elements like wall etc.) due to its varied sustainable benefits such as low cost, low embodied energy etc., (e.g. Reddy et al., 2014 etc.). In spite of the upsurge in research interest on rammed earth constructions, due to the lack of adequately validated useful structural design regulations, building designers and engineers often use design rules developed for masonry constructions, often without modification (Maniatidis and Walker, 2008). Some of the well-known structural design standards/guidelines for modern earth constructions are NZS 4297 (1998), IS 2110 (2002), AS HB 195 (2002) and ASTM E2392/E2392M (2010). Many of these standards are used in conjunction with masonry standards, such as the stress/capacity reduction factors (*k*) available in earthen standards are directly adopted from the masonry standards (AS 3700, 1988; IS 1905, 2002; BS 5628 Part 1, 1992). As such, there is indeed a need to systematically investigate structural elements *viz.*, beams, columns, walls etc. made of rammed earth, if such techniques are to be made acceptable to practicing planners, designers and engineers. Amongst the structural elements, columns form an important structural element where rammed earth could have a potential application. In the literature, to the best of author's knowledge a very limited study is available on the structural behaviour of unreinforced rammed earth

columns (e.g. Maniatidis and Walker, 2008). Maniatidis and Walker (2008) first attempted to validate the use of masonry design rules for the design of unstabilised rammed earth square columns. However, their study did not explicitly explain the stress reduction factors for concentrically axially loaded columns. Hence, there is a need for further validation of masonry design rules considering structural parameters such as slenderness ratio (λ = height (h) / thickness (d) ratio), aspect ratio (Φ = width (a) / thickness (d) ratio) etc., on the capacity reduction factors of axially loaded columns.

In this chapter, the effects of slenderness ratio (λ), cross-sectional aspect ratio (Φ) on stress-reduction (k) factors, load-deformation, and load-capacity of columns, which are subjected to axial compression, are investigated. Furthermore, the ultimate compressive strength (σ_u) (where $\sigma_u = P_u/A$; P_u = ultimate load of test specimen and A = cross-sectional area of specimen) of columns is also determined using Engesser's tangent modulus theory (Bleich, 1952) and compared with the experimental results with respect to slenderness ratios. Experimental stress reduction factors and the corresponding values in masonry design standards are compared. At last, factor of safety values are determined to verify the design requirement of CSRE columns.

4.2 Experimental programme

4.2.1 Materials

Properties of the soil and cement used in the present experimental programme are similar to those explained in Section 3.2.1 and is shown in Table 4.1. Generally, 4 – 12% cement (by weight) is used for soil stabilisation to gain higher strength and durability of rammed earth structures (Ngowi, 1997; Guettala et al., 2006; Jayasinghe and Kamaladasa, 2007; Reddy and Kumar, 2011). Therefore, 10% cement was used for production of test specimens throughout the test programme. However, as discussed in Section 3.3.2, it must be noted that improvement in compressive strength could be obtained by increasing the cement content beyond 10%, however such effort is likely to affect the sustainability and cost of construction.

4.2.2 Equipments used for production of test specimen

For production of prisms and columns, the following equipments were used:

1. A 5.6 kg mild steel rammer with a 95 mm square ramming face and 1.02 m long solid handle of 25 mm diameter was used for ramming/compaction (Fig. 4.1a).
2. A wooden mould of 150 mm square section (inner dimension) and 1.5 m height having 20 mm wall thickness was fabricated and fastened with nuts and bolts and further provided with a wooden base plate for fixing the mould in position (Fig. 4.1b). The same mould was used for the production of rectangular columns, which was provisioned in such a way (i.e., extra holes have been provided to fix the bolts and nuts ensuring to obtain the desired cross-section) that the desired cross-sectional dimension of 190 mm x 150 mm and 230 mm x 150 mm (width x thickness) respectively can be easily set.
3. Out of four walls of the mould, one part of the wall was cut into half along the transverse direction to facilitate better compaction and positioning of rammer in the mould during compaction.
4. Collar guide as shown in Fig. 3.3a of Chapter 3, was used to facilitate the location of the rammer in the mould whenever required. Fig. 4.1c shows a typical CSRE square column.

Similarly, for the production of cylinder (height = 300 mm) and circular columns the following equipments were used:

1. A 5.6 kg mild steel rammer with a 107 mm diameter ramming face and 1.02 m long solid handle of 25 mm diameter was used for compaction (Fig. 4.2a).
2. Plastic pipe of 150 mm internal diameter and 0.3 mm wall thickness was used for production of columns. The top portion of the pipe was left with 400 mm extra height of each column to facilitate the location of the rammer in the mould (or act as collar). Mild steel clamps, ropes and wooden base plate were used for fixing the mould in position (Fig. 4.2b). A typical CSRE circular column is shown in Fig. 4.2c.

During the test programme, compaction was carried out with the help of a compaction machine developed in the laboratory, in which the rammer is connected to have a free fall of height of about 300 mm approximately.

4.2.3 Production of prism, cylinder and column specimens

Five prisms of 150 mm x 150 mm in cross-section and λ equals to two were produced to determine the compressive strength (σ) and stress-strain curve. In total 45 columns of three different cross-sections (i.e. Square (S) = 150 mm x 150 mm; Rectangular (R1) = 190 mm x 150 mm; and Rectangular (R2) = 230 mm x 150 mm) were produced having λ equals to 6, 8 and 10, comprising of five specimens from each series with an approximate height of 0.9 m (denoted by S-0.9, R1-0.9 and R2-0.9), 1.2 m (denoted by S-1.2, R1-1.2 and R2-1.2), and 1.5 m (S-1.5, R1-1.5 and R2-1.5), respectively. The dimensions are so chosen that length of one side remain constant i.e., thickness, d =150 mm, while the other side, i.e., width, a varies from 150 to 230 mm (see Fig. 4.3b), thereby increasing the values of Φ by about 26.7% and 53.3% for R1 and R2 respectively as compared to S columns.

Similarly, five cylinders of 150 mm diameter and λ equals to 2 were produced to determine the compressive strength and stress-strain curve. Overall 15 columns were produced having λ equals to 6, 8 and 10, comprising of at least five specimens from each series with an approximate height of 0.9 m (denoted C-0.9), 1.2 m (C-1.2), and 1.5 m (C-1.5) respectively.

The soil sample was sun – dried, ground and passed through 4.75 mm sieve prior to production of test specimens. Dry mixing of soil with 10% cement (by mass of dry soil) was carried out before mixing with an optimum quantity of water equals to 19% (corresponding to 10% cement content; see Fig. 3.2). Further, a rapid moisture meter test was performed prior to adding optimum water to every freshly prepared soil-cement mix in order to maintain optimum water content of the mix. The mass of the mix and compaction on each layer was controlled, through prior experimentation, to provide compaction energy close to the equivalent of standard Proctor effort in order to achieve the required density. The compaction energy/effort was calculated using Equation 3.1. The inner walls of the mould were covered/pasted with either thin polythene or sellotape to avoid adhesion of test specimen with the mould walls. The wetted mix was then poured into a mould and compacted into 100 mm thick layers (approximately). This process was continued until the desired height was reached.

After about 30 minutes of casting, the test specimens were removed from the mould. Prior to wet curing the specimens were left for a night in an ambient laboratory condition (temperature of 27 ºC – 35 ºC and relative humidity of 70% – 80%) soon after removal from the mould. The specimens were then shifted to tray containing water of 50 mm depth (to allow capillary action), covered with wet gunny cloths, and wrapped with polythene to prevent loss of moisture. Wetting of gunny cloths and spraying of water on the specimens were done at regular interval of about 8 hours. After 28 days, curing was discontinued and the specimens were removed from the tray and allowed to dry in ambient laboratory conditions for 4 weeks as commonly practiced (e.g. Maniatidis and Walker, 2008; Reddy and Kumar, 2011) such that no further weight loss (through evaporation etc.) is observed and to ensure uniform distribution of moisture along the height of column, prior to testing.

4.2.4 Testing of specimens

Prior to testing of prisms, cylinders and columns, a thin capping layer of lean cement-mortar (cement: sand = 1:10 nominal mix) of 2-3 mm was used for capping surfaces, in order to have a level surface for uniform distribution of stresses. A 20 mm thick mild steel capping plate was placed on top of each specimen prior to loading. Based on trial and error, an optimum-loading rate of 2.5 kN/min was arrived at to give reasonably reliable results, without excessively increasing testing time. Universal Testing Machine (UTM) of 400 kN capacity was used to test prisms, cylinders and shorter columns of 0.9 m height. Test setup for longer columns of 1.2 m and 1.5 m heights is shown in Figs. 4.3a, b and c. Lateral restraint at both the ends of column was obtained by providing 20 mm thick mild steel plates. In addition, the lateral movement at the top of the column in the direction perpendicular to the plane was constrained by the loading system. The vertical load was applied using a 500 kN motorized hydraulic jack suspended from a stiff steel frame and a 250 kN load cell placed in between the loading arm of the jack and the articulated plate, was used to measure the applied loads on columns.

Lateral movement of each column was recorded at every 10 kN loading interval using digital dial gauges. Six digital dial gauges – two at the top, two in the middle, and two at the bottom were fixed at right angles in each of the square and circular columns

(Fig. 4.3). However, knowing the preferential direction of deformation (perpendicular to minor axis) of rectangular columns, only three digital dial gauges were fixed as shown in Fig. 4.3b. In addition, a digital dial gauge was fixed on top of each column, to monitor the vertical movement under incrementally increasing loads. As collapse was difficult to predict, some instruments were removed as a measure of precaution before reaching the P_u. One representative sample from each of the three locations (i.e., top, middle and bottom) of the failed column at which the measurement was taken were collected immediately in a beaker to determine the moisture content and density at the time of testing by drying at 110°C in an oven for 24 h. Test results are shown in Tables 4.3 and 4.4.

4.3 Results and discussion

4.3.1 Strength and failure pattern of prisms and cylinders

Test results are summarized in Table 4.3. The following points were observed from the test results:

1. The average compressive strength of prism is found to be ~5.30 MPa with an average density of 1820 kg/m^3 and an average moisture content of 5.01% at the time of testing. On the other hand, the average compressive strength of cylinder is seen to be ~4.60 MPa with an average density of 1810 kg/m^3 and an average moisture content of 4.87% at the time of testing.
2. The stress – strain relationships are linear initially followed by non–linear portion until peak stress value. A considerable deformation can be seen beyond the peak stress. This may be due to the presence of cement in the soil mix, which contributes to the strength and control the deformation of specimens under compression as discussed in sub-section 3.3.4 of Chapter 3.
3. Fig. 4.4 shows a typical stress-strain curve for prism and cylinder. The initial tangent modulus (ITM) for both prism and cylinder is determined to be about 2 GPa and the complete failure of prism and cylinder occurs at the strain value of about 0.034 and 0.017 respectively.

4.3.2 Failure patterns of column

Post-ultimate load failure patterns of test specimens of columns and prism are shown

in Fig. 4.5. Initially i.e. initiation of some lateral deformation of the columns (not prism) could be observed at pre-ultimate load (more discussion on lateral deformation in Section 4.3.3), suggesting buckling of the columns, however at the time of failure splitting and shear cracks are observed. The formation of shear wedge is distinctly visible at the support end along with vertically split long cracks at the middle portion (except for prism where the middle portion is too small as compared to the height of the shear wedge (Figs. 4.6a and b). Fig. 4.7a shows the onset of cracks at the support end of circular columns. Figs. 3.7b and c show the progressive spalling of loosened/fractured material surrounding the top shear wedge of circular columns. The shear wedge is shown in Fig. 4.7d, while the remaining portion of the column after the removal of the top shear wedge is shown in Fig. 4.7e. Based on the test observations typical failure mechanism of the columns is presented in Fig. 4.8. Failure of column can be divided into three zones i.e., shear failure dominated zones at top and bottom, and tension dominated failure zone at the middle. Nearly 65° - 75° (with respect to the flat horizontal surface) shearing cracks/surfaces begin to appear at 60 - 70% of P_u resulting in pyramidal shear wedges at both the ends, although the visible appearance of the shear wedge occurred earlier at the support end in comparison to the loaded end. The appearance of the shear wedge was consistent with the platen effect where the platen surface offers shear resistance at the interface between steel platen and the contacted specimen surfaces. On the other hand, tension dominates the middle portion of the column and due to this force acting outward perpendicular to the axis of column, led to splitting of the column into two halves. It was also observed that the split failure of the middle portion was progressively enhanced by the ‘axe action’ of the shear wedges. However, in case of circular columns the normal tension in conjunction with the ‘axe action’ of the shear wedge let to equally inclined (~ 120°) splitting vertical cracks. Visual/touch examination of the fractured surfaces in the middle and ends showed relatively rougher and smoother respectively, i.e., showing characteristics of mode I (i.e. tensile/opening) and mode II (shear) failure / fracture mechanisms. Similar failure patterns i.e. split and shear wedge types are also reported by Ciancio and Gibbings (2012), for the tests on CRSE prisms. Ideally, as demonstrated by Ciancio and Gibbings (2012), shear wedge failure/zone could be

avoided if low/negligible friction inducing materials such as Teflon mats are placed in between the specimen and the platens.

4.3.3 Load-deformation response of column

Figs. 4.9, 4.10 and 4.11 show lateral deformation (δ_l) of columns of heights 1.5 m, 1.2 m and 0.9 m (i.e. S, R1 and R2 columns with heights of 1.5, 1.2 and 0.9 m) respectively, at various stages of loading and with corresponding values of P_u (ultimate load) being marked. As expected, maximum lateral deformation occurred at the mid-height of the column and these profiles are typical of the column responses up to the last available measurement. It may be noted that load vs. deformation curves are plotted up to some pre-ultimate loads (e.g. up to ~ 60 kN for square/rectangular sections, and up to ~40 kN for circular columns). After reaching those loads, dial gauges were removed as a measure of precautions against the approaching nearly sudden failures. However, continuous load values beyond the ultimate load are monitored through the load cell (even after the removal of dial gauges). It was observed that the lateral deformations are in the range of 0.6 – 2.3 mm, 0.3 – 1 mm and 0.2 – 0.8 mm for the column series S-1.5, S-1.2 and S-0.9 respectively, at the corresponding loads of 10 to 60 kN. Similarly, corresponding values of lateral deformations for R1-1.5, R1-1.2 and R1-0.9 columns are 0.4–2.1 mm, 0.2–0.8 mm and 0.12–0.6 mm; and for R2-1.5, R2-1.2 and R2-0.9 columns are 0.34–2.0 mm, 0.15 –0.7 mm and 0.1–0.5 mm respectively. In circular columns, lateral deformations were in the range of 0.4 – 1.6 mm, 0.6 – 2.8 mm and 0.8 – 4.2 mm for the column series C-0.9, C-1.5, and C-1.2 respectively, at the corresponding load of 10 to 40 kN (Fig. 4.12). As the slenderness ratio of the column was increased from 6 to 10, the deformation increased by about 164%. Thus, it is clear that with the increasing λ the lateral deformation also increases at comparable loads.

Fig. 4.13 shows load vs. vertical deformation (P vs. δ_v) curves for square and rectangular columns. The vertical deformation for the column series S-1.5, S-1.2 and S-0.9 are in the range of 0.37 – 3.46 mm, 0.38 – 2.68 mm and 0.31 – 2.29 mm respectively, at the corresponding loads of 10 to 70 kN (as noted above, these loads correspond to pre-ultimate loads). Similarly, the corresponding values for R1-1.5, R1-1.2 and R1-0.9 columns are 0.44 – 3.46 mm, 0.35 – 2.58 mm and 0.31 – 2.09 mm;

and for R2-1.5, R2-1.2 and R2-0.9 columns are 0.4 – 3.4 mm, 0.3 – 2.5 mm and 0.3 – 2.1 mm, respectively. It can be noted that the deformation of S-type columns is comparatively higher than R1 and R2 column types at the specified loads. This may be due to lesser cross-sectional area of S-type columns as compared to R1 and R2 columns. With the increase in λ from 6 to 10 the lateral deformation increased by about 250% to 300%, and the vertical deformation increased by about 52% to 66% at a given load. This shows that the deformation of the column increases with the increase in λ values (see Table 4.3). Fig. 4.14 shows load vs. vertical-deformation curves for circular columns. It was observed that the vertical deformation increases from 2 – 3.9 mm with increasing load at about 40 kN. As λ was increased from 6 to 10 the vertical deformation also increased by about 95%. Thus, it is clear that with increasing λ the vertical deformation also increases at a given load.

4.3.4 Moisture content and density of column

Moisture content and density play a vital role in gaining strength and durability of rammed earth structures. Bui et al., (2014) reported that, when the moisture content of rammed earth specimen is greater than 4%, the compressive strength decreases quickly for all types of soil studied, and the effect is more in clayey soil than sandy soil. However, this effect is negligible to the soil stabilised with 8% natural hydraulic lime and it was noted that the stabilisation by hydraulic lime decrease the sensitivity to water of rammed earth material. Likewise, the effect of moisture content on strength and density of test specimens is expected to be negligible in the present study due to use of sandy soil and 10% cement. However, it is important to determine the moisture variation along the height of the specimen to ascertain the exact percentage of moisture and its effect on strength and behaviour of the column specimen. Details of moisture content and density of columns during test is shown in Table 4.2. The average moisture content of the test specimens varies from 4.93% to 6.09% with a standard deviation of 0.13% to 0.23%; and the average dry density varies from 1750 kg/m^3 to 1820 kg/m^3 with a coefficient of variation 0.23% to 0.33% respectively. On the other hand, the average moisture content of circular columns varies from 4.82% to 5.40% with a corresponding standard deviation of 0.15% to 0.34%; and average dry density varies from 1800 kg/m^3 to 1820 kg/m^3 with coefficient of variation of 0.21%

to 0.46%, respectively. It can be observed that there exists a marginal variation of average dry density and average moisture content between the test specimens of the same series of column during testing.

4.3.5 Effect of aspect ratio (Φ)

The value of P_u decreases linearly (R^2 = 0.99) with the increase in λ and increases linearly (R^2 = 0.99) with the increase in Φ values as shown in Figs. 4.15a and b respectively, for the range of λ (6 -10) and Φ (1-1.53) considered. It is interesting to note that like any column strength profile, the plot of P_u is likely to get flattened / asymptotic with increasing value of λ. However, the variation of P_u is likely to increase with increasing Φ values (keeping d constant at 150 mm), because the gross cross-sectional area increases with a. It was observed that when the aspect ratio is increased from 1.0 to 1.27 and 1.53, the P_u of column increased by about 20% and 40.5% respectively, for λ = 6, 8 and 10 of all the column sets. The increase in P_u for increasing values of Φ agrees with the increase in cross-sectional area, however, the load-capacity decreases with the increase in λ irrespective of any values of Φ. This confirms that besides λ, Φ also significantly influences the values of P_u of columns.

4.3.6 Strength and design of column

The values of P_u of square and rectangular columns range from 81 kN - 135.6 kN as shown in Table 4.3. It is observed that R2 columns possess higher values of P_u than R1 and S columns. In general, P_u of columns decreases with increasing values of λ. The value of P_u declined by about 9% to 19% when λ is increased from 6 to 10. The values of capacity reduction factor, k (where $k = P_u / P_{u6}$; P_{u6} = ultimate load corresponding to λ value of 6) (NZS 4297, 1998; AS HB 195, 2002; IS 1905, 2002) at λ equal to 8 and 10 are determined to be 0.92 and 0.84 respectively. The P_u of circular columns range from 55.1 - 67.2 kN (Table 4.4). It was observed that P_u declined by about 10% to 18% when λ was increased from 6 to 10. The values of k for λ equal to 8 and 10 was determined to be 0.90 and 0.82 respectively as shown in Table 4.5.

The ultimate strength (σ_u) of CSRE column was determined using Engesser's tangent modulus theory as discussed by Bleich (1952), as done in the case of brick masonry (e.g. Sahlin, 1971) and CSRE walls (e.g. Reddy and Kumar, 2011). For comparison of

test results obtained from experimentation and tangent modulus theory, the following formula was used to compute the buckling strength (σ_{cr}) Bleich (1952):

$$\sigma_{cr} = \frac{P_{cr}}{A} = \frac{\pi^2 E_t}{(l/r)^2} \tag{4.1}$$

where P_{cr} = buckling load (N); E_t = tangent modulus at failure/ultimate stress, (MPa); l/r = slenderness ratio; l = effective height of the column (mm); r = radius of gyration = $\sqrt{(I/A)}$ (mm); and I = moment of inertia (mm^4). Values of E_t were estimated from the stress-strain curve of prism as shown in Fig. 4.4 (see Tables 4.3 and 4.4). It can be observed that the values of E_t and σ_{cr} range from 155 to 375 MPa and 2.2 to 4.8 MPa respectively. In case of circular columns, the values of E_t and σ_{cr} range from 283 to 370 MPa and 2.3 to 4.9 MPa respectively. The effect of λ on σ_u of column is shown in Figs. 4.16, 4.17 and 4.18.

Experimental variations of ultimate / buckling stress (σ_u) with λ (6-10) for S, R1 and R2 columns are shown in Fig. 4.16. It can be seen that the experimental variation of σ_u with λ is nearly linear and decreases with increasing values of λ (6 – 10). Further, there is an increase in σ_u values of ~ 8% as the cross-sections changes from R2 to R1 and R1 to S. It is interesting to note that although the values of P_u are of the order S < R1 < R2 (see Fig. 4.15), the values of σ_u are of the opposite trend i.e. values for S > R1 > R2 (Fig. 4.16). The higher values of σ_u associated with cross-sections having lower aspect ratio may possibly be due to the preference or tendency for higher cross-sectional slenderness (or higher cross sectional aspect ratio) to buckle at lower stress levels (as in plate buckling where the buckling stress is inversely proportional to width/thickness ratio (Bleich, 1952)). Comparison of experimental and those predicted by Engesser's tangent modulus theory (Bleich, 1952) are shown in Figs. 4.17a,b and c, respectively for S, R1 and R2 columns. It can be seen from Fig. 4.17 that as the cross-sectional aspect ratio increases (S to R1 and R2) the values of σ_u gets increased, in contrast to the experimental observations (see Fig. 4.16), and as such the theoretical predictions changes from under predictions (S and R1) to over prediction at higher cross-sectional aspect ratio (for lower λ value of 6). This is may be related to increasing values of tangent modulus associated with decreasing values of experimental σ_u (see Fig. 4.4 and Eqn.4.1). It may further be noted that in the work of

Reddy and Kumar (2011), it was reported that tangent modulus theory predicted very high values of σ_u for λ < ~68.38, which is in contrast to the present work. This may be because in their work, the experimental σ_u obtained at lower value of λ (e.g. 2) appears to be higher than that of the referral prism (150 mm x 150 mm x 150 mm) strength, which is in contrast to the common understanding of increasing strength with lower λ. Fig. 4.18 shows a similar comparison of σ_u between experimental and those predicted by tangent modulus theory for circular column. Again, the behaviour is similar to that of R2 column (see Fig. 4.17c). Predicted higher values of σ_u at lower values of λ can again be attributed to the improved experimental strength at shorter column height.

Thus it can be seen that the predictions made by tangent modulus theory are sensitive (for the ranges of λ considered) to the stress level at which the tangents are considered i.e. it can lead to under predictions when the experimental ultimate stress is high and closure to the peak stress of the referral characteristic stress strain curve and vice-versa, however the decreasing pattern of σ_u with increasing values of λ is well captured. However, it needs to be noted that as the λ increasing sufficiently, it is expected that both the experimental and predicted values should merge asymptotically, as at higher values of λ, the behaviour of the columns should tend to respond elastically.

4.3.7 Comparison of capacity reduction factors (*k*)

Table 4.5 shows the comparison of experimental *k* values with published values for structural masonry. The values of *k* obtained from the current investigation tend to differ from the values outlined in structural masonry standards. Figs. 4.19 and 4.20 show the comparison of experimental and codal values of *k*, in terms of P_{ur} and λ (where $P_{ur} = P_u \times k$). The values outlined in earthen standards such as NZS 4297 (1998) and AS HB 195 (2002), and masonry standard IS 1905 (2002) are in a close range to the experimental values i.e., differ by about 2% - 4.5% and 3% - 5.6% respectively, for all series of columns. Whereas, the values outlined in masonry standard BS 5628 Part 1 (1992) are found to be the least conservative and about 8% - 13.8% higher than the experimental values. Now, considering the experimental variations of about ~4.0% (see standard deviation values in Table 4.3), it can be observed that the current experimental values can be thought to be in agreement with

the predictions made by earthen standards NZS 4297 (1998) and AS HB 195 (2002). However, the predictions made by BS 5628 Part 1 (1992) can be considered relatively higher even after consideration of the experimental variations. Similar trend can be seen in circular columns. The values outlined in earthen standards and masonry standard are higher by about 4.4% to 7.3% and 5.2% to 7.9%, respectively, i.e., ~7% higher, thus showing relatively un-conservative, and the values outlined in BS 5628 Part 1 (1992) are found to be the least conservative i.e., ~15% higher than the experimental values. This may be due to the improved strength (compressive as well as flexure) of brick masonry as compared to that of CSRE. Hence, the rate of drop of strength (σ_u) with λ is likely to be higher than that of CSRE, thereby predicting a higher value of σ_u. However, further studies may be required to reconfirm the validity of these codes.

4.3.8 Characteristic strength of column

Eqn. 4.2 (BS 5628 Part 1, 1992) has been used to compute the characteristic compressive strength (f_k) as reported in the literature by Jayasinghe and Kamaladasa (2007) related to stabilised rammed earth. As may be seen from Eqn. 4.2, the expression for f_k is quite simple and straight forward, as it involves the product of compressive strength with a factor (i.e. 1/1.2) associated with the conversion of mean compressive strength to f_k . As mentioned by Jayasinghe and Kamaladasa (2007), the factor '1.2' comes from BS 5628 Part 1 (1992), for calculation of f_k where statistical values are not readily available (especially for stabilised rammed earth), as in the current research programme with smaller testing results.

$$f_k = \frac{F_m}{A} \times \frac{\psi_m \psi_u}{1.2} \tag{4.2}$$

where F_m = mean of the maximum loads carried by the two test panels (mean values of five specimens are considered in the present study); A = cross-sectional area of each column; Ψ_m = reduction factor for strength of mortar; and Ψ_u = unit reduction factor for sample structural strength. The value of Ψ_m is taken as 1.0 since there is no mortar joint and Ψ_u is taken from Table 4.5, and the average compressive strength is taken from Tables 4.3 and 4.4 for the respective columns. The values of f_k are shown in Table 4.6. Jayasinghe and Kamaladasa (2007) stated that the vertical stress due to self-weight of the walls and the portion of the roof supported is usually in the range of

0.1 MPa for a single storey construction. Using a factor of safety for dead loads (γ_f) equal to 1.4 and, material strength variations and workmanship factors (γ_m) equal to 3.5 as recommended in BS 5628 Part 1 (1992), the characteristic column strength is determined to be about 0.5 MPa. Hence, the overall factor of safety is equal to 5, which is at par with NZS 4297 (1998). In the present study, factor of safety ranges between 21.3 to 36 and these values are much higher than the value of 5 that is usually used. Furthermore, Jayasinghe (1999) showed that in a two storey load-bearing houses for small and carefully planned layouts, the maximum design strengths required can be maintained within 0.8 and 1.0 MPa when the ground floor wall widths are about 250 mm. Thus, it can be observed that the characteristic strength obtained for CSRE column yields relatively higher safety factor indicating a possibility of using CSRE columns for load-bearing houses.

4.4 Summary and conclusions

This chapter deals with a detailed study on the load-capacity of unreinforced CSRE columns under axial compression. Tests on CSRE cylinders, prisms and columns of circular, square and rectangular cross-sections were performed. The effects of concentric axial loading, slenderness ratio (λ) and aspect ratio; moisture effect and stress reduction factors were assessed. A comparative study was made between the ultimate compressive strength (σ_u) of columns determined using tangent modulus theory and experimental values. Furthermore, the validity of using masonry design rules for the design of CSRE columns was evaluated. Lastly, the safety factors of columns were determined to assess the possibility of constructing a single storey load bearing houses. From the test results the following conclusions have been drawn:

1. Lateral and vertical deformation increases with increasing value of λ. Typically, columns tested failed by formation of vertical cracks initially at the platen-column interface followed by shearing and splitting at the later stages of loading. Shear dominates near the platen ends and shearing cracks typically occurred at nearly 65° - 75° angle and at 60% - 70% of P_u, and thus forming a shear wedge. At the same time, tension dominates in the middle of the column and due to this force acting outward perpendicular to the axis of column led to splitting of the column into two halves. Similar type of failure can be observed

in case of circular columns except the formation of equally inclined (~ 120°) splitting vertical cracks due to 'axe action' of the shear wedge.

2. Predictions made by tangent modulus theory are sensitive (for the ranges of λ considered) to the stress level at which the tangents are considered i.e. it can lead to under predictions when the experimental ultimate stress is high and closure to the peak stress of the referral characteristic stress strain curve and vice-versa, however the decreasing pattern of σ_u with increasing values of λ is well captured. The values of k at λ equal to 8 and 10 were determined to be 0.92 and 0.84 for rectangular columns and 0.90 and 0.82 for circular columns respectively.
3. At increasing values of Φ the load-capacity, P_u of rectangular columns increases. It was observed that when Φ is increased from 1.0 to 1.27 and 1.53, the P_u of column increased by about 20% and 40.5% respectively, for λ = 6, 8 and 10 of all the column sets. It may be noted that the increase in P_u for increasing values of Φ agrees with the increase in cross-sectional area.
4. The k values outlined in earthen standards such as NZS 4297 (1998) and AS HB 195 (2002), and masonry standard IS 1905 (2002) are in a close range to the experimental values by about ~4.0% at λ equal to 8 - 10. However, in case of circular columns, the codal values are higher by about ~7%, thus showing relatively un-conservative.
5. The characteristic strength obtained for CSRE column yields relatively higher factor of safety ranging from 21 to 36. Hence, CSRE columns can be used with confidence for construction of single storey load bearing houses or even two storeys or more when designed properly.

Table 4.1. Properties of soil.

Soil property	Values
Grain size distribution:	
Sand	79%
Silt	13%
Clay	8%
Atterberg limits:	
Liquid limit	31.70%
Plastic limit	22.90%
Plasticity index	8.80%
Compaction characteristics:	
(a) Soil with 10% cement	
Optimum moisture content	19%
Maximum dry density (kg/m^3)	1710

Table 4.2. Details of moisture content and density.

	Moisture content of specimen (%)						
	Location						
Specimen	Top	Middle	Bottom	Average	Standard deviation	Average dry density (kg/m^3)	Coefficient of variation (%)
S-1-0.9	4.25	3.83	3.98	4.02	0.21	1830	0.20
S-2-0.9	4.65	5.04	5.15	4.95	0.26	1810	0.25
S-3-0.9	4.88	6.11	5.41	5.47	0.62	1800	0.58
S-4-0.9	4.72	5.52	5.13	5.12	0.40	1810	0.38
S-5-0.9	5.16	5.41	6.18	5.58	0.53	1800	0.50
S-1-1.2	4.38	5.76	5.81	5.32	0.81	1800	0.77
S-2-1.2	5.25	3.93	4.56	4.58	0.66	1820	0.63
S-3-1.2	4.25	5.93	5.56	5.25	0.88	1810	0.84
S-4-1.2	4.65	3.93	5.27	4.62	0.67	1820	0.64
S-5-1.2	5.24	4.93	4.56	4.91	0.34	1810	0.32
S-1-1.5	6.27	7.30	6.50	6.69	0.54	1780	0.51
S-2-1.5	6.41	6.79	5.45	6.22	0.69	1780	0.65
S-3-1.5	5.43	6.79	5.45	5.89	0.78	1790	0.73
S-4-1.5	6.29	5.79	4.85	5.64	0.73	1800	0.69
S-5-1.5	5.67	6.56	5.78	6.00	0.49	1790	0.46

Note: *S – square column; 1, 2, 3, 4, 5, 6 – sl. no. of column; 0.9, 1.2, 1.5 – height of column in meter.*

Table 4.3. Test results of square and rectangular columns.

Specimen series	Average ultimate load, P_u (kN) [a]	Average comp. Strength, σ_u (MPa)[a]	Standard deviation (MPa)	Average moisture content at test (%)[a]	Standard deviation (%)	Average dry density at test (kg/m^3) [a]	Coef. of variation (%)	Average lateral deformation at 60 kN load at mid-height (mm) [a]	Standard deviation (mm)	Aspect ratio (a/d)	Height to thickness ratio (λ)	Slenderness ratio (l/r)	Tangent modulus at a stress level of ultimate strength, E_t (MPa)	σ_{cr} (MPa)[b]
Prism	119.3	5.30	0.29	5.01	0.06	1820	0.25	-	-	1	2	-	-	-
S-0.9	96.5	4.29	0.14	5.03	0.17	1810	0.27	0.8	0.28	1	6	20.8	155	3.5
S-1.2	88.4	3.93	0.13	4.93	0.21	1810	0.33	1.0	0.37	1	8	27.7	208	2.7
S-1.5	81.0	3.60	0.26	6.09	0.13	1800	0.23	2.3	0.26	1	10	34.6	272	2.2
R1-0.9	116.9	4.10	0.28	5.05	0.15	1810	0.25	0.6	0.19	1.26	6	20.8	161	3.7
R1-1.2	107.4	3.77	0.19	5.36	0.23	1790	0.32	0.8	0.22	1.26	8	27.7	222	2.9
R1-1.5	96.0	3.37	0.23	4.68	0.20	1810	0.27	2.1	0.25	1.26	10	34.6	340	2.8
R2-0.9	135.6	3.93	0.25	4.99	0.18	1750	0.29	0.5	0.23	1.53	6	20.8	210	4.8
R2-1.2	124.5	3.61	0.18	6.06	0.24	1780	0.31	0.7	0.18	1.53	8	27.7	276	3.6
R2-1.5	114.2	3.31	0.20	5.62	0.23	1800	0.28	2.0	0.20	1.53	10	34.6	357	2.9

[a] *Average of five specimens tested.*

[b] *Critical buckling stress based on tangent modulus theory.*

Table 4.4. Summary of test results of circular columns.

Specimen series	Average ultimate load, P_u (kN) [a]	Average compressive strength (MPa) [a]	Standard deviation (MPa)	Average moisture content at test (%) [a]	Standard deviation (%)	Average dry density at test (kg/m^3) [a]	Coef. variation (%)	Average lateral deformation at 40 kN load at mid-height (mm) [a]	Standard deviation (mm)	Height to thickness ratio (λ)	Slenderness ratio (l/r)	Tangent modulus at a stress level of ultimate strength, E_t (MPa)	σ_{cr} (MPa)[b]
Cylinder	81.3	4.60	0.31	4.87	0.23	1820	0.23	-	-	2	-	-	-
C-0.9	67.2	3.80	0.11	5.40	0.34	1810	0.21	1.5	0.31	6	24	283	4.9
C-1.2	60.4	3.42	0.23	5.26	0.27	1800	0.46	2.7	0.27	8	32	345	3.3
C-1.5	55.1	3.12	0.27	4.82	0.15	1810	0.34	4.1	0.34	10	40	370	2.3

[a]*Average of five specimens tested.*

[b]*Critical buckling stress based on tangent modulus theory.*

Note: *C – circular column; 0.9, 1.2, 1.5 – height of column in meter.*

Table 4.5. Comparison of experimental and published capacity reduction factors (k).

		Capacity reduction factor (k) for slenderness ratio (λ)				
Column series	Slenderness ratio, λ	Experimental	NZS 4297-1998	IS 1905-2002	AS HB 195-2002	BS 5628-1:1992
S-0.9	6	1	1	1	1	1
S-1.2	8	0.92	0.94	0.95	0.94	1
S-1.5	10	0.84	0.88	0.89	0.88	0.97
R1-0.9	6	1	1	1	1	1
R1-1.2	8	0.92	0.94	0.95	0.94	1
R1-1.5	10	0.84	0.88	0.89	0.88	0.97
R2-0.9	6	1	1	1	1	1
R2-1.2	8	0.92	0.94	0.95	0.94	1
R2-1.5	10	0.84	0.88	0.89	0.88	0.97
C-0.9	6	1	1	1	1	1
C-1.2	8	0.90	0.94	0.95	0.94	1
C-1.5	10	0.82	0.88	0.89	0.88	0.97

Table 4.6. Characteristic strength (f_k) and factor of safety.

Column series	F_m/A	f_k	Factor of safety
S-0.9	4.29	3.58	35.8
S-1.2	3.93	3.01	30.1
S-1.5	3.6	2.52	25.2
R1-0.9	4.10	3.42	34.2
R1-1.2	3.77	2.89	28.9
R1-1.5	3.37	2.36	23.6
R2-0.9	3.93	3.28	32.8
R2-1.2	3.61	2.77	27.7
R2-1.5	3.31	2.32	23.2
C-0.9	3.80	3.17	31.7
C-1.2	3.42	2.57	25.7
C-1.5	3.12	2.13	21.3

(a) Rammer (b) Wooden mould (c) Typical square column

Fig. 4.1. Equipments and typical square column.

(a) Rammer (b) Plastic mould (c) Typical circular column

Fig. 4.2. Equipments and typical circular column.

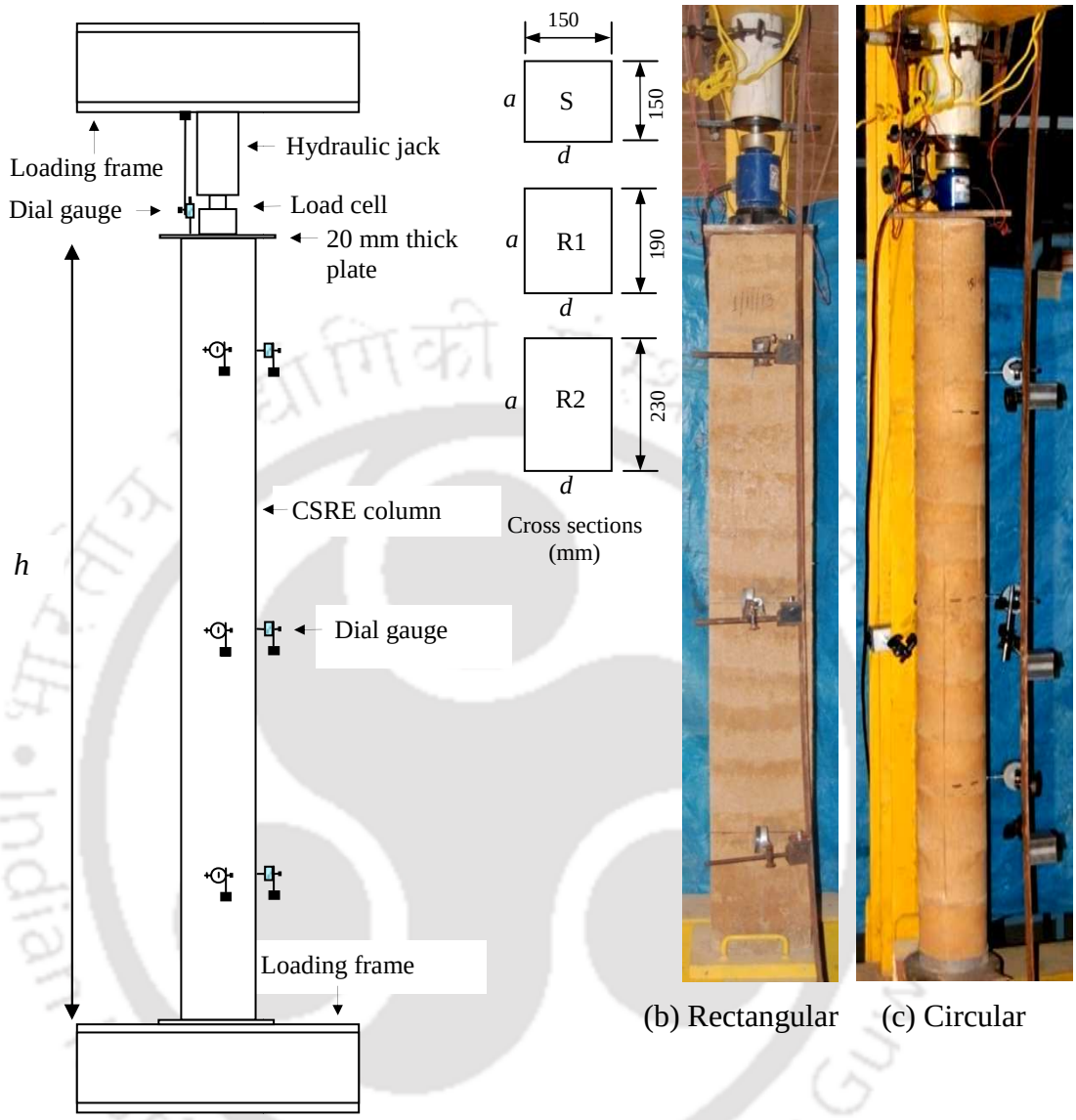

(a) Schematic diagram of test setup

(b) Rectangular (c) Circular

Fig. 4.3. Test setup.

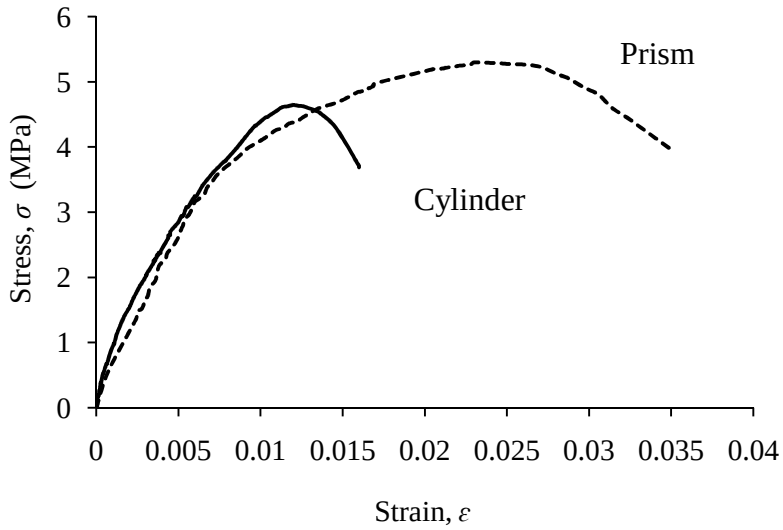

Fig. 4.4. Typical stress-strain curve for prism and cylinder (moisture content during testing is 5.01% and 4.87% respectively).

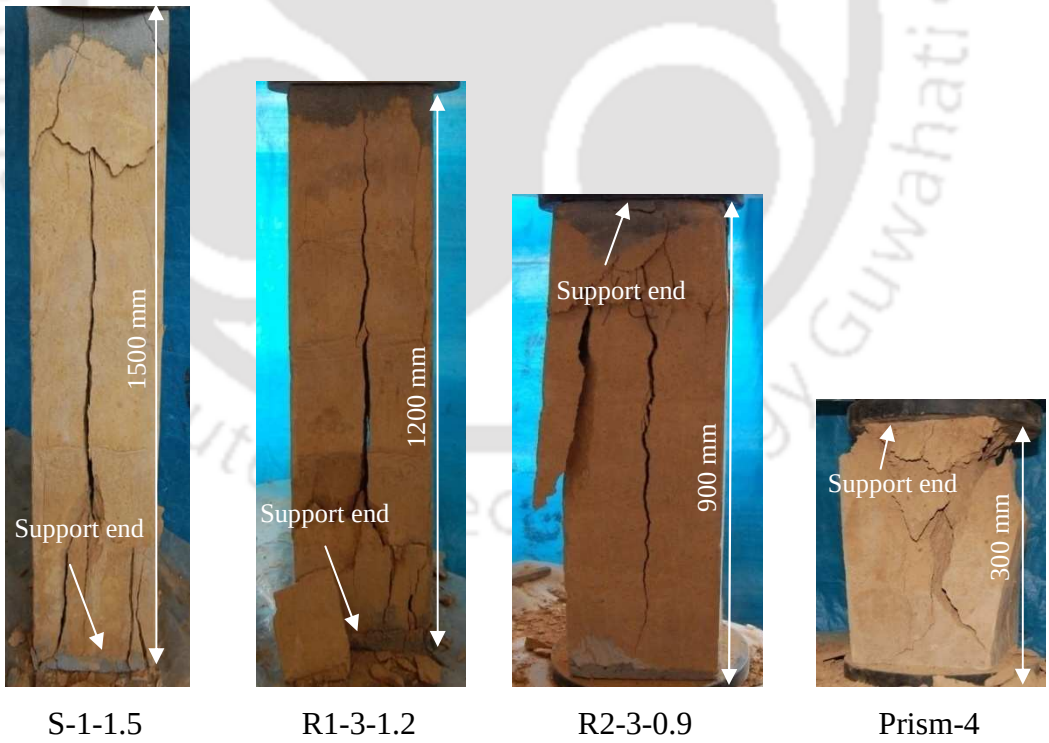

Fig. 4.5. Failure pattern of test specimens (columns and prism).

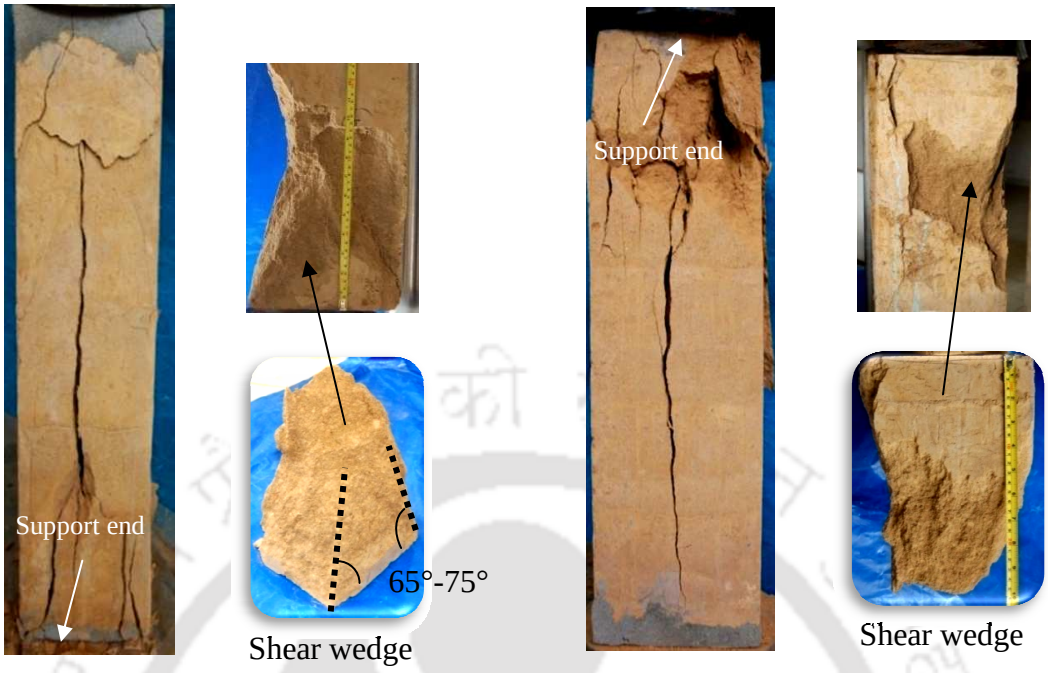

S-1-1.5 R2-1-1.2

(a) Failure of square column (b) Failure of rectangular column

Fig. 4.6. Typical failure modes of columns.

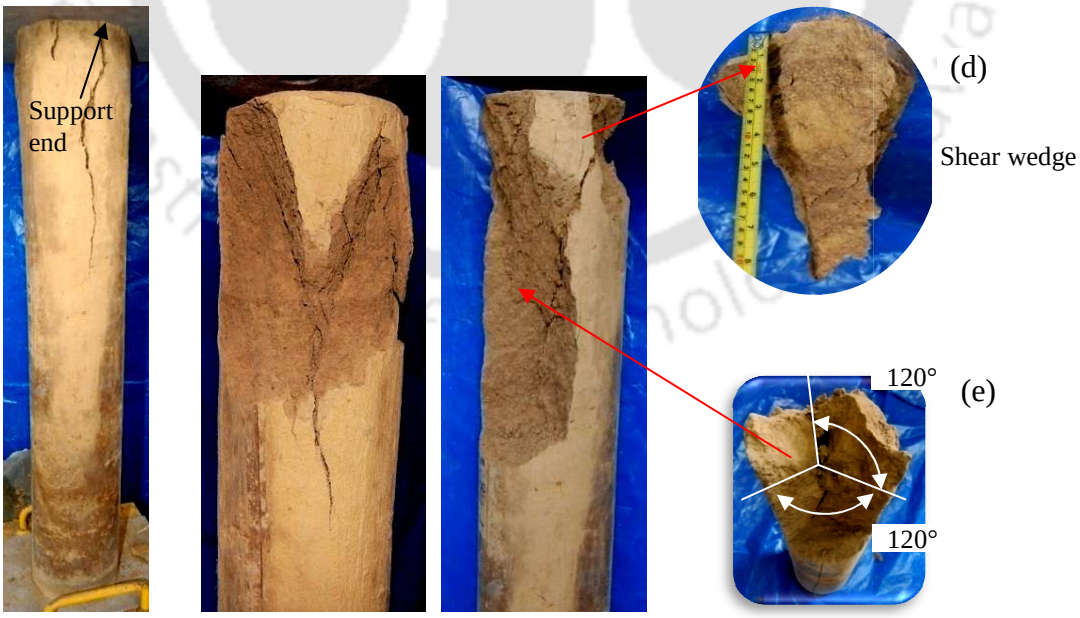

(a) (b) (c)

Fig. 4.7. Failure pattern of circular column (C-3-1.2).

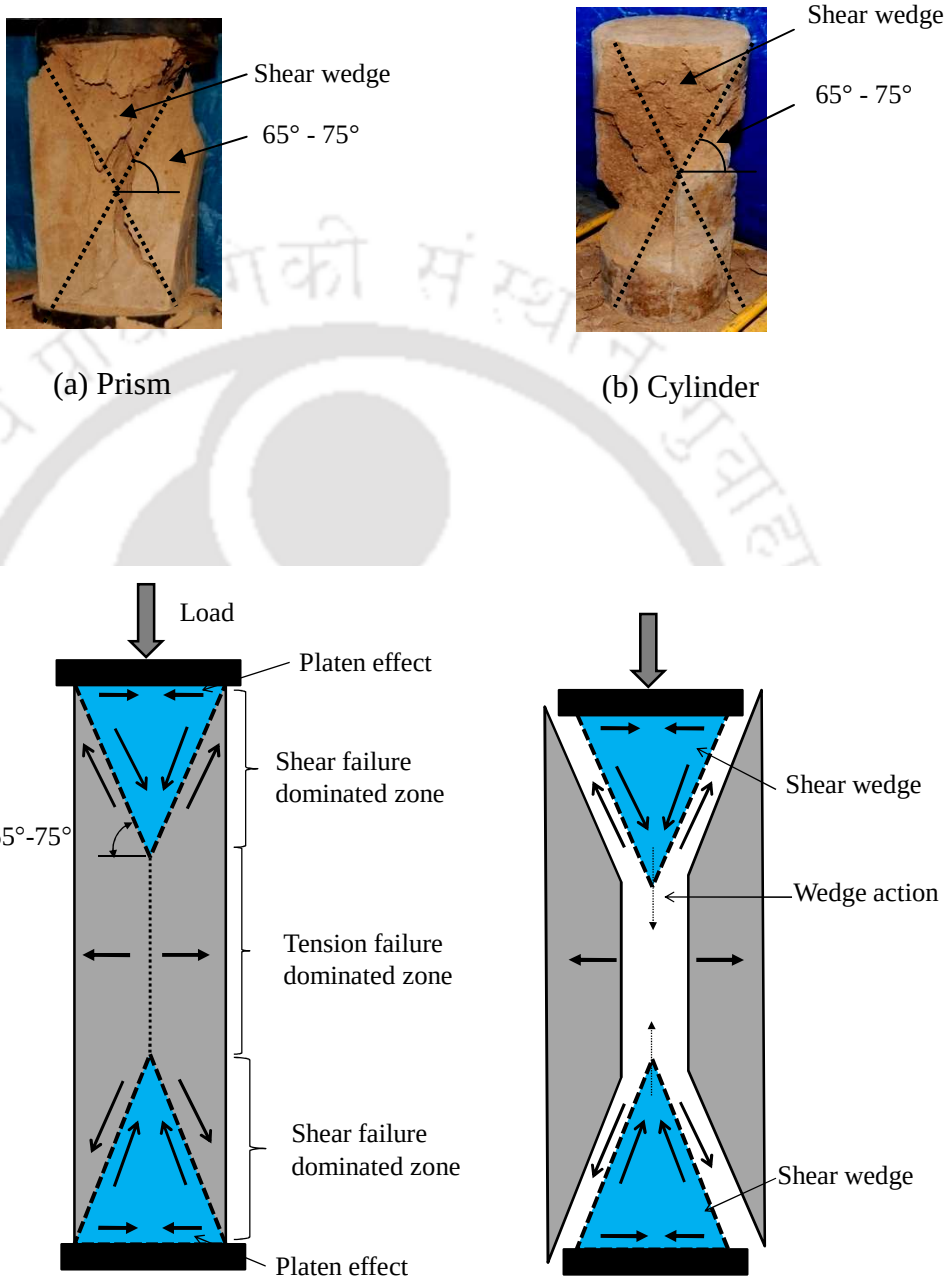

(a) Prism (b) Cylinder

(c) Details of failure mechanism

Fig. 4.8. Typical failure mechanism of prism, cylinder and column.

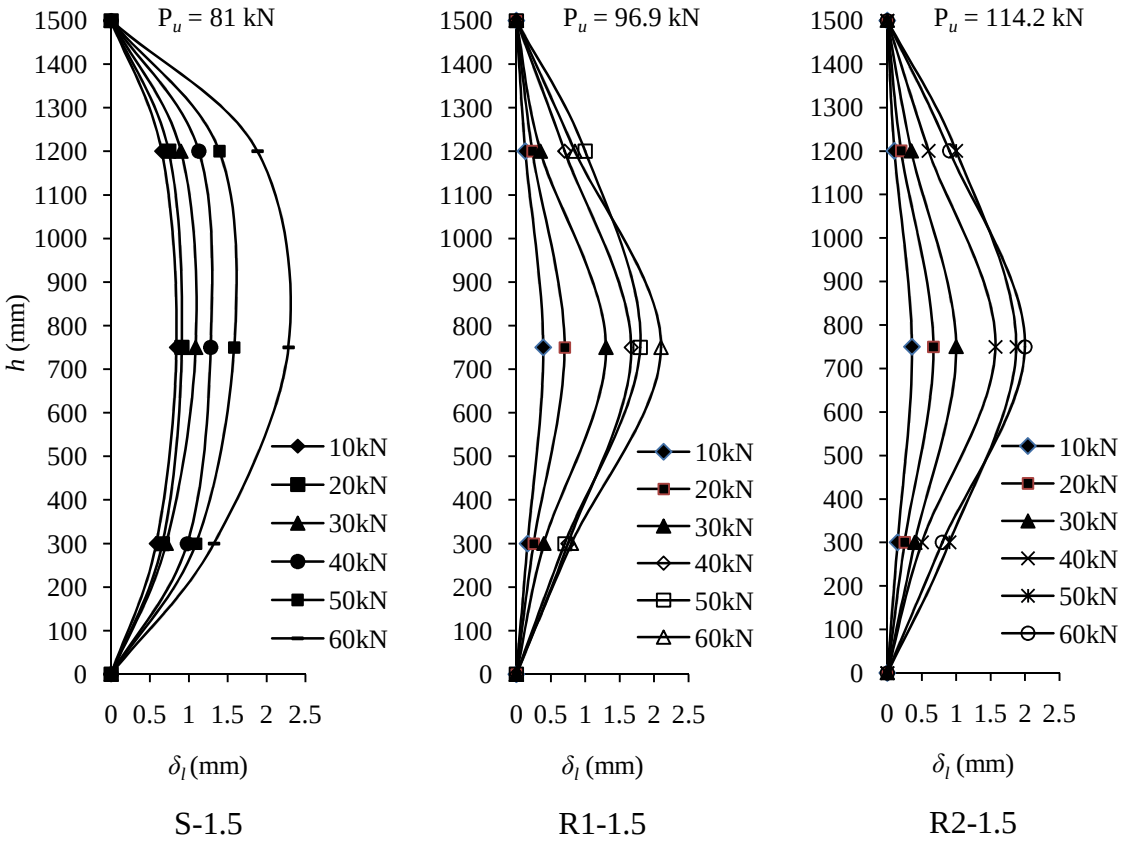

Fig. 4.9. Lateral deformation of 1.5 m high column at various stages of loading.

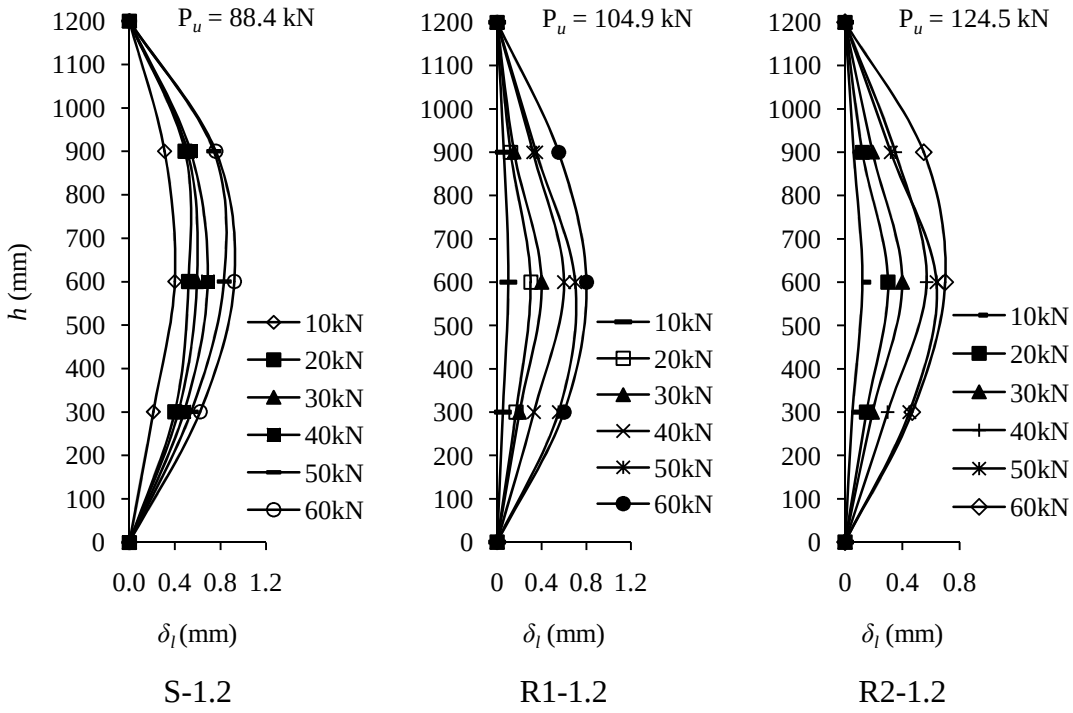

Fig. 4.10. Lateral deformation of 1.2 m high column at various stages of loading.

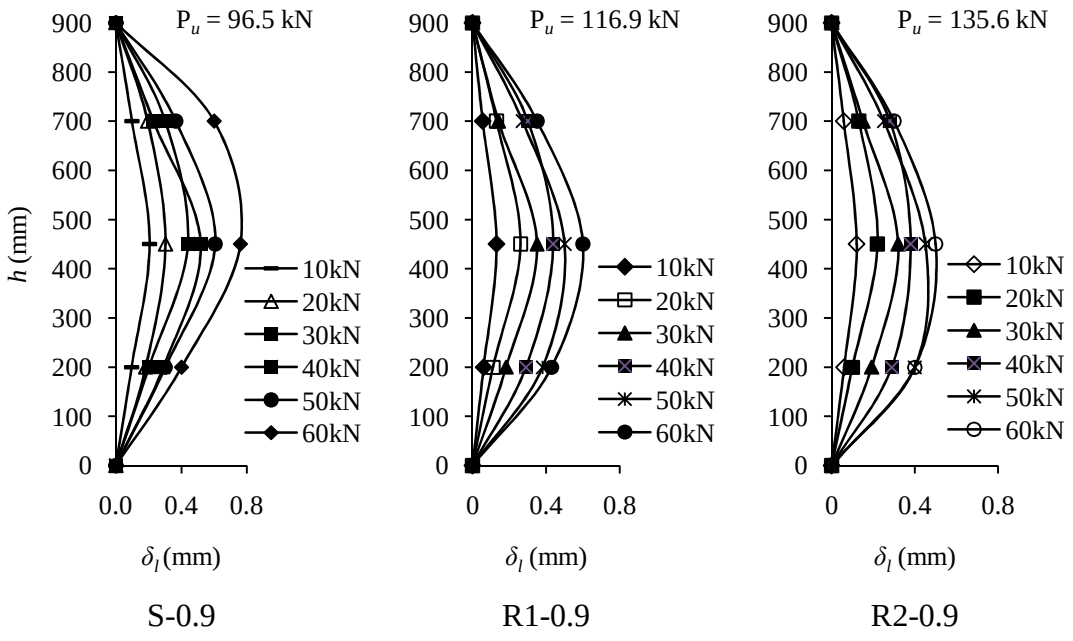

Fig. 4.11. Lateral deformation of 0.9 m high column at various stages of loading.

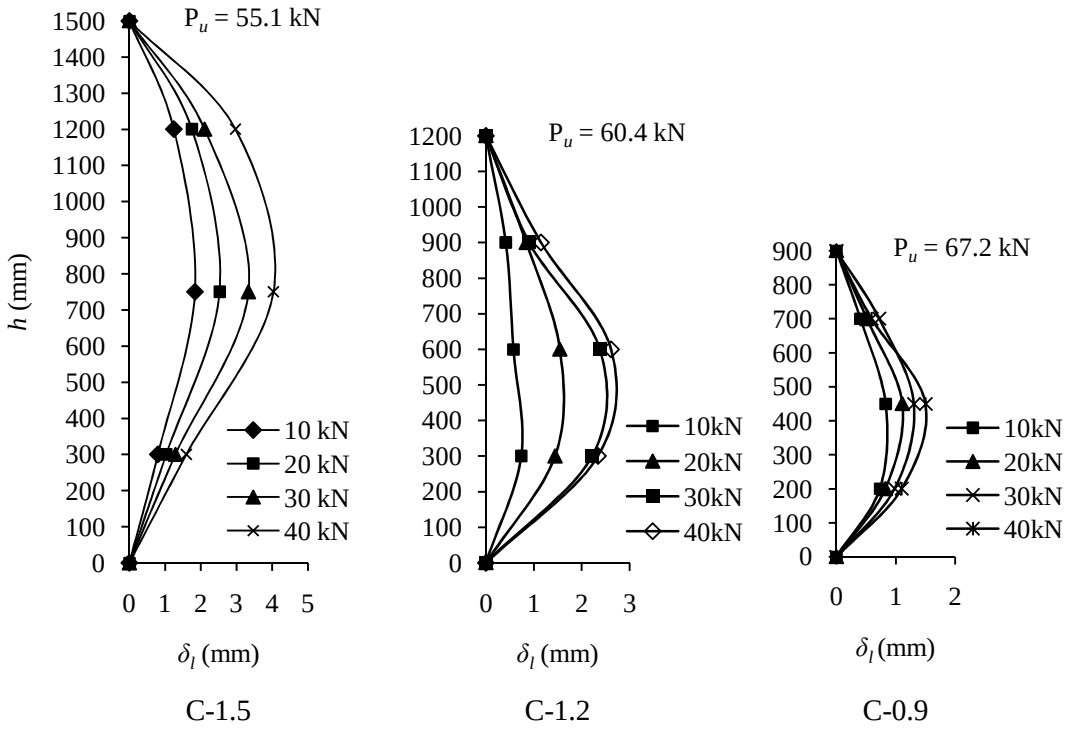

Fig. 4.12. Lateral deformation of circular columns at various stages of loading.

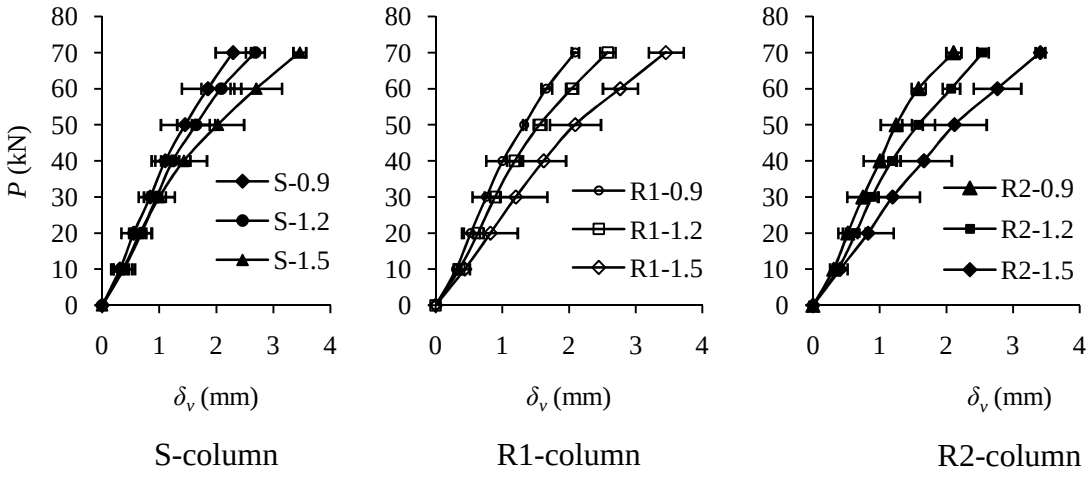

Fig. 4.13. Load-vertical deformation curves of square and rectangular columns.

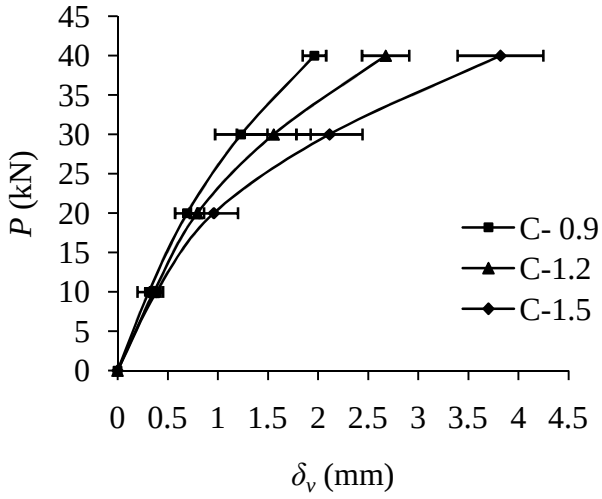

C-column

Fig. 4.14. Load-vertical deformation curves of circular columns.

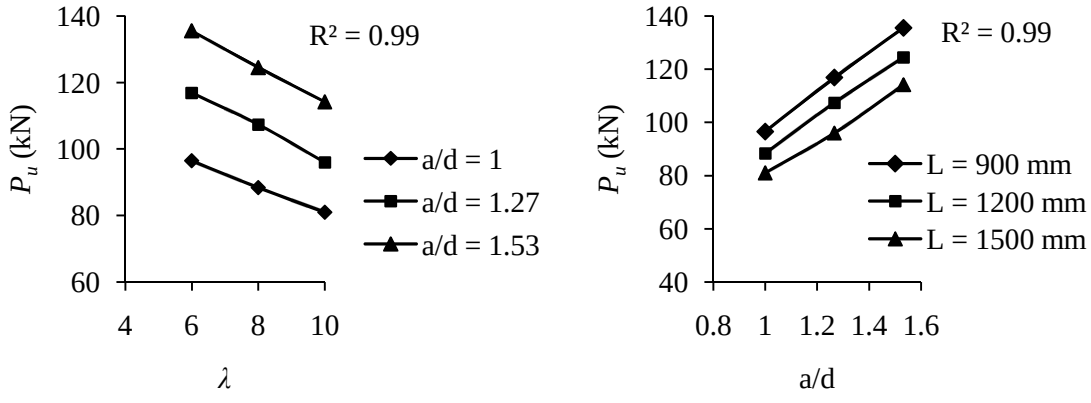

(a) (b)

Fig. 4.15. Effect of aspect ratio on load-capacity.

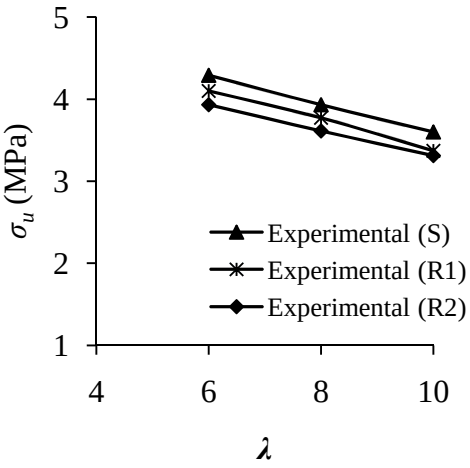

Fig. 4.16. Effect of slenderness ratio on strength of columns.

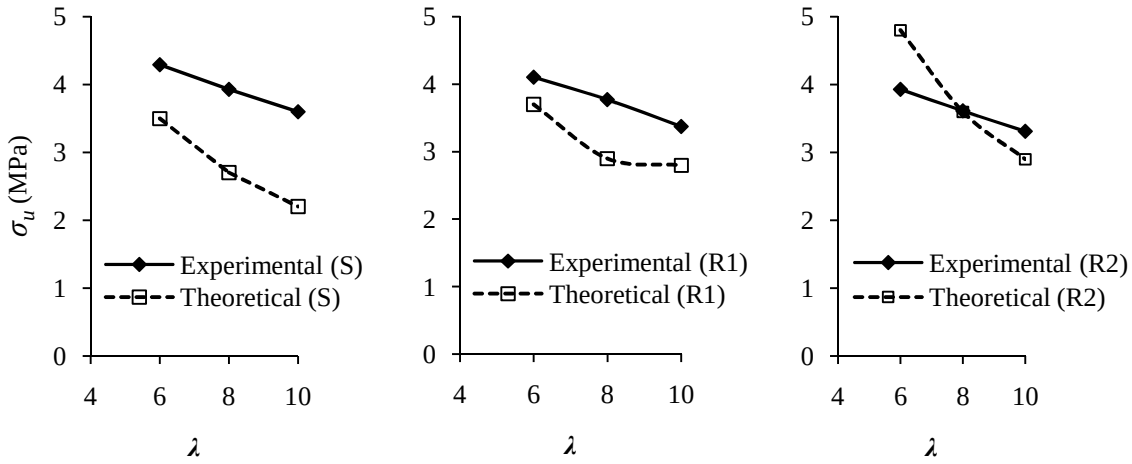

(a) S-column (b) R1-column (c) R2-column

Fig. 4.17. Effect of slenderness ratio on compressive strength of square and rectangular columns.

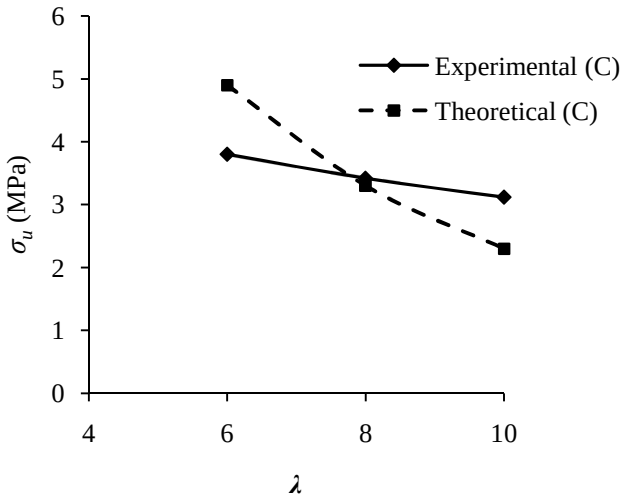

Fig. 4.18. Effect of slenderness ratio on compressive strength of circular columns.

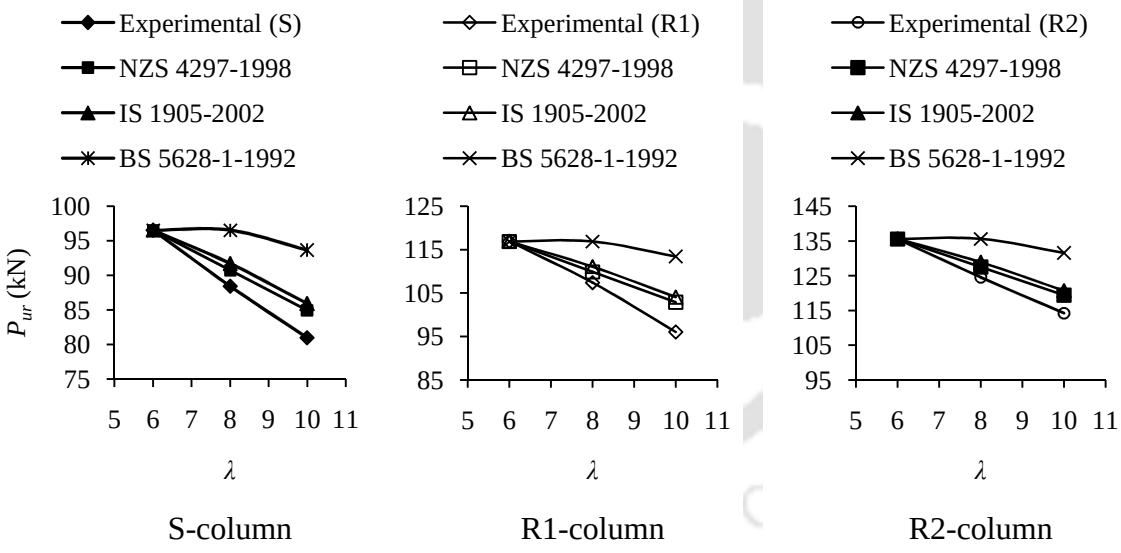

Fig. 4.19. Comparison of experimental and codal reduction factors for square and rectangular columns.

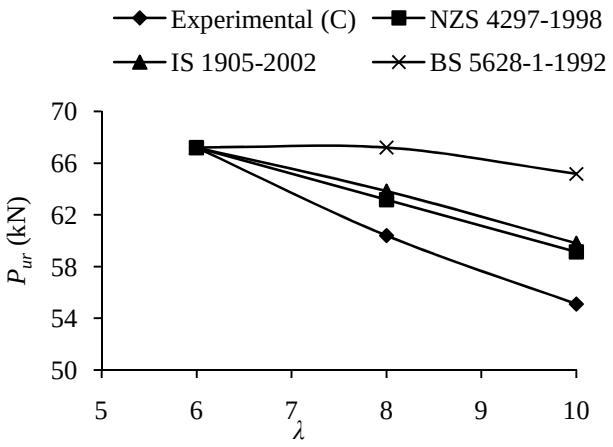

Fig. 4.20. Comparison of experimental and codal reduction factors for circular columns.

Chapter 5

Structural Behaviour of Steel Reinforced CSRE Column

This chapter presents an experimental study on the behaviour of CSRE columns reinforced with steel under concentric axial compression. Effects of structural parameters such as lateral reinforcement ratio, total reinforcement ratio etc., on the failure pattern; load-lateral deformation and load-axial deformation of columns were studied.

5.1 Introduction

In the previous chapter (Chapter 4), the structural behaviour of 'unreinforced' CSRE columns of square, rectangular and circular cross-sections have been presented, with a focus on the cross-sectional effects and slenderness ratios on column strength. As the requirement for improved structural behaviour (e.g. strength, deformation capacities) is expected by modern building professionals, with an intention to use rammed earth materials in a more challenging and innovative ways such as construction of structural elements like columns, walls, beams, lintels etc. (Maniatidis and Walker, 2008), it has become increasingly important to investigate on reinforced CSRE structural elements. As highlighted in the literature review (Chapter 2), in the recent past steel have been introduced as reinforcing materials in order to attain higher strength of rammed earth elements for innovative applications. It has been observed that rammed earth beams reinforced with steel (Gaind and Char, 1983), improves the load carrying capacity by about 383% to 570% and flexibility of the soil beams substantially. Bond property of steel bars (12 mm diameter) embedded in rammed earth (Walker and Dobson, 2001), gave a reasonable bond force of 1.08 to 19.52 kN useful for rammed earth constructions. Rammed earth columns made of diagonal ties carry significantly higher load of about 167% more than the column with horizontal ties (Gupta, 2014). Thus, it is seen that strength of CSRE elements are considerably improved when reinforced with steel. However to the best of author's knowledge, no detailed studies could be found on use of steel as reinforcing materials in CSRE compression members like columns under axial loading, considering the effects of important

structural parameters such as lateral reinforcement ratio, total reinforcement ratio etc., on load-capacity, deformation, failure patterns etc. Hence, in the present chapter an attempt has been made to study the behaviour of steel reinforced CSRE columns under axial compression, considering the effects of above cited structural parameters.

5.2 Materials and equipments used for production of test specimen

5.2.1 Soil

The property of soil used in the present experimental programme is similar to that explained in Section 4.2.1 (Table 4.1).

5.2.2 Cement

The property of cement used is explained in Section 3.2.1. Similar to the studies made for unreinforced CSRE columns (Chapter 4), only 10% cement by dry mass of soil was used for production of test specimens throughout the test programme, so that a comparison with the unreinforced CSRE columns could also be made.

5.2.3 Steel

Steel bars of 6 mm and 8 mm diameter (Fe 500 grade) confirming IS 1786 (1985) was used for lateral (or tie) and longitudinal reinforcement respectively. Figs. 5.1a and 5.1b show the details of testing and load-deformation curve of steel. The tensile strength of steel is determined to be 558 MPa (average of 3-sample test). Lateral (or tie) reinforcement was provided at center-to-center spacing of 200 mm, 100 mm and 50 mm approximately, to assess the effects of lateral reinforcement spacing. Two legged steel ties of 90 mm x 90 mm size bent at 90° were used for lateral reinforcement. Fig. 5.2 shows the details of column reinforcement and Table 5.1 shows the reinforcement data.

5.2.4 Equipments and techniques

For production of test specimens, the following equipments were used:

1. The mould and rammer are similar to the one used in Chapter 4, explained in Section 4.2.2. Figs. 5.3a and 5.3b show the details of mould with steel reinforcement and rammer used.

2. For production of reinforced columns, a mild steel rammer weighing 5 kg with a solid handle of 25 mm diameter and 1.02 m length attached with a 70 mm x 70 mm mild steel ramming face was used for compaction (Fig. 5.3b).
3. A 20 mm thick mild steel plate of size 140 mm x 140 mm with 12 mm diameter holes at four corners, about 30 mm away from the edge was employed (Fig. 5.3b). This plate was inserted in the mould in such a way that the steel bars were penetrated through the perforations, thereby enabling the positioning of bars vertically upright and uniform compaction of soil-cement mix (wetted mix). Furthermore, the compaction plate was tied with thin ropes at four corners in such a way that it can be lifted easily after compaction of every layer. Fig. 5.3c shows a typical steel reinforced CSRE column.

Compaction throughout the test programme was carried out with the help of a compaction machine developed in the laboratory as discussed in Section 4.2.2.

5.2.5 Production of test specimen

Square columns of size 150 mm x 150 mm x 1500 mm (width x thickness x height) were prepared for the experimental investigation. It may be noted that unlike the study presented in Chapter 4 for unreinforced CSRE columns, only one size of column is considered here, as the focus is on reinforcement effects. Three series of columns were considered, comprising three specimens for each series of columns. The steel reinforced (SR) columns with 200 mm, 100 mm and 50 mm tie spacing were marked as SR200, SR100 and SR50, respectively.

Prior to production of test specimens the soil sample and mould was prepared as explained in Section 4.2.3. The compaction energy/effort was calculated using Equation 3.1. For preparation of steel reinforced columns, at first a 20 mm thick layer (cover) of wetted mix was compacted at the bottom of the mould before placing the longitudinal steel reinforcement. The steel bars tied within the four corners of the steel ties were placed upright inside the mould followed by pouring/placing of requisite amount of wetted mix and leveled (Fig. 5.3a). The perforated steel plate was then placed over the wetted mix by allowing the steel bars to pass through the four holes of the plate. The compaction was carried out with a rammer height of fall 300 mm

dropped uniformly on the perforated plate. After the completion of compaction, the plate was taken out and a steel tie was inserted and placed over the compacted layer followed by pouring of fresh wetted mix and re-insertion of perforated plate over the mix for compaction. This process was continued until the desired height was attained. It is to be noted that the amount of compaction energy required for each level of tie spacing was calculated separately. Removal of test specimens from the mould and curing procedure is similar to the one explained in last paragraph of Section 4.2.3.

5.2.6 Column test

A detail of column test set up is shown in Fig. 5.4 and is similar to the test set-up for unreinforced CSRE columns test (see Section 4.2.4). Load, lateral and axial displacements were recorded, and failure pattern was observed.

5.3 Results and discussions

5.3.1 Failure and load-deformation response of column

5.3.1.1 Effect of 200 mm tie spacing

Fig. 5.5a shows the failure pattern of steel reinforced columns with 200 mm (i.e. ~133% of column width) tie spacing (SR200). It was observed that the column did not show any sign of distress (e.g. visible cracks, or compression crushing) until 60 kN load, but as soon as the load approached to 70 kN the vertical cracks near the location of longitudinal bars were generated near the loading end, which eventually led to spalling of the cover gradually. This can be attributed to outward buckling of steel bars in between the ties. Further, this type of failure is found to localize within a lateral tie spacing at the end, with little or no failure impact on the rest of the column length. This implies that the lateral tie spacing provided is sufficiently large enough to allow lateral buckling of the longitudinal steel reinforcement, thereby leading the column to ultimate failure. This type of localised failure in SR200 column may be due to development of localised stress concentration because of end rotation near the loaded end in conjunction with the weak shear wedge zone resulting from platen effect, leading to the early failure of longitudinal steel reinforcement. It can also be noticed from Fig. 5.5a that the altitude of the shear wedge pyramid is ~ 97-167 mm

(the base of the shear wedge being equal to the tie width of 90 mm), which is shorter than that of the UCSRE (see Fig. 4.6), although similar angle of inclination of the shear planes (65-75°; see Fig. 5.5a) is seen. Hence, it is possible that with relatively large tie spacing of 200 mm (~ 133% of the column width) the confining effect from the tie is not sufficient to prevent such local failure due to the formation of shear wedge. Values of δ_l are in the range of 0.5 - 2 mm from the axis at the corresponding load of 10 - 60 kN respectively. It was observed that the failure of column occurred corresponds nearly to the location where δ_l is maximum as shown in Fig. 5.5b. The load-capacity of steel reinforced column (P_{us}) was determined to be 83.6 kN with a standard deviation of 1.56 kN, which is about 4.58% higher than the corresponding UCSRE columns (see Table 5.2).

5.3.1.2 Effect of 100 mm and 50 mm tie spacing

Fig. 5.6a shows the failure pattern of steel reinforced columns of 100 mm (67% of column width) tie spacing (SR100). Unlike UCSRE and SR200 columns, the sign of distress is not seen in SR100 columns even after reaching a load of 70 kN. However, as soon as the load approached to 80 kN and above (i.e., at about 85% - 90% of the ultimate load) the vertical cracks near the location of longitudinal bars were generated near the end supports, similar to that of SR200 columns. Spalling of cover occurred near the mid-height of the column where the maximum deformation occurred followed by bending of steel bars leading to ultimate failure. P_{us} of SR100 column is about 92.9 kN with a standard deviation of 2.37 kN, which is about 16.1% and 11.1% higher than corresponding UCSRE and SR200 (see Table 5.2) columns respectively. Variation of P_{us} vs. δ_l is shown in Fig. 5.6b and it is about 0.6 to 2.6 mm at 10 to 60 kN load. It can be seen that relatively, there is an enhancement of δ_l as compared to that of SR200 columns (see Fig. 5.5).

Fig. 5.7a shows the failure pattern of steel reinforced columns of 50 mm (33% of column width) tie spacing (SR50). The failure of this column is similar to that of SR100 columns. The P_{us} vs. δ_l curve is shown in Fig. 5.7b and it is about 0.7 to 5 mm at 10 to 60 kN load. It can be observed from the figures that the failure of columns occurs at the point where the maximum deformation occurred. P_{us} of SR50 column is about 109 kN with a standard deviation of 1 kN, which is about 17.3% higher than

SR100 columns. Similar localised failure pattern (compression side crushing and tension side cracking) can be observed for both SR100 and SR50 columns, closer to the mid-height, along with spalling of cover near the support. It may be seen that the compression crushing for both SR100 and SR50 extends to about ~100 mm (i.e. around half the face width) at the face. However, presence of relatively distributed micro-cracks can be seen on the tension side of SR50, in contrast to SR100 where a well-defined macro-crack appears on the tension side of the failure zone. This led to a relatively smoother curvature of the failure zone in SR50 (see Fig. 5.7a) and this can be attributed to the improved distributed stress with increased confinement effect, with decreasing tie spacing (i.e. with higher lateral reinforcement ratio, ρ_w (see Appendix C.2)). The reason for the shifting of localised failure zone (or development of hinge) closer to the mid-height for SR50 column in relation to that of SR100, can again be linked to better or improved distribution of the stresses as a result of increasing confinement effect from the ties. The relatively closer spaced ties in SR50 column inhibited the possibility of premature formation of shear wedge failure zone near the supports (ties are known to provide/enhanced capacity, see e.g. Cusson and Paultre (1994)), thereby greatly diminishing localised stress concentrations near the supports, which further arrests the possibility of localised cover spalling and buckling of longitudinal reinforcements closer to the supports.

5.3.1.3 Load- deformation response of column

Fig. 5.8 shows the plot of load vs. axial deformation from three samples each for UCRSE, SR200, SR100 and SR50. The results for USCRE from Fig. 4.13 is re-plotted again for comparison (Fig. 5.8a). It can be seen from Fig. 5.8 that with the increase in ρ_w (i.e. as the tie spacing decreased from 200 mm to 100 mm to 50 mm) the values of P_{us} increases and the ductility property of the column is enhanced. It may be noted that when reinforcements are provided, measurement of post-peak deformations are made possible with the present test setups, as sudden failure (i.e. brittle) did not occur like that of UCSRE columns. The axial deformation of the column is much higher than the UCSRE columns by about 71% at the corresponding load of 60 kN.

Unlike UCSRE and SR200 columns (Fig. 5.8b), the P vs. δ_v curve behaves differently for SR100 and SR50 columns (Figs. 5.8c and 5.8d). It can be observed that the curves posses two peak points. During the ascending part of loading, confinement has little or no effect and the CSRE cover is visually free of cracks up to the first peak load equal to 65 to 75 kN for SR100 columns and 70 to 80 kN for SR50 columns, approximately, (i.e., at about 75 to 80% of ultimate load). There was a gradual fall of load by about 5 to 8 kN, followed by increase in load up to second peak and beyond this there was gradual decrease in P. The sudden fall in load after first peak can be attributed to gradual formation of micro-cracks on the tension side and de-bonding of the CSRE from the reinforcement leading to spalling of cover. Because of the tension cracks and spalling of cover, the effective cross-section available to resist the axial load drops and hence the drop in P. At this stage, the lateral CSRE strains increase significantly and, as a result, the inner confinement becomes very significant. The CSRE core gains strength, while the cover gradually disappears (Figs. 5.6a and 5.7a) at the failure zone. Generally, the P vs. δ_v curve for the specimen shows a strength gain and reaches a second peak of average load equal to 92.9 kN (SR100) and 109 kN (SR50), when the CSRE core reaches the maximum stress. At this load level, the longitudinal steel bars tend to bend. Axial deformation at peak load (δ_{uv}) increased by about 6.3% and 19.1%; whilst lateral deformation at 60 kN (δ_{l60}) (pre-peak) by 13.6 % and 100%; when the stirrup spacing decreased from 200 mm to 100 mm and 100 mm to 50 mm respectively, suggesting an improved ductility with core confinement (Fig. 5.9). As mentioned in Section 4.2.4, lateral deformation at ultimate load was not monitored due to the removal of measuring dial gauges.

Unlike the studies made by Cusson and Paultre (1994), on high strength concrete columns confined by rectangular ties, the value of P of columns at second peak did not fall below the value at first peak, in the present study. On the other hand, specimens with low confinement (specimens SR200) did not show the second peak (UCSRE and SR200 columns). This can be attributed to relatively brittle nature of failure (see Fig. 4.6) for UCSRE and end localised shear wedge type failure for SR200 columns (see Fig. 5.5). Finally, at the end of testing (Figs. 5.5a, 5.6a, and 5.7a) most of the columns failed by simultaneous failure of CSRE and bending of longitudinal bars.

5.3.2 Effect of reinforcement on load-capacity

Fig. 5.10 shows the influence of reinforcement on load ratio (P_{us}/P_u) of columns at longitudinal reinforcement ratio, ρ_l = 0.89. It can be seen from Fig. 5.10a, that when the total reinforcement ratio ($\rho_l+\rho_w = \rho_t$) is ~< 1.5 the capacity of reinforced column approaches toward the capacity of UCSRE column, indicating that there is no significant improvement in column strength when the reinforcement or steel confinement is low. Further, it is also noted that the rate of increase in column strength with increasing reinforcement ratio is relatively slow, as compared to higher reinforcement ratios. At higher value of ρ_t i.e., ~> 1.5, an increase in the rate of strength gain can be observed, although it may be seen that there is an apparent tapering (or drop) in the rate of increase at relatively higher ρ_t i.e. > 3.0. The plateauing effect of P_{us}/P_u at higher reinforcement ratio is consistent with the intuition that at vanishing tie spacing the column would approach a rammed earth filled steel tube (just like concrete filled steel tubes (Gardner and Jacobson, 1967; Han, 2000; Patton and Singh, 2014)) with a finite strength value. The effect on P_{us}/P_u due to changes in ρ_w for a fixed ρ_l = 0.89 is plotted in Fig. 5.10b. The positive effect of lateral steel confinement is clearly seen for ρ_w > ~ 0.5. It can be seen that there is an increase in P_{us}/P_u by about 30% when ρ_w is increased by about 300% from 0.6. The increase in P_{us}/P_u with decreasing tie spacing (or increasing ρ_w) is consistent with similar studies done for steel reinforced concrete columns (e.g. Cusson and Paultre, 1994). At lower values of ρ_w (i.e. <~ 0.5), when the tie spacing is lesser than 200 mm (or 133% of the column size), the effect of lateral confinement is not very significant on the column strength. Thus it can be seen that the overall response of P_{us}/P_u of column with confinement effect of the steel reinforcement appears to follow a non-linear S-curve (i.e. a double curvature curve) plateauing at both the ends.

5.3.3 Moisture content and density of column

Determination of moisture content and density of the materials used for rammed earth construction should be born in mind to achieve better strength and durability of the structure. Bui et al., (2014) reported that, when the moisture content of rammed earth specimen is greater than 4%, the compressive strength decreases quickly for all types of soil studied, and the effect is more in clayey soil than sandy soil. However, this

effect is negligible to the soil stabilised with 8% natural hydraulic lime and it was noted that the stabilisation by hydraulic lime decrease the sensitivity to water of rammed earth material. Therefore, moisture content of CSRE was determined to assess its effect on strength and behaviour of column specimen. Details of moisture content and density of columns during testing are presented in Table 5.2. In general, the average moisture content of the CSRE samples varies from 4.25% to 6.89% with a standard deviation of 0.13% to 0.91%; and the average dry density varies from 1790 kg/m^3 to 1990 kg/m^3 with a standard deviation of 0.003% to 0.016% respectively. There exists a negligible variation in moisture content between the test specimens during testing.

5.4 Summary and conclusions

This chapter presents an experimental study on the structural behaviour CSRE columns reinforced with steel under concentric axial loading. Effects of key variables such as total reinforcement ratio (ρ_t), lateral reinforcement ratio (ρ_w), etc., are studied. Furthermore, the failure pattern, load-lateral deformation and load-axial deformation of columns are also assessed. Based on the study the following conclusions have been drawn:

1. The behaviour of CSRE columns reinforced with close tie spacing is characterized by gradual spalling of cover at the failure zone leading to a loss of axial capacity before the lateral confinement becomes effective.
2. The P_{us} of SR200, SR100 and SR50 column is about 4.6%, 16% and 33% higher than UCSRE column, respectively. P_{us} increases due to reduction in tie spacing and toughness gain of confined CSRE.
3. Linear increase in percent P_{us} is observed as ρ_t ratio was increased from 0% to 3.41%. There is a gradual increase on percent P_{us} as the ρ_t ratio was increased from 0% to 1.52%, 2.15% and 3.41% with the values of 4.5%, 16% and 36% respectively. The P_{us} also increases by about 11% to 30% when the percent ρ_w ratio was increased from 0.63% to 1.26% and 2.51% respectively.
4. The ductility property of column is enhanced due to reinforcement, and unlike the UCSRE columns, the failure of reinforced column is not sudden. This type

of column can be used as structural member for construction of low-rise rammed earth houses.

5. Steel can be a potential reinforcing material in CSRE columns with close tie spacing in order to achieve higher strength and better seismic performance.

Table 5.1. Details of steel reinforcement.

Column	a (mm)	d (mm)	h (mm)	s (mm)	ρ_l (%)	ρ_w (%)	$\rho_l + \rho_w$ (%)
1SR200	150	150	1500	200	0.89	0.63	1.52
2SR200	150	150	1500	200	0.89	0.63	1.52
3SR200	150	150	1500	200	0.89	0.63	1.52
1SR100	150	150	1500	100	0.89	1.26	2.15
2SR100	150	150	1500	100	0.89	1.26	2.15
3SR100	150	150	1500	100	0.89	1.26	2.15
1SR50	150	150	1500	50	0.89	2.51	3.41
2SR50	150	150	1500	50	0.89	2.51	3.41
3SR50	150	150	1500	50	0.89	2.51	3.41

Table 5.2. Summary of steel reinforced column test results.

Column	Ultimate load (kN)	Compressive strength (MPa)	Moisture content of test specimen (%)			Average moisture content at test (%)	Standard deviation (%)	Average dry density of soil-cement (kg/m^3)	Standard deviation (%)
			Locations						
			Top	Middle	Bottom				
1UCSRE	81.0	3.6	5.43	6.79	5.45	5.89	0.78	1790	0.014
2UCSRE	80.3	3.6	6.29	5.79	4.85	5.64	0.73	1800	0.014
3UCSRE	81.6	3.5	5.67	6.56	5.78	6.00	0.49	1790	0.009
1SR200	83.4	3.7	4.93	3.91	4.22	4.35	0.52	1990	0.010
2SR200	82.2	3.7	5.83	4.33	2.13	4.10	1.86	2000	0.036
3SR200	85.3	3.8	5.24	4.13	3.51	4.29	0.88	1990	0.017
1SR100	90.4	4.0	5.32	6.19	6.66	6.06	0.68	1960	0.013
2SR100	93.3	4.1	8.06	8.02	7.53	7.87	0.29	1930	0.005
3SR100	95.1	4.2	6.21	7.13	6.87	6.74	0.47	1950	0.009
1SR50	108.0	4.8	5.88	6.73	4.28	5.63	1.24	1970	0.023
2SR50	110.0	4.9	5.25	4.55	5.21	5.00	0.39	1980	0.007
3SR50	109.0	4.8	5.73	5.23	4.86	5.27	0.44	1970	0.008

Note: *UCSRE = Unreinforced Cement stabilised Rammed Earth; SR = Steel Reinforced; 1, 2, 3 = Serial number of columns; 50, 100, 200 = Spacing of lateral ties in mm.*

Test setup

Failed sample

(a) Steel bar

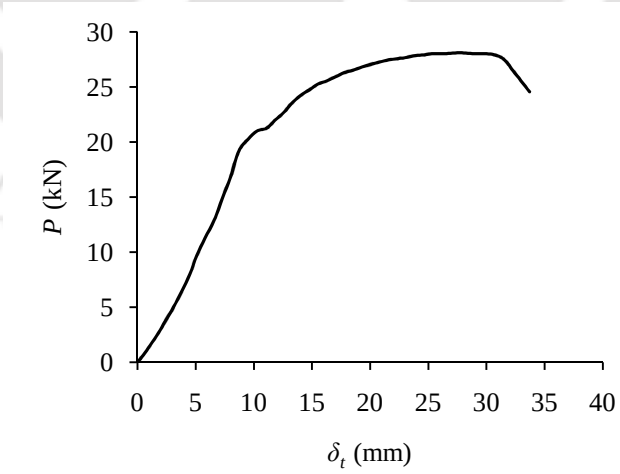

(b) Typical load-deformation curve of steel

Fig. 5.1. Testing of steel bar.

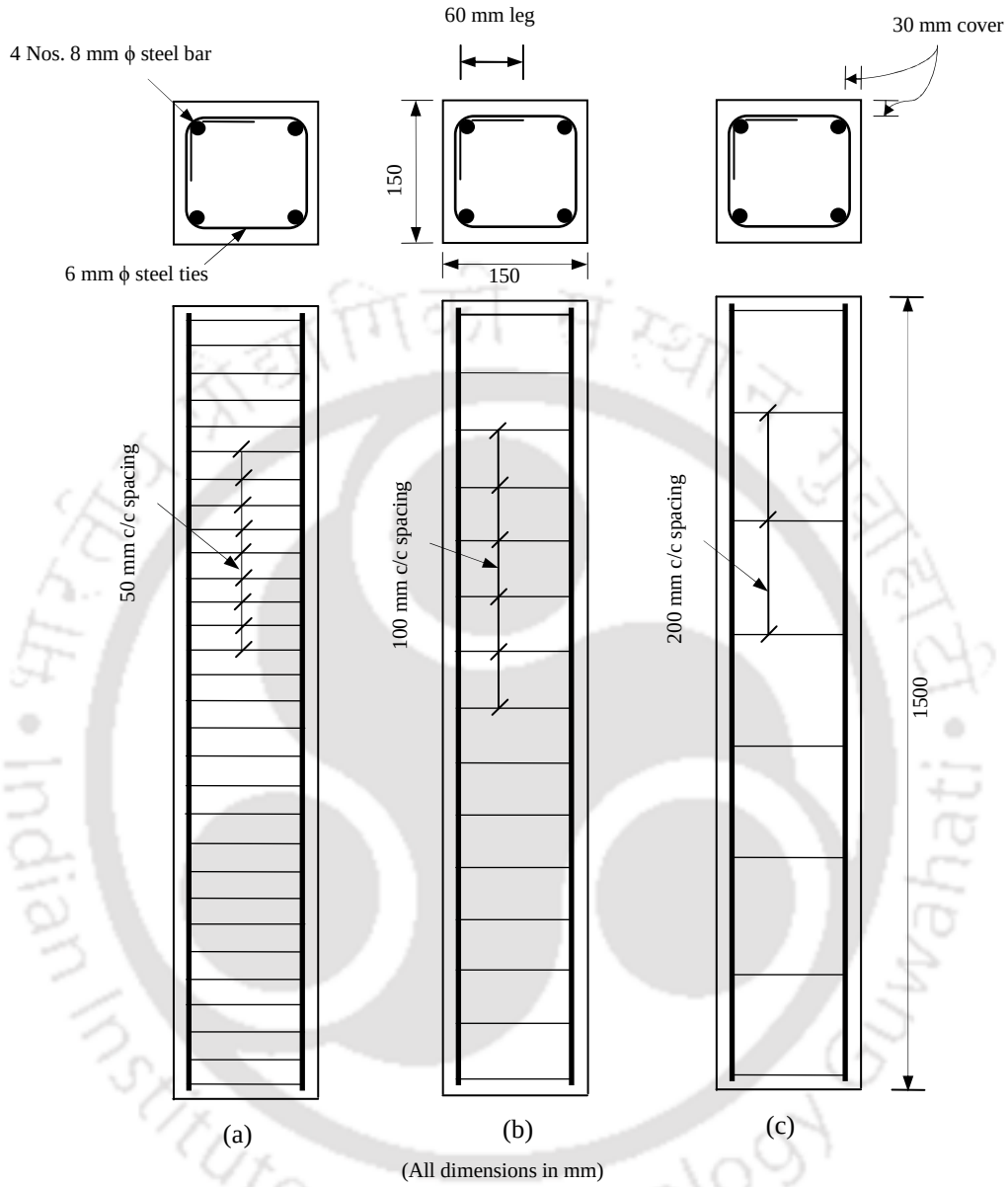

Fig. 5.2. Reinforcement details of column with tie spacing: (a) 50 mm; (b) 100 mm; and (c) 200 mm.

Fig. 5.3. Equipments: (a) mould; (b) rammer and compaction plate with holes; and (c) typical steel reinforced CSRE column.

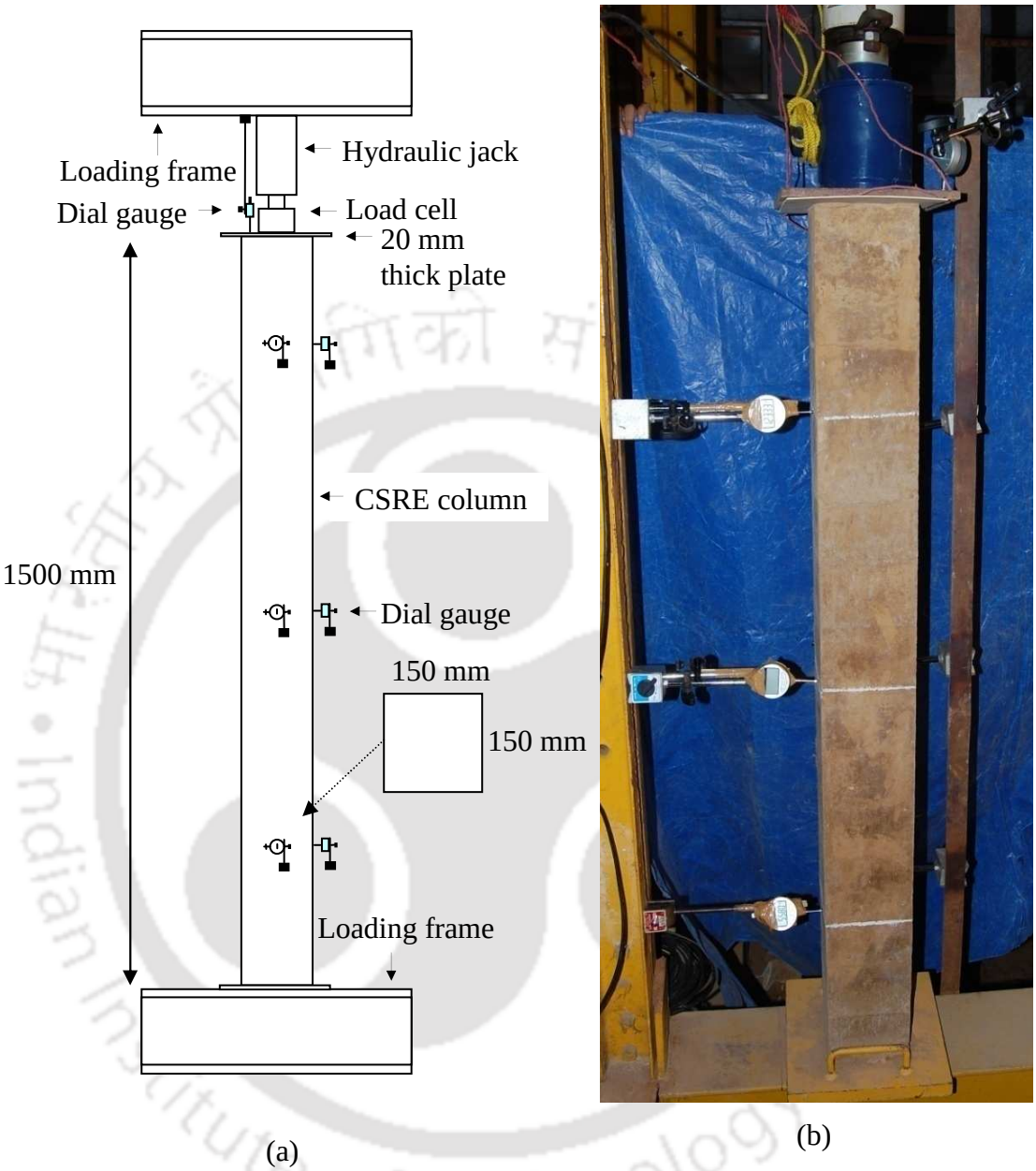

Fig. 5.4. Column test setup: (a) schematic diagram; and (b) experimental set up for steel-reinforced CSRE column.

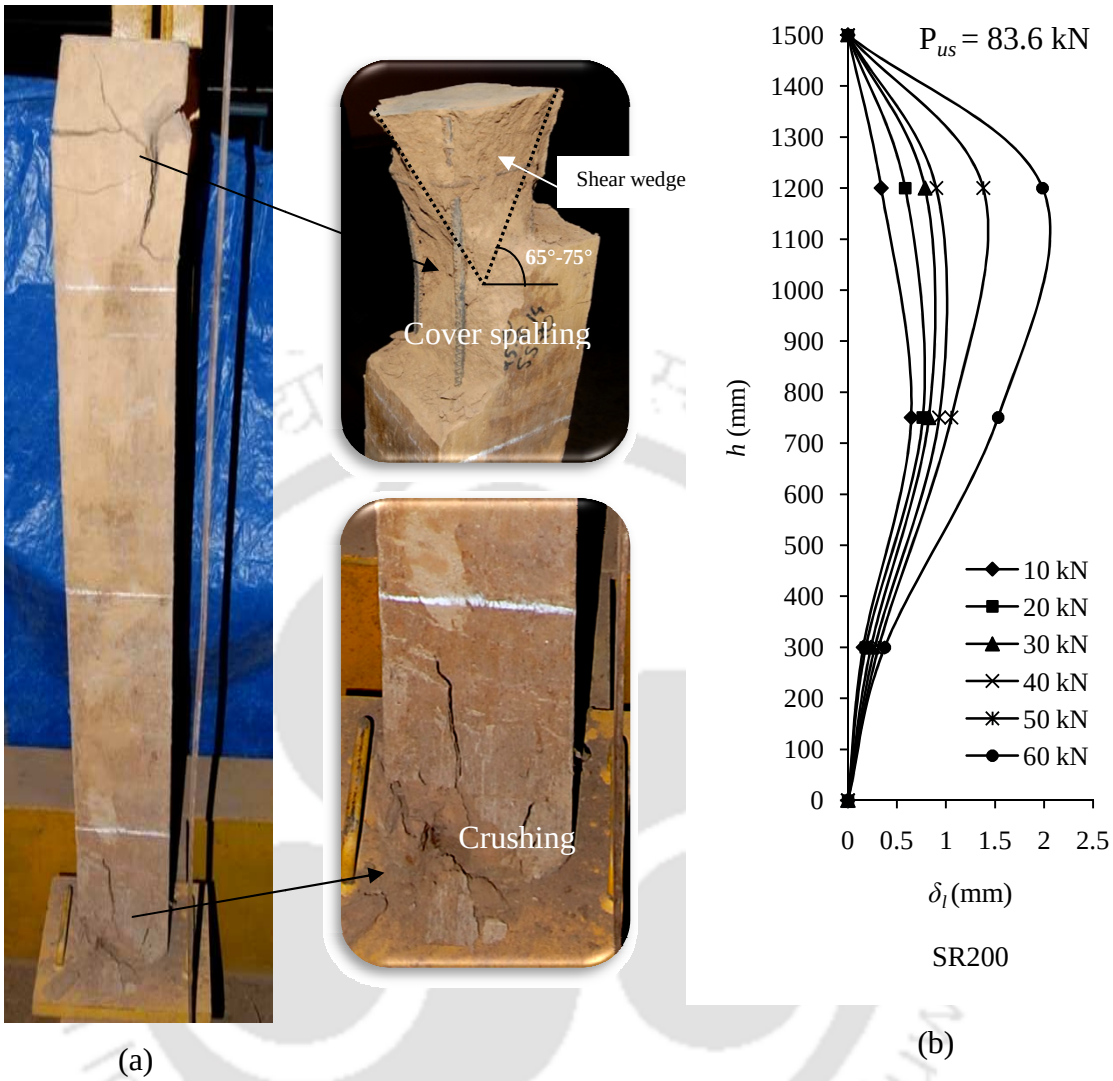

Fig. 5.5. Failure of column with 200 mm tie spacing: (a) failure pattern; and (b) load-lateral deformation curve.

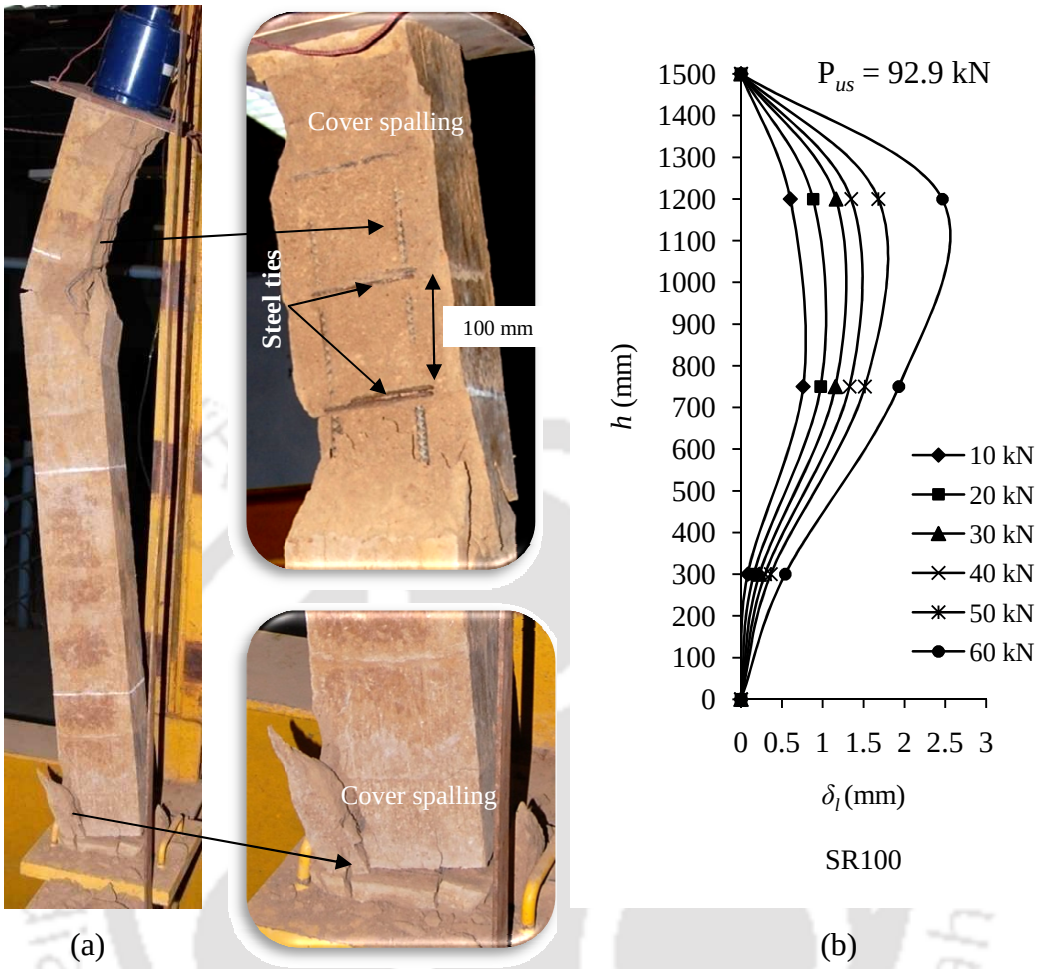

Fig. 5.6. Failure of column with 100 mm tie spacing: (a) failure pattern; and (b) load-lateral deformation curve.

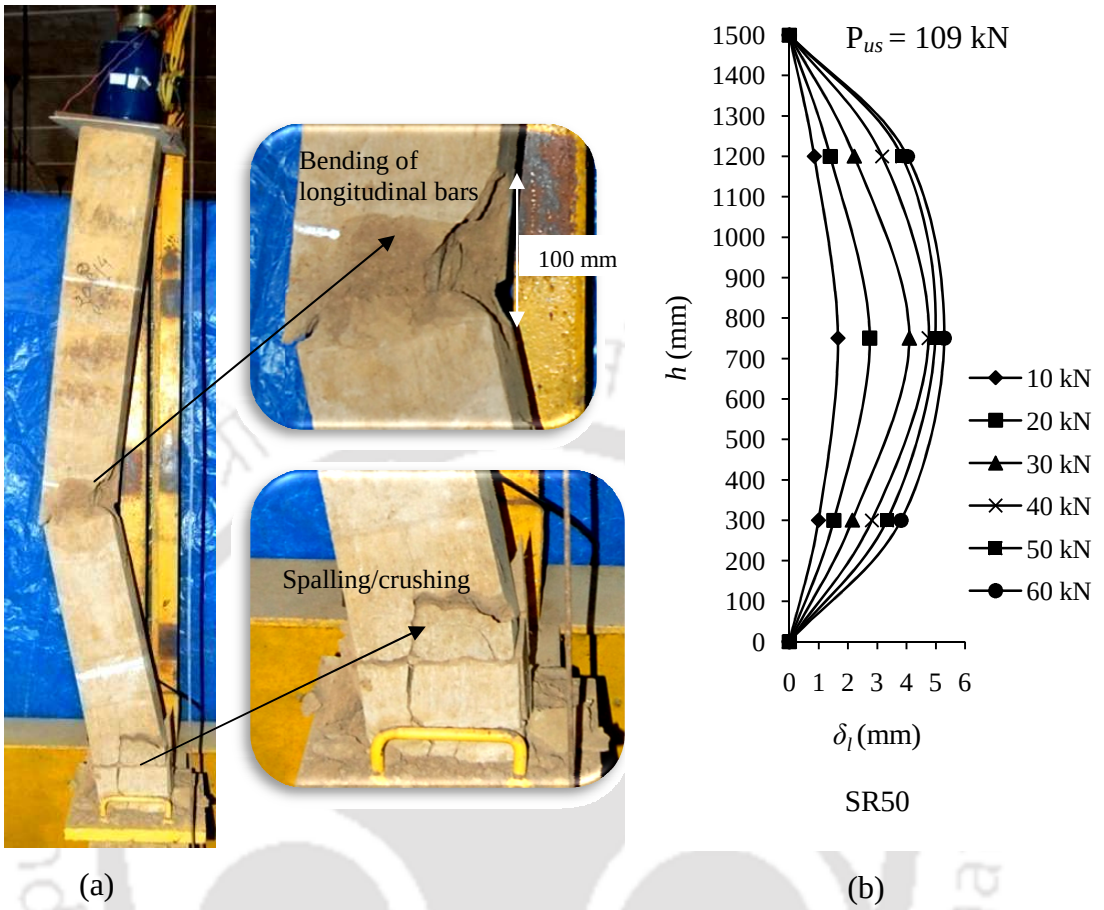

Fig. 5.7. Failure of column with 50 mm tie spacing: (a) failure pattern; and (b) load-lateral deformation curve

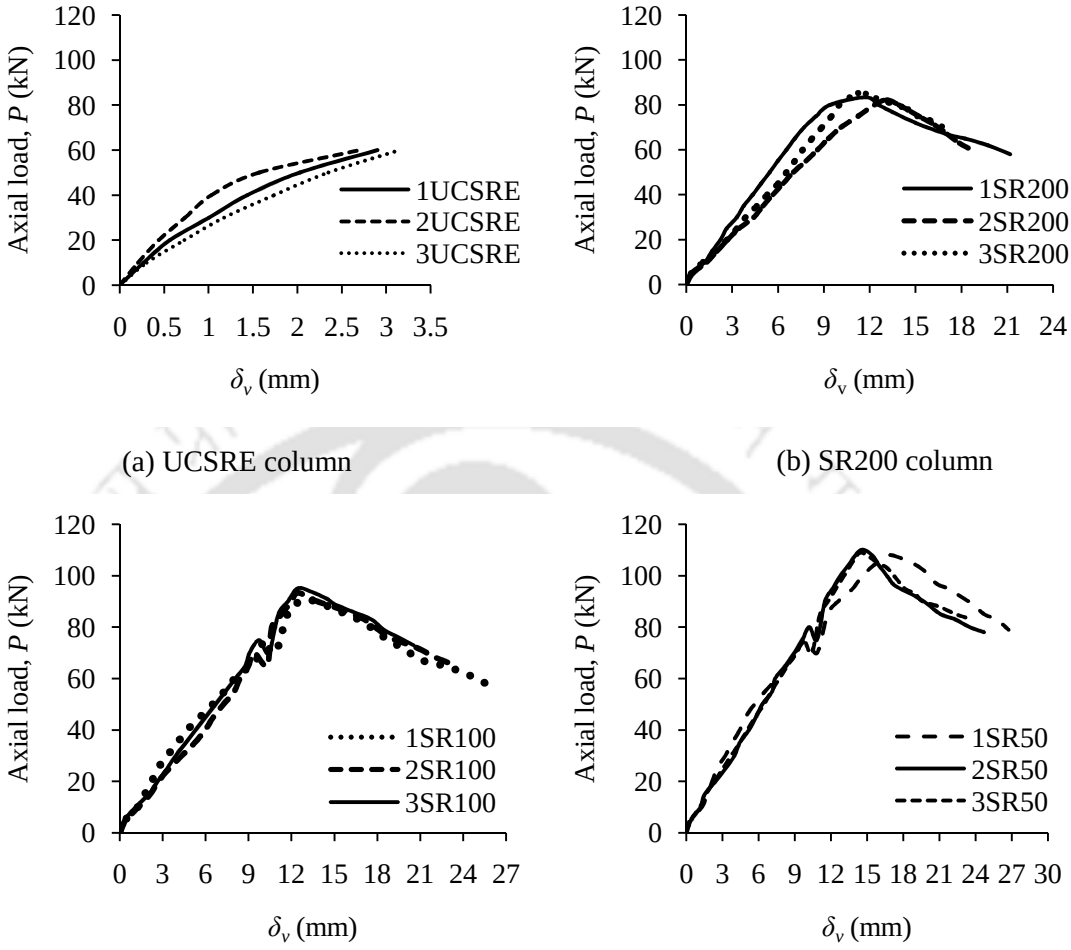

(a) UCSRE column

(b) SR200 column

(c) SR100 column

(d) SR50 column

Fig. 5.8. Load-axial deformation curves.

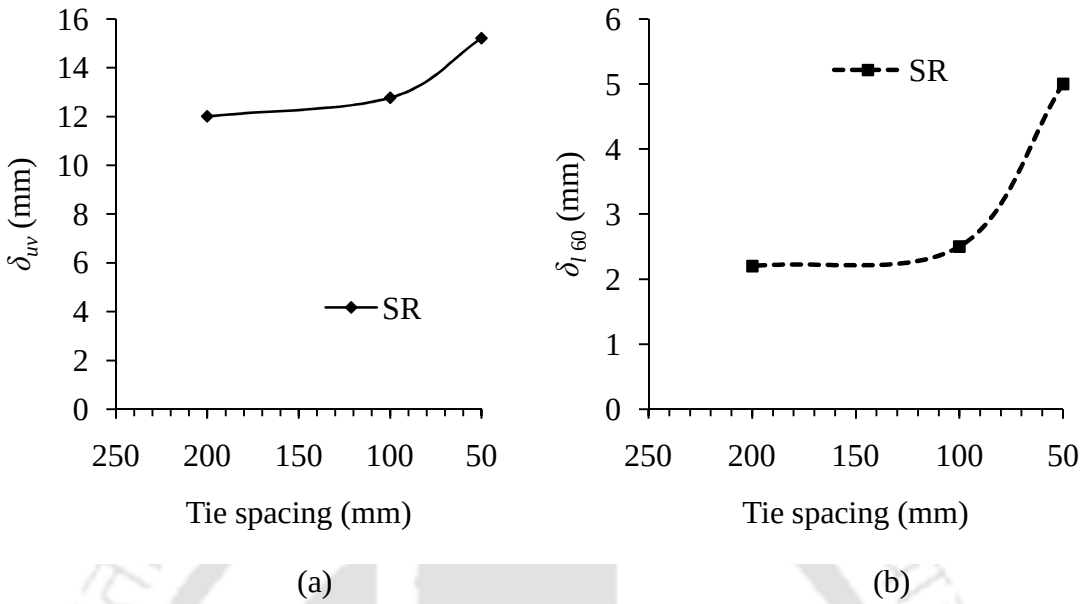

Fig. 5.9. (a) Axial deformation of columns at ultimate load; and (b) lateral deformation of columns at 60 kN load.

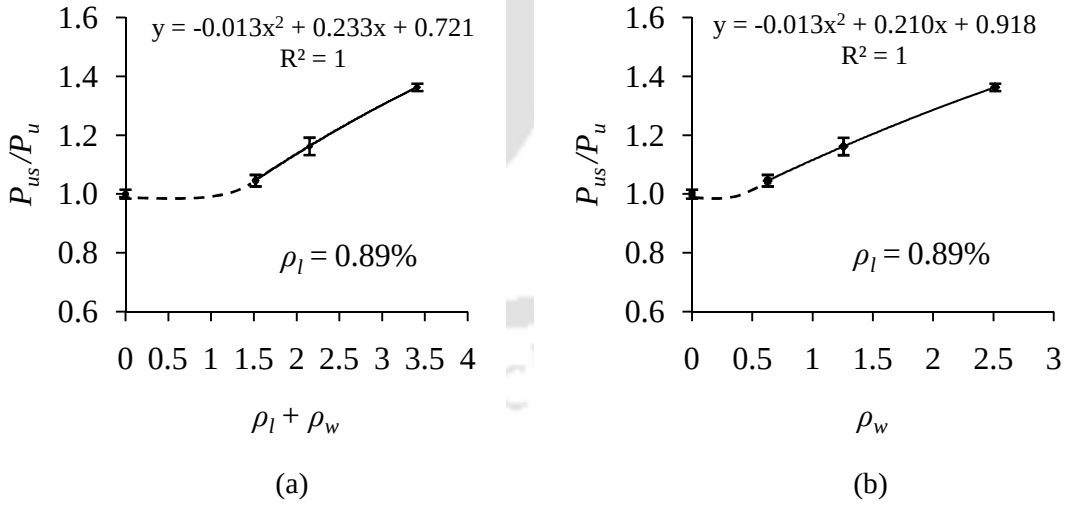

Fig. 5.10. Effect of reinforcement on load-capacity of column: (a) load vs. total reinforcement; and (b) load vs. lateral reinforcement.

Chapter 6

Structural Behaviour of Bamboo-Steel Reinforced CSRE Column

This chapter presents an experimental study on the capacity of CSRE columns reinforced with bamboo and steel under concentric axial compression. Effects of structural parameters such as lateral reinforcement ratio, total reinforcement ratio etc., on the failure pattern; load-lateral deformation and load-axial deformation of columns are studied.

6.1 Introduction

In tropical and sub-tropical parts of the world, traditionally bamboo has been used as a construction material, especially its uses is extensive in rural areas of developing countries like India, Brazil, Myanmar, Nigeria, Bangladesh, Vietnam, etc. Bamboo is known to possess several attractive properties such as relatively high strength/weight ratio, easy workability, ability to reduce carbon footprint, being a rapidly renewable resource, etc., (Sharma et al., 2014; Greenleafdoors, 2015). As such, as mentioned in Chapter 2 (literature review) in the recent past, bamboo has attracted the attention of several researchers (e.g. Gavami, 2005; Gao et al., 2009; Agarwal et al., 2014; Tripura and Sharma, 2014, etc.) to validate and check its suitability as reinforcement materials in concrete, rammed earth construction etc. Ghavami (2005) extensively studied the performance of bamboo as reinforcement in structural concrete elements, and observed that bamboo can substitute steel satisfactorily in many building constructions. Agarwal et al., (2014) investigated the behaviour of chemically treated bamboo reinforced concrete beams and columns, and concluded that bamboo can provide reasonable strength as reinforcement for beam and column like members. Bond behaviour/anchor property of bamboo embedded in rammed earth have been assessed and found reasonable bond strength useful for rammed earth constructions (Tripura and Sharma 2014). Gao et al., (2009) showed that rammed earth wall reinforced with bamboo could improve ductility, when subjected to horizontal load. Hence, in this chapter, an attempt is made to study the feasibility of using bamboo

splints substituting the longitudinal steel bars in CSRE columns under axial loading (see preceding chapter for steel reinforced CSRE columns), considering the effects of structural parameters such as total reinforcement ratio, lateral reinforcement ratio, etc. Thus this chapter is an extension of the previous chapter i.e. Chapter 5, except for the replacement of longitudinal bars with bamboo splints.

6.2 Materials and equipments used for production of test specimen

6.2.1 Soil

Properties of the soil used in the present experimental programme are similar to those explained in Section 4.2.1 (see Table 4.1).

6.2.2 Cement

Ordinary Portland cement conforming to IS 8112 (1989) was used in the experimental investigations. The property of cement used is explained in Section 3.2.1. Similar to Chapters 4 and 5, only 10% cement by dry mass of soil was used for production of test specimens throughout the test programme.

6.2.3 Bamboo

For production of reinforced CSRE columns, the bamboo species namely Bambusa Balcooa was used as longitudinal reinforcing bars. This species of bamboo is commonly available and widely used for construction of houses locally (Agartala, India). The specimens were harvested at an age greater than 3 years, and were then seasoned by air-drying for 4 weeks in a standing upright position in the laboratory at ambient temperature. The bamboo was further chemically treated as per IS 401 (2001) with Copper-Chrome-Boron (CCB) solution confirming to IS 9096 (2006). The CCB solution was prepared by mixing Boric Acid, Copper Sulphate and Potassium dichromate in the ratio 1.5:3:4 respectively. After soaking the bamboo splints in the CCB solution for a week, the splints were further, allowed to dry in air for about 10 days prior to tensile strength test. The tensile strength of bamboo was determined as per IS 6874 (2008). Figs. 6.1a and b show the details of testing and load-deformation curve of bamboo splints. The tensile strength of bamboo splints is about 315 MPa (average of 3 sample test), and this value is very close to the value obtained by

Tripura and Sharma (2014). Bamboo splints having cross sectional area equivalent to 8 mm diameter of steel bars were used for longitudinal reinforcement. Table 6.1 outlines the details of reinforcement data.

6.2.4 Steel

The property of the steel used is similar to that explained in Section 5.2.3. Reinforcement details of column are shown in Fig. 6.2 and Table 6.1.

6.2.5 Equipments and techniques

The equipments and compaction process used for production of test specimens; in the present test programme is similar to the one explained in Section 5.2.4. Figs. 6.3a, b, and c shows the equipments and typical bamboo-steel reinforced CSRE column.

6.2.6 Production of test specimen

The size of the columns used in bamboo-steel reinforced column experimentation programme was chosen same (150 mm x 150 mm x 1500 mm) as that of steel-reinforced columns presented in Chapter 5. The column dimensions were made equal to facilitate comparison of structural properties between bamboo-steel and steel reinforced columns. Three series of columns were prepared comprising of three columns for each series. The bamboo steel reinforced (BSR; bamboo as longitudinal reinforcement and steel as lateral reinforcement) are then designated as BSR200, BSR100 and BSR50, depending on the tie spacing, where BSR200 denotes column with 200 mm center-to-center tie spacing. Prior to production of test specimens the soil sample and mould was prepared as explained in Section 4.2.3. The compaction energy/effort was calculated using Equation 3.1. Production and curing procedure of test specimens are similar to that explained in Section 5.2.5.

6.2.7 Column test

Column test setup and testing procedure is similar to that explained in Section 5.2.6 (see Fig. 5.4). Moisture content was determined for bamboo splint and CSRE samples at the time of testing.

6.3 Results and discussions

6.3.1 Failure and load-deformation response of column

6.3.1.1 Effect of 200 mm tie spacing

Failure pattern of bamboo-steel reinforced columns with tie spacing of 200mm (i.e. 133.3% of the column width) (BSR200) is shown in Fig. 6.4a. Results from the experimental programme shows that the vertical cracks were generated near the loading end as the load approaches to about 75% of ultimate load. On subsequent loading gradual spalling of cover occurred due to outward buckling (more like a triangle, unlike in steel reinforced column, SR200 where only little localised steel buckling is seen; see Fig. 5.5) of bamboo splints in between the ties (Fig.6.4a, inset), thereby drastically reducing the load-capacity (P_{ubs}) and leading to complete failure of the column. Interestingly, the failure occurred near the loading end in between the ties due to localised stress concentration, and there was a little or no visible damage or distress on the rest of the column length. This localised failure may again be related to development of stress concentration due to end rotation near the loaded end, where weak shear wedge zone from platen effect also exists. leading to the early failure of longitudinal steel reinforcement. Similar type of pyramidal shear wedge (base = ~90 mm, and altitude = ~ 97-167 mm, corresponding to 65°-75° shear plane) as that of SR200 (see Fig 5.6) is observed. Localised bamboo splint breaking or buckling may have been caused by insufficient or larger tie spacing, which in this case is much larger than the width of the column itself.

The value of P_{ubs} of BSR200 column was determined to be 83.1 kN with a standard deviation of 0.78 kN, which is about 2.6% higher than UCSRE columns (see Table 6.2). From Fig. 6.4b, it can be seen that lateral deformation (δ_l) of the column is in the range 0.3 - 2.6 mm for load value of 10-60 kN. It was observed that the failure of column occurred corresponds nearly to the location where δ_l is maximum as shown in Fig. 6.4b.

6.3.1.2 Effect of 100 mm and 50 mm tie spacing

Failure pattern of columns with tie spacing of 67% of the column width (BSR100) is shown in Fig. 6.5a. It was observed that at about 85 - 90% of the ultimate load the

vertical cracks were generated near the end supports, because of the end rotations followed by gradual spalling of cover near the mid-height of the column, unlike in BSR200 column, where the failure is localised at one of the ends only. Subsequent loading led to complete spalling of cover at the mid-height of the column, due to buckling followed by breaking of bamboo splints. The occurrence of tensile crack on the tension side and crushing of the cover can be seen on the compression side. The zone of compression crushing or spalling is about two times the lateral ties spacing i.e. ~ 200 mm. Such, very localised failure is not seen in the case of SR100 column (Fig. 5.6), and this may be related to relatively weaker strength of bamboo splints as compared to steel, and also due to weaker bond between bamboo splint and earth. The spalling of cover near the end support may be related to the formation of cracks because of end rotation. The value of P_{ubs} was determined to be 87.7 kN, which is about 8.3% and 5.2% higher than that of UCSRE and BSR200 (see Fig. 6.4) columns respectively, and δ_l is about 0.5 to 1.7 mm at 10 to 60 kN load. The load - deformation curve is shown in Fig. 6.5b.

Failure pattern of columns with lesser tie spacing such as BSR50 (i.e., 33.3% of the column width) is shown in Fig. 6.6a. Failure pattern of BSR50 columns resembles to that of BSR100 columns. It was observed that δ_l ranges from 0.5 to 1.6 mm at corresponding load of 10 to 60 kN. The P_{ubs} vs. δ_l curve is shown in Fig. 6.6b. The value of P_{ubs} of BSR50 column is about 93.3 kN, which is about 14.3%, 11.2%, 6% higher than UCSRE, BSR200 and BSR100 columns respectively. Similar type of failure pattern can be observed at the compression zone of BSR100 and BSR50 columns, closer to the mid-height, and spalling of cover near the support. In comparison to BSR100, the curvature at the failure zone for BSR50 is relatively smoother (see Figs. 6.5a and 6.6a), and this may be related to the closer tie spacing (resulting in higher lateral reinforcement ratio, ρ_w) in BSR50 wherein a better level of confinement and distribution of the stresses is achieved. Further, zone of cover cracks at the tension side is found to spread in a wider area in BSR50 as compared to that of BSR100. The compression failure zone is enhanced to about five times the tie spacing i.e. (~ 250 mm) which is more than that of BSR100.

6.3.1.3 Load- deformation response of column

Variation of load vs. axial deformation is plotted in Figs. 6.7a,b,c and d considering three samples each of BSR200, BSR100 and BSR50 respectively. For comparison, the results for UCSRE columns are also plotted again. It can be observed that both ultimate load (P_{ubs}) and ductility properties of the columns are enhanced due to addition of tie reinforcements (i.e., ρ_w = 0% to 0.63%), further, δ_v of the column increased by about 70% higher than UCSRE columns at the corresponding load of 60 kN. *P* vs. δ_v curves of BSR100 and BSR50 columns posses two peak points as shown in Figs. 6.7c and d, which is absent in case of UCSRE (Fig. 6.7a) and BSR200 (Fig. 6.7b) columns (similar to that observed for steel reinforced columns; see Fig. 5.8), and can be attributed to confinement effect of the inner core due to lateral ties. A negligible confinement effect persists during the ascending part of loading and the CSRE cover is visually free of cracks up to the first peak load equal to 70% to 80% of ultimate load for both BSR100 and BSR50 columns. On further loading, a gradual fall of load by about 7% to 10% of ultimate load from the first peak was observed. Subsequently, the load reached up to a second peak and beyond which there was a gradual decrease in *P*. The formation of micro-cracks on the tension side and de-bonding of the CSRE from the reinforcement may be regarded as key parameters causing the gradual fall in load after the first peak. Due to tension cracks and spalling of cover, there is a considerable drop in the effective cross-section available to resist the axial load, thereby dropping *P* after first peak, as shown in Figs. 6.7c and d. As the load rises again after first peak, the inner core confinement becomes very effective as a result of increase in lateral CSRE strains, which is characterized by the formation of second peak at ultimate load equal to 87.7 kN for BSR100 and 93.3 kN for BSR50 columns (Figs. 6.7c and d). At this load level, the longitudinal bamboo breaks/shears off (i.e., BSR100 and BSR50 columns), however the lateral steel being stronger in tension show no sign of distress.

Similar to the observations made for steel reinforced CSRE columns (see Section 5.3.1.4), the second peak load was found to be higher than the first, which is again in contrast to the behaviour reported by Cusson and Paultre (1994) on high strength concrete columns confined by rectangular ties. It was observed that the reinforced columns failed by successive failure of CSRE and bamboo splints as shown in Figs.

6.4a, 6.5a, and 6.6a, respectively. A nearly linear increase in axial deformation at peak load (δ_{uv}) and lateral deformation at 60 kN (δ_{l60}) (pre-peak) have been observed i.e., around ~10% and 14% increase respectively, when the stirrup spacing decreased from 200 mm to 50 mm, thus showing an improvement in ductility (Fig. 6.8) with reducing tie spacing.

6.3.2 Effect of reinforcement on load-capacity

Effect of total (longitudinal steel (ρ_l) + lateral bamboo ties (ρ_w) = ρ_t) and ρ_w on load ratio i.e. P_{ubs} /P_u (P_u is the ultimate load for UCSRE columns) are presented in Fig 6.9, for a fixed value of ρ_l = 0.89. As can be seen from Fig. 6.9 that a marginal difference in P_{ubs} exists between UCSRE and BSR200 columns (shown by dotted line). This shows that reinforcement in BSR200 column is insufficient to bring a significant effect on P_{ubs}. At higher ρ_t i.e., ~>1.5 (and up to ~3.5), an increase in strength by about 10% to 16% can be observed, although it may be seen that there is a noticeable dropping in the rate of increase at relatively higher ρ_t i.e. >3.0. As mentioned in Section 5.3.2, the plateauing effect of P_{ubs} at high reinforcement ratios, it is likely that P_{ubs} would tend to a finite strength limit, consistent with the common perception that at vanishing tie spacing, the column would behave like a rammed earth filled steel tube (similar to concrete filled steel tubes (Gardner and Jacobson, 1967; Han, 2000; Patton and Singh, 2014)). The effect of ρ_w on P_{ubs} /P_u for ρ_l = 0.89 is shown in Fig. 6.9b and this effect is prominent when ρ_w > ~ 0.5. It can be seen that there is an increase in P_{ubs} by about 12% when ρ_w is increased by 300% (from ρ_w = 0.6). It may be noted that this increase is about half of the value observed for steel reinforced CSRE columns (see Fig. 5.10), as expected of the greater strength exhibited by longitudinal steel as compared to longitudinal bamboo splints). The increase in P_{ubs} with decreasing tie spacing agrees with similar studies done for steel reinforced concrete columns (e.g. Cusson and Paultre, 1994). At lower values of ρ_w (i.e. <~ 0.5), when the tie spacing is lesser than 200 mm (or 133.3% of the column width), the effect of lateral confinement is not very significant on the column strength. Thus, it can be seen that the overall response of the column capacity i.e. P_{ubs} with confinement effect of the steel reinforcement appears to follow a non-linear S-curve (i.e. a double curvature curve) plateauing at both the ends.

6.3.3 Moisture content and density of column

Moisture content and density of CSRE columns during the time of testing was determined to assess the effect on strength of column. In the present study, the average moisture content of the CSRE samples varies from 5.64% to 7.73% with a standard deviation of 0.49% to 1.20%; and the average dry density varies from 1790 kg/m^3 to 1960 kg/m^3 with a standard deviation of 0.009% to 0.029% respectively (see Table 6.2). Bui et al., (2014) observed that the effect of moisture content on compressive strength in soil stabilised with 8% natural hydraulic lime, as mentioned in Section 5.3.4, hence the moisture content observed in the present study is likely to have negligible effect on the column strength. In case of bamboo splints the average moisture content ranges from 3.32% to 5.69% with standard deviation ranging from 0.34% to 1.90% respectively.

6.3.4 Comparison of BSR and SR columns

Fig. 6.10a shows P_u relationship of BSR and SR column based on ρ_t. It is observed that both BSR and SR column possess higher P_{ubs} by about 3.8 - 16.6% and 4.6 - 33% than UCSRE column, respectively. This shows that reinforcement increases the P_{ubs} of columns. It is further observed that the P_{ubs} of SR column increases gradually higher than BSR columns. Although these values are not much different at 1.52 and 2.15 reinforcement ratios, however SR50 column possess higher P_{ubs} by about 17% than BSR50 column at 3.14 reinforcement ratios. Fig. 6.10b shows the P_{ubs} relationship of BSR and SR columns with respect to ρ_w. It is observed that the P_{ubs} increases gradually with the increase in reinforcement ratio in both BSR and SR columns. Furthermore, the SR columns possess higher P_{ubs} by about 6% to 11% than BSR columns at the rate of two times increase in reinforcement ratio. Fig. 6.11 shows the influence of longitudinal reinforcement type on P_{ubs}. Here the CSRE strength and tie spacing is considered as constant and material type for longitudinal reinforcement as variable. It can be seen that the difference in P_{ubs} is negligible between BSR200 and SR200 columns. This shows that both bamboo and steel carries similar amount of load at this reinforcement ratio (i.e., 0.63). However, the difference is highest between BSR50 and SR50 columns by about 17%, which shows that the longitudinal steel

becomes more effective and carries more load than bamboo at ρ_w equal to 2.51. The reason for this difference can be due to steel being stronger material than bamboo.

The comparison of δ_{uv} and δl_{60} between SR and BSR CSRE columns are shown in Figs. 6.12a and b respectively. It can be seen that the values of δ_{uv} and δl_{60} for SR are found to be higher than those of BSR by ~8% and ~16 % respectively, for greater tie spacing i.e. 100 mm and 200 mm. However, a relatively sharp improvement in δ_{uv} and δl_{60} can be seen for SR when the tie spacing is reduced towards 50 mm from 100 mm, in comparison to BSR wherein a gradual trend is maintained for all the tie spacing considered (i.e. 200 mm to 50 mm). The enhanced deformation improvement trend in SR as compared to BSR, may be related to the improved confinement core strength achieved as a result of the higher strength in longitudinal steel (i.e. confinement effect has relatively increasing effect in mobilising the strength/stiffness of higher strength steel as compared to bamboo).

6.4 Summary and conclusions

This chapter presents an experimental study on the behaviour of bamboo-steel reinforced CSRE column under concentric axial loading. Effects of key variables such as total reinforcement ratio (ρ_t), lateral reinforcement ratio (ρ_l) etc., on load-capacity (P_{ubs}), failure patterns etc., was studied. Based on the study the following conclusions have been drawn:

1. Similar failure patterns as those of steel reinforced CSRE columns are observed for bamboo-steel reinforced CSRE columns, except for post-ultimate snapping or breaking of buckled bamboo longitudinal reinforcement.
2. P_{ubs} (ultimate load for bamboo-steel reinforced column) of bamboo-reinforced CSRE columns are about 3.7% to 15% higher than that of unreinforced CSRE column when total (bamboo and steel) reinforcement ratio is increased from 1.52% to 3.41%.
3. The increase of P_{ubs} is about 6% to 12% when the transverse reinforcement ratio was increased from 0.63% to 1.26% and 0.63% to 2.51% respectively. P_{ubs} of SR50 column is about 17% higher than that of BSR50 (BSR = Bamboo-Steel Reinforced), however only minor differences are seen for larger tie spacing, i.e. 200 mm.

4. Linear increase in percent P_{ubs} is observed as ρ_t was increased from 0% to 3.41%. There is a gradual increase on percent P_{ubs} as ρ_t was increased from 0% to 1.52%, 2.15% and 3.41% with the values of 4%, 10% and 16% respectively. The P_{ubs} also increases by about 6% to 12% when ρ_w was increased from 0.63% to 1.26% and 2.51% respectively, thus showing an improvement in ductility.
5. Bamboo possess reasonably high tensile property i.e., half the strength of steel, hence it can be used as a potential reinforcing material and a substitute to steel to some extent for construction of rammed earth structures in order to achieve higher strength and better seismic performance.

Table 6.1. Details of bamboo-steel reinforcement.

Column	a (mm)	d (mm)	h (mm)	s (mm)	ρ_l (%)	ρ_w (%)	$\rho_l + \rho_w$ (%)
1BSR200	150	150	1500	200	0.89	0.63	1.52
2BSR200	150	150	1500	200	0.89	0.63	1.52
3BSR200	150	150	1500	200	0.89	0.63	1.52
1BSR100	150	150	1500	100	0.89	1.26	2.15
2BSR100	150	150	1500	100	0.89	1.26	2.15
3BSR100	150	150	1500	100	0.89	1.26	2.15
1BSR50	150	150	1500	50	0.89	2.51	3.41
2BSR50	150	150	1500	50	0.89	2.51	3.41
3BSR50	150	150	1500	50	0.89	2.51	3.41

Table 6.2. Summary of bamboo-steel reinforced column test results.

Column	Ultimate load (kN)	Comp. strength (MPa)	Moisture content of specimen (%)						Average moisture content at test (%)		Standard deviation (%)		Average dry density of CSRE (kg/m^3)	Standard deviation (%)
			Locations											
			Top		Middle		Bottom							
			CSRE	Bamboo	CSRE	Bamboo	CSRE	Bamboo	CSRE	Bamboo	CSRE	Bamboo		
1UCSRE	81.0	3.60	5.43	-	6.79	-	5.45	-	5.89	-	0.78	-	1790	0.012
2UCSRE	80.3	3.57	6.29	-	5.79	-	4.85	-	5.64	-	0.73	-	1800	0.015
3UCSRE	81.6	3.49	5.67	-	6.56	-	5.78	-	6.00	-	0.49	-	1790	0.013
1BSR200	83.7	3.72	5.52	2.82	6.97	3.85	7.91	3.87	6.80	3.34	1.20	0.73	1950	0.029
2BSR200	82.2	3.65	5.97	2.80	6.28	4.02	7.04	7.92	6.43	3.41	0.56	0.86	1930	0.010
3BSR200	83.3	3.70	5.62	3.33	6.77	3.85	7.81	3.97	6.70	3.72	1.10	0.34	1950	0.011
1BSR100	89.1	3.96	7.97	3.09	5.27	3.80	8.12	3.80	7.12	3.56	1.60	0.50	1940	0.022
2BSR100	87.3	3.88	7.39	4.60	7.15	3.99	6.32	3.11	6.95	3.90	0.56	0.43	1940	0.010
3BSR100	86.8	3.86	7.12	3.73	6.12	3.63	7.15	3.47	6.64	3.72	0.77	0.47	1950	0.020
1BSR50	95.0	4.22	8.49	5.57	7.52	6.67	7.19	4.82	7.73	5.69	0.68	0.78	1930	0.014
2BSR50	91.3	4.06	6.73	6.19	6.81	3.50	5.35	5.41	6.30	5.03	0.82	1.90	1960	0.014
3BSR50	93.7	4.16	7.23	5.61	5.84	4.73	6.21	5.13	6.78	5.42	0.63	0.97	1950	0.009

Note: *UCSRE = Unreinforced Cement stabilised Rammed Earth; BSR = Bamboo-Steel Reinforced; 1, 2, 3 = Serial number of columns; 50, 100, 200 = Spacing of lateral ties in mm.*

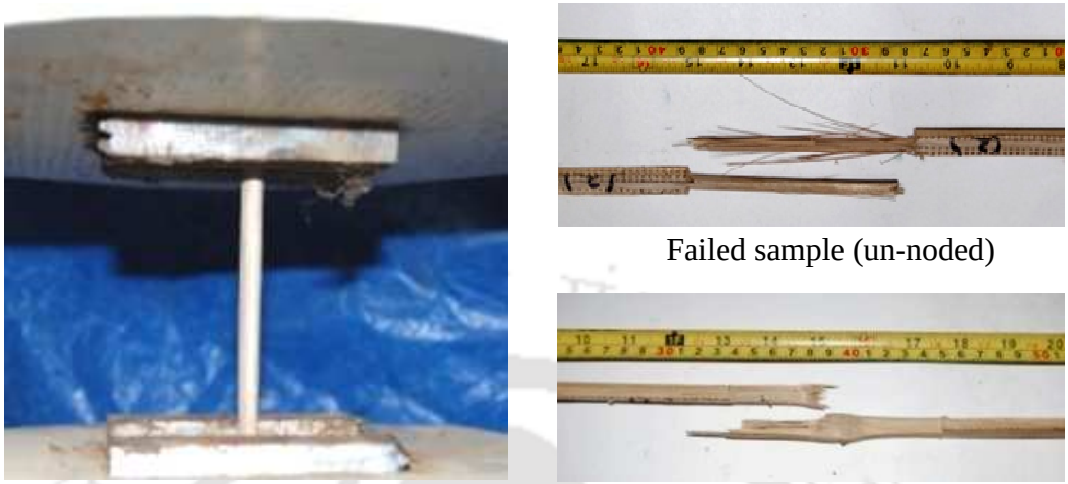

Test setup

Failed sample (un-noded)

Failed sample (noded)

(a) Bamboo splint.

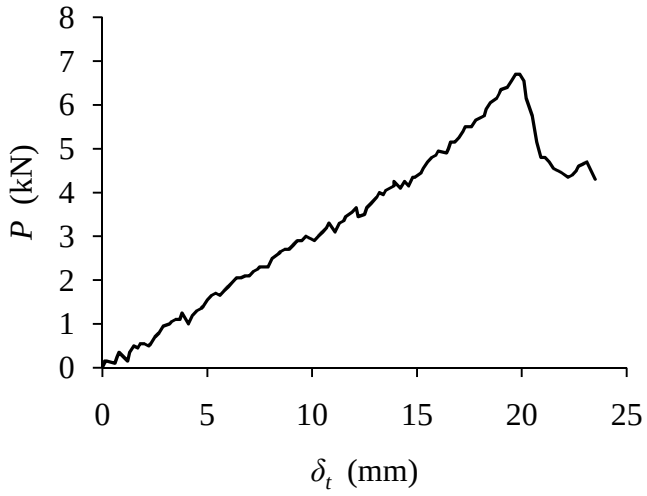

(b) Typical load-deformation curve of bamboo splint.

Fig. 6.1 Testing of bamboo splint.

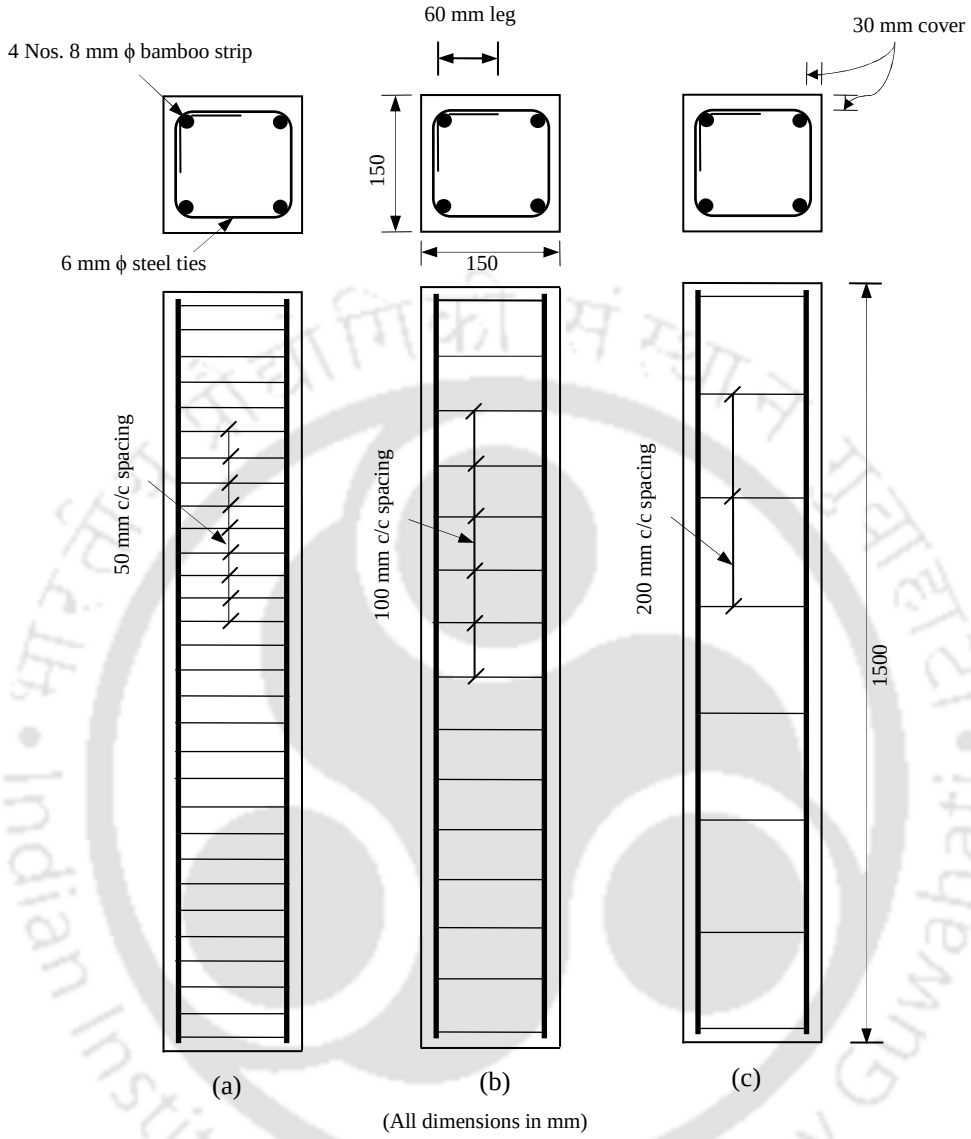

Fig. 6.2. Reinforcement details of column with tie spacing: (a) 50 mm; (b) 100 mm; and (c) 200 mm.

Fig. 6.3. Equipments: (a) mould; (b) rammer and compaction plate with holes; and (c) typical bamboo-steel reinforced CSRE column.

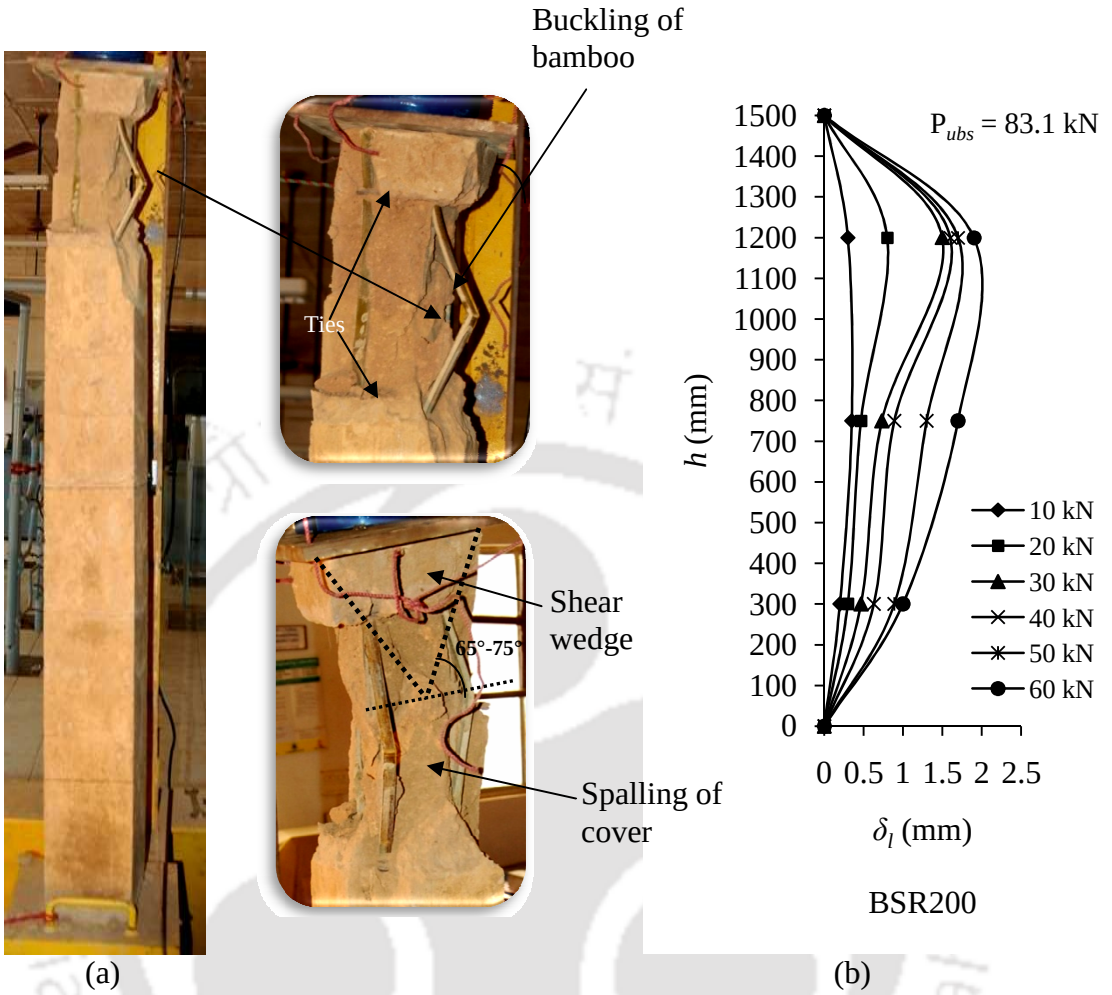

Fig. 6.4. Failure of column with 200 mm tie spacing: (a) failure pattern; and (b) load-lateral deformation curve.

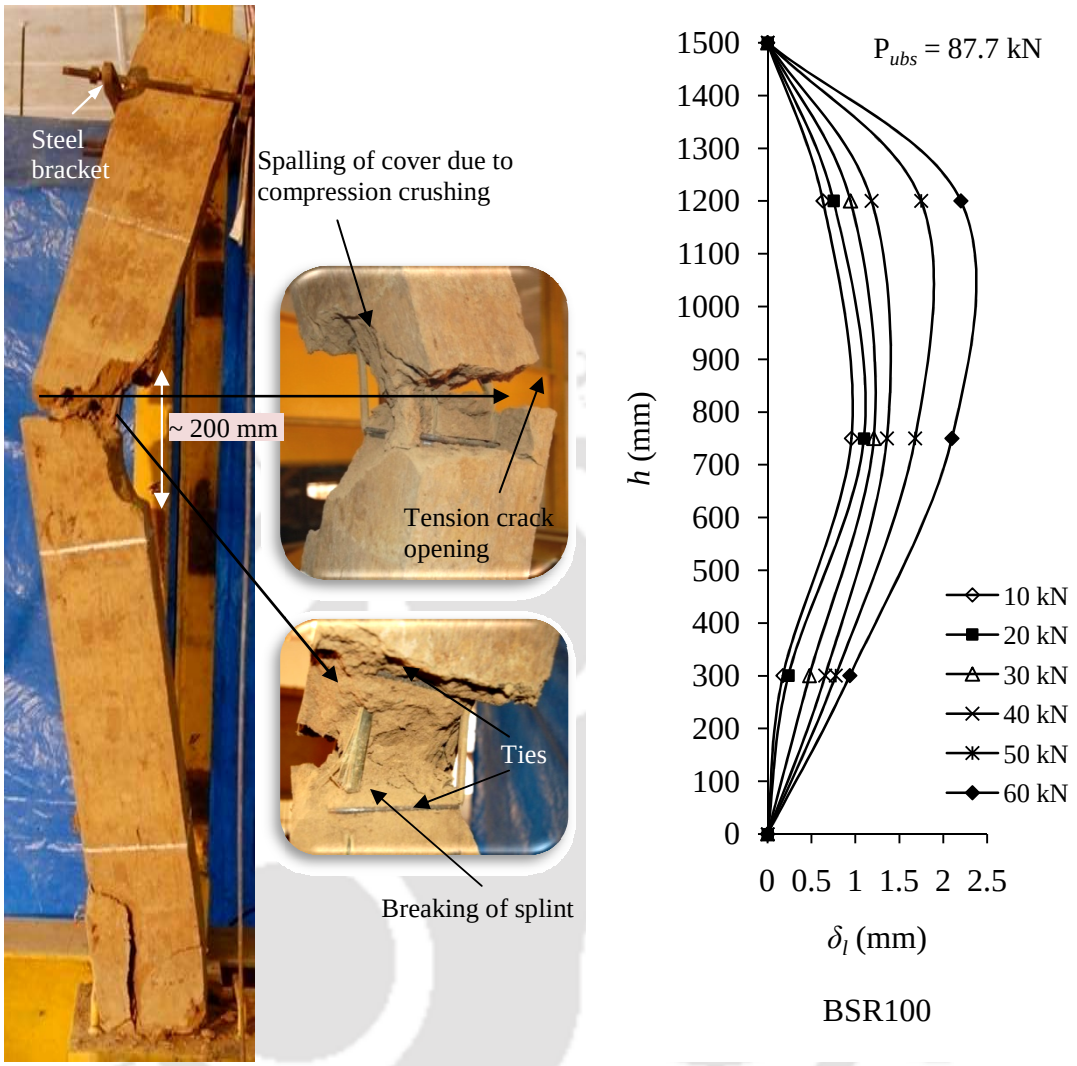

Fig. 6.5. Failure of column with 100 mm tie spacing: (a) failure pattern; and (b) load-lateral deformation curve.

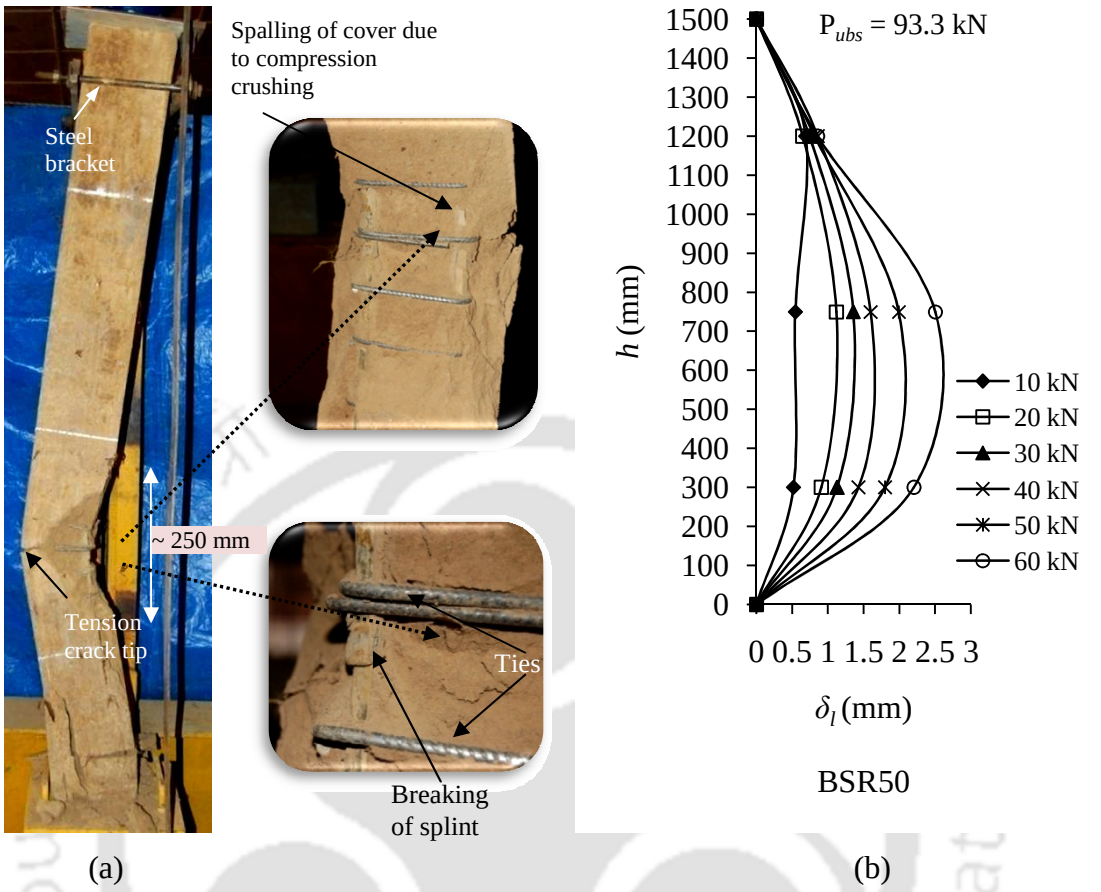

Fig. 6.6. Failure of column with 50 mm tie spacing: (a) failure pattern; and (b) load vs. lateral deformation curve.

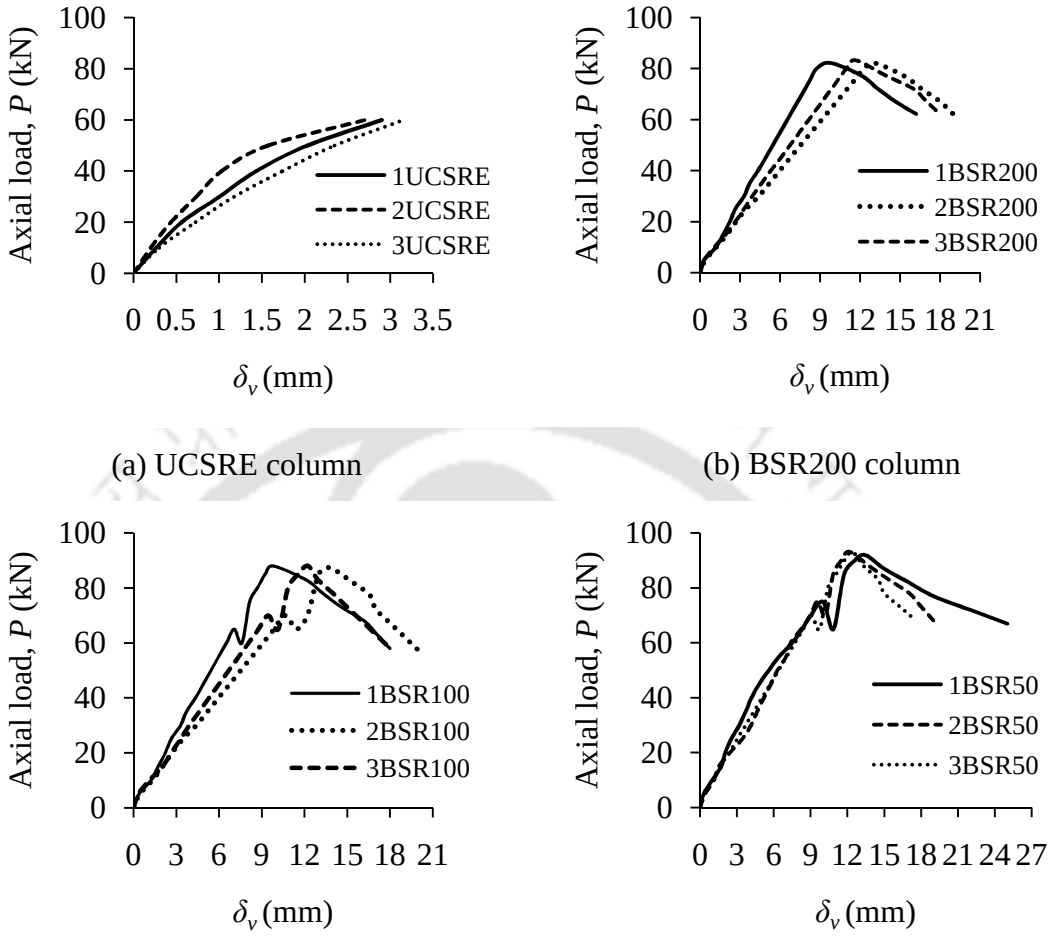

(a) UCSRE column

(b) BSR200 column

(c) BSR100 column

(d) BSR50 column

Fig. 6.7. Load vs. axial deformation curves.

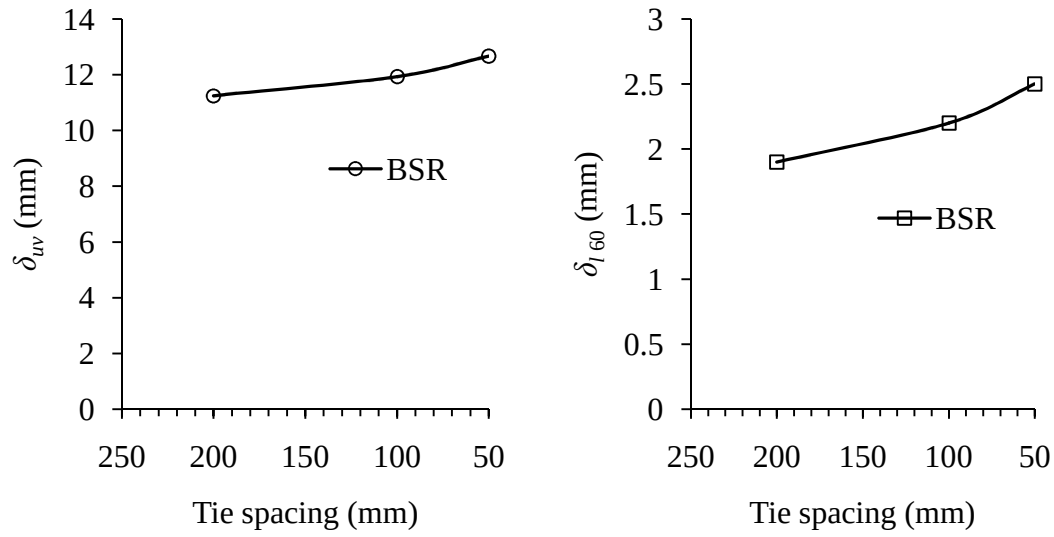

Fig. 6.8. Effect of tie spacing: (a) axial deformation of columns at ultimate load (δ_{uv}); and (b) lateral deformation of columns at 60 kN load ($\delta_{l\,60}$).

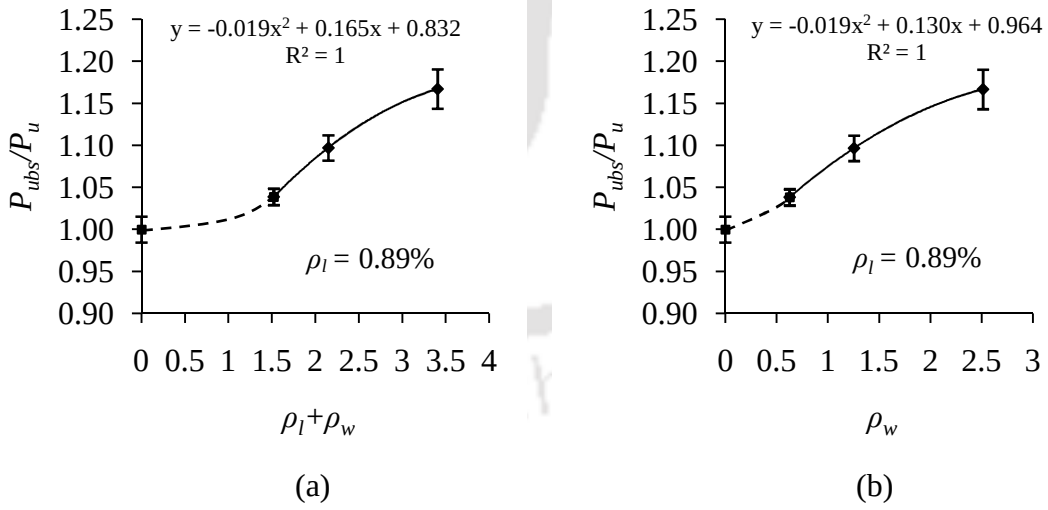

Fig. 6.9. Effect of reinforcement on load ratio (P_{ubs}/P_u) of column: (a) load ratio vs. total reinforcement; and (b) load ratio vs. lateral reinforcement.

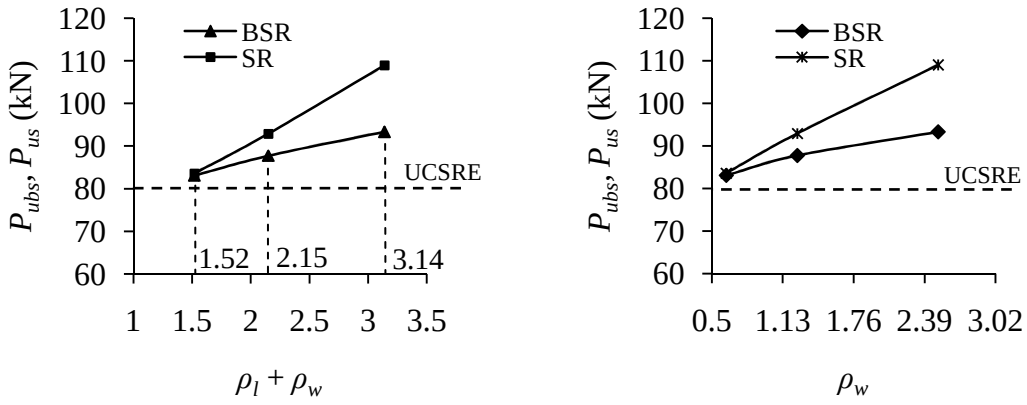

Fig. 6.10. (a) Load-capacity of BSR and SR columns with respect to total reinforcement ratio; and (b) load-capacity of BSR and SR columns with respect to lateral reinforcement.

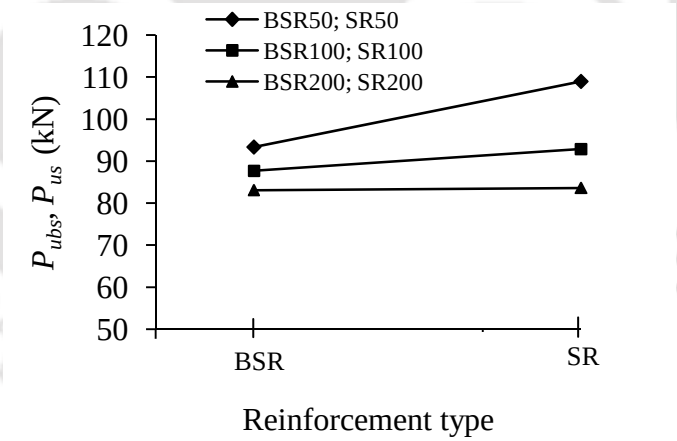

Fig. 6.11. Effect of longitudinal reinforcement type on load-capacity.

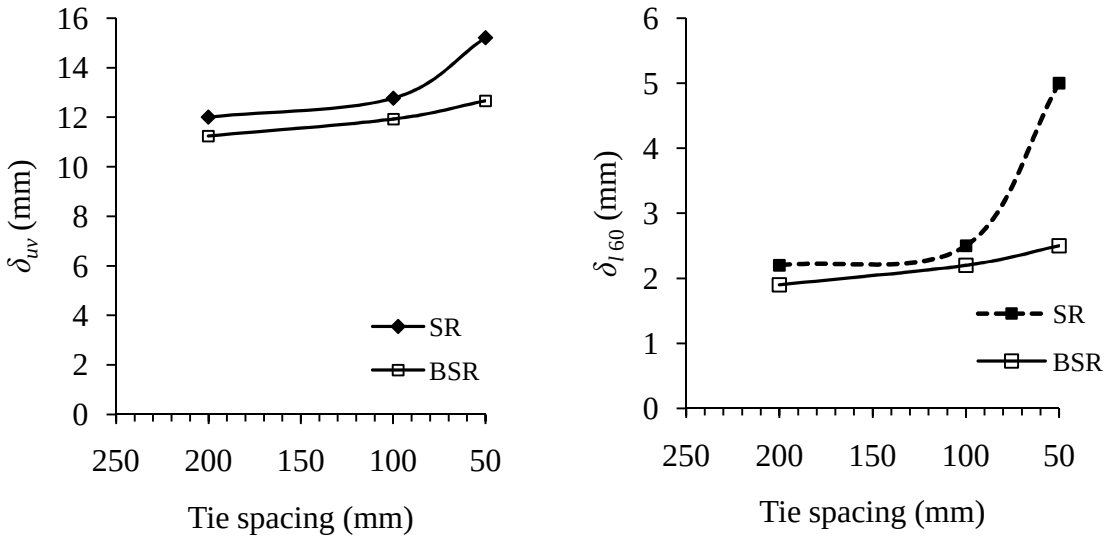

Fig. 6.12. Comparison of SR and BSR columns on (a) axial deformation at ultimate load (δ_{uv}); and (b) lateral deformation at 60 kN load ($\delta_{l\,60}$).

Chapter 7

Conclusions and Future Scope of Work

This chapter summarizes the important conclusions drawn from the experimental studies on unreinforced and reinforced (steel and bamboo-steel reinforced) cement stabilised rammed earth (CSRE) columns, using locally available soil at Agartala (India). The study includes determination of the characteristic properties of unstabilised and cement stabilised rammed earth blocks; structural behaviour of axially loaded CSRE columns of circular, square and rectangular cross-sections and behaviour of steel and bamboo-steel reinforced CSRE columns under axial compression.

7.1 Introduction

In the preceding chapters, studies on the characteristic properties of soil and structural behaviour of unreinforced and reinforced CSRE columns have been presented. The properties of unstabilised and cement stabilised rammed earth blocks in terms of density, strength, compaction energy, and durability in both cured and uncured condition were studied. An attempt was made to select and validate the block-making equipment and technique, which can be used for construction of rammed earth structures. Detailed study on load-capacity of unreinforced CSRE columns of circular, square and rectangular cross-sections under axial loading were carried out. The effects of concentric axial loading on failure pattern, slenderness and aspect ratio; moisture variation and stress reduction factors were assessed. A comparative study was made on ultimate compressive strength (σ_u) of columns obtained from experimentation and Engesser's tangent modulus theory. Validity of using masonry design rules for the design of CSRE column was evaluated. Factor of safety for columns were determined to assess the possibility of constructing a single storey load bearing houses. In addition, a study was carried out on the behaviour of steel and bamboo-steel reinforced CSRE columns under axial loading. The effects of structural parameters such as transverse reinforcement ratio, total reinforcement ratio, tie spacing, etc., on the failure pattern; load-lateral deformation and load-axial deformation of columns

were studied. Based on the study summary of the conclusions are enumerated in the following sections.

7.1.1 Characteristics properties of CSRE blocks

1. The compressive strength of both cured and uncured CSRE blocks increases with increasing cement content and the average characteristic strength of cured samples is about two times higher than uncured samples.
2. At optimum moisture content, it is not possible to achieve the maximum dry density and compressive strength of CSRE blocks although the compaction energy is increased beyond the standard Proctor effort.
3. Strength and density of CSRE blocks is quite sensitive to the variations in compaction energy up to a specified limit and on an increase in compaction energy from 7.26 to 16.94 kg-cm/cc tends to increase in strength and density up to 1.2 times and 16% higher than that obtained at an energy level equivalent to the standard Proctor test.
4. The locally available soil (Agartala, India) used for production of CSRE blocks using the proposed block-making equipment and technique satisfy the design criteria outlined in various standards.

7.1.2 Structural Behaviour of CSRE columns of circular, square and rectangular sections

1. Failure of column can be divided into three zones i.e., shear failure zones at top and bottom, and tension failure zone at the middle. Shear dominates near the platen ends and shearing cracks typically occurred at nearly 65° - 75° angle and at 60 - 70% of ultimate load, and thus forming a shear wedge. At the same time, tension dominates in the middle of the column and due to this force acting outward perpendicular to the axis of column led to splitting of the column into two halves. Similar pattern of failure was observed in case of circular columns except the formation of equally inclined (~ 120°) splitting vertical cracks due to ‘axe action’ of the shear wedge.
2. Predictions made by Engesser's tangent modulus theory are sensitive (for the ranges of λ considered) to the stress level at which the tangents are considered

i.e. it can lead to under predictions when the experimental ultimate stress is high and closure to the peak stress of the referral characteristic stress strain curve and vice-versa, however the decreasing pattern of σ_u with increasing values of λ is well captured. The values of k at λ equal to 8 and 10 were determined to be 0.92 and 0.84 for rectangular columns and 0.90 and 0.82 for circular columns respectively.

3. The load-capacity increases with the increase in aspect ratio. It was found that when the aspect ratio was increased from 1.0 to 1.27 and 1.53, the load-capacity of column increased by approximately 20% and 40.5% respectively, for λ = 6, 8 and 10 of all the column sets. It may be noted that the increase in load-capacity for increasing aspect ratio agrees with the increase in cross-sectional area.
4. The reduction factors outlined in earthen standards such as NZS 4297 (1998) and AS HB 195 (2002), and masonry standard IS 1905 (2002) are in a close range to the experimental values by about ~4.0% at slenderness ratio equal to 8 - 10. However, in case of circular columns, the codal values are higher by about ~7%, thus showing relatively un-conservative.
5. Factor of safety obtained for CSRE column is quite high, which ranges from 21 to 36. This indicates that CSRE columns can be used for construction of single storey load bearing houses or even two storeys or more when designed properly.

7.1.3 Structural behaviour of steel reinforced CSRE columns

1. The load-capacity of SR200, SR100 and SR50 column is about 4.6%, 16% and 33% higher than UCSRE column, respectively. Load-capacity increases due to reduction in tie spacing and toughness gain of confined CSRE.
2. There is a gradual increase on percent load-capacity as the total reinforcement ratio is increased from 0% to 1.52%, 2.15% and 3.41% with the values of 4.5%, 16% and 36% respectively. The load-capacity also increases by about 11% to 30% when the percent transverse reinforcement ratio is increased from 0.63% to 1.26% and 2.51% respectively.
3. As compared to UCSRE columns, steel reinforced CSRE columns shows significant load carrying capacity and an improvement in ductility, and

capacity could be obtained with closer tie spacing. Hence, steel can be a potential reinforcing material in CSRE columns with closer tie spacing in order to achieve higher strength and better seismic performance.

7.1.4 Structural behaviour of bamboo-steel reinforced CSRE column

1. Similar failure patterns as those of steel reinforced CSRE columns are observed for bamboo-steel reinforced CSRE columns, except for post-ultimate snapping or breaking of buckled bamboo longitudinal reinforcement.
2. Load capacities (ultimate load for bamboo-steel reinforced column) of bamboo-reinforced CSRE columns are about 3.7% to 15% higher than that of unreinforced CSRE column when total (bamboo and steel) reinforcement ratio is increased from 1.52% to 3.41%.
3. The increase of load capacity is about 6% to 12% when the transverse reinforcement ratio was increased from 0.63% to 1.26% and 0.63% to 2.51% respectively. Load-capacity of SR50 column is about 17% higher than that of BSR50 (BSR = Bamboo-Steel Reinforced), however only minor differences are seen for larger tie spacing, i.e. 200 mm.
4. Linear increase in percent load-capacity is observed as total reinforcement was increased from 0% to 3.41%. There is a gradual increase on percent load-capacity at total reinforcement was increased from 0% to 1.52%, 2.15% and 3.41% with the values of 4%, 10% and 16% respectively. The load-capacity also increases by about 6% to 12% when lateral reinforcement was increased from 0.63% to 1.26% and 2.51% respectively, thus showing an improvement in ductility.
5. Bamboo possess reasonably high tensile property i.e., half the strength of steel, hence it can be used as a potential reinforcing material and a substitute to steel to some extent for construction of rammed earth structures in order to achieve higher strength and better seismic performance.

7.2 Future scope of work

Although an attempt has been made to experimentally study the structural behaviour of both unreinforced and reinforced (steel and bamboo-steel reinforced) cement

stabilised rammed earth (CSRE) columns, considering several important variables like cross-sectional shape, cross-sectional aspect ratio, slenderness ratio, steel reinforcement, bamboo reinforcements, etc., several areas can be identified which can lead to further understanding of CSRE structural elements. Some of the areas where research can be focused in the future are enumerated below:

1. As the present study deals only with single soil type, further study is recommended to determine the suitability of proposed block making equipment and technique using different soil types.
2. A further investigation needs to be carried out on CSRE columns in order to derive stress reduction factors useful for design calculations. Some of the works are as follows: (a) determination of stress-reduction factors for higher slenderness ratio and eccentricities, (b) behaviour of bamboo-steel and steel reinforced CSRE columns under biaxial loading, and (c) however, further studies may be required to reconfirm the validity of these codes.
3. Investigations on biaxial loaded reinforced CSRE columns considering the effects of structural parameters such as longitudinal reinforcement ratio, transverse reinforcement ratio, tie configuration, CSRE compressive strength and spalling of covers.
4. Test on durability in terms of corrosion of steel and alteration of bamboo to humidity.
5. Development of finite element models based on the understanding gained from experimental studies to explore further variations in parametric space of columns.
6. Development of design guidelines/charts based on experimental and finite element simulations.

References

Agarwal, A., Nanda, B., and Maity, D. (2014). "Experimental investigation on chemically treated bamboo reinforced concrete beams and columns." *Construction and Building Materials*, 71, 610–617.

Alhambra.http://www.planetware.com/granada/alhambra-hill-e-and-ah.htm. Accessed on March 2015.

AS 3700. (2001). "Masonry structures." Standard Australia, Sydney, Australia.

AS HB 195. (2002). "Australian earth building handbook." Standards Australia, Sydney, Australia.

ASTM E2392/E2392M-10. (2010). "Standard guide for design of earthen wall building systems." West Conshohocken, PA.

ASTM D698-12. (2012). "Standard test methods for laboratory compaction characteristics of soil using standard effort." West Conshohocken, PA.

Bahar, R., Benazzoung, M., and Kenai, S. (2004). "Performance of compacted cement stabilised soil." *Cement and Concrete Composites*, 26(7), 811–820.

Beckett, C., and Ciancio, D. (2014). "Effect of compaction water content on the strength of cement stabilised rammed earth materials." *Canadian Geotechnical Journal*, 51, 583-590.

Berge, B. (2009). "The ecology of building materials." 2nd Edn. Architectural Press, Oxford.

Bleich, F. (1952). *Buckling strength of metal structures*, McGraw-Hill, New York.

BS 5628 (Part 1). (1992). "Structural use of unreinforced masonry." British Standard Institute, United Kingdom.

Bui Q.B., Hans S., and Morel J.C., "The compressive strength and pseudo elastic modulus of rammed earth." *Proceeding of International symposium on earthen structures*, Bangalore, India, Interline Publishers.

Bui, Q.B., Hans, S., Morel, J.C., and Do, A.P. (2011). "First exploratory study on dynamic characteristics of rammed earth buildings." *Engineering Structures*, 33, 3690–3695.

Bui, Q.B., Morel, J.C., Hans, S., and Walker, P. (2014). "Effect of moisture content on the mechanical characteristics of rammed earth." *Construction and Building Materials,* 54, 163-169.

Bui, Q.B., Morel, J.C., Reddy, B.V. V., and Ghayad, W. (2009). "Durability of rammed earth walls exposed for 20 years to natural weathering." *Building and Environment,* 44, 912-919.

Burroughs, S. (2008). "Soil property criteria for rammed earth stabilisation." *Journal of Materials in Civil Engineering,* 10.1061/(ASCE)0899-1561(2008)20: 3(264), 264–273.

Chayet, A., Jest, C., and Sanday, J. (1990). "Earth used for building in the Himalaya, the Karakoram and central Asia – Recent research and future trends." *6th International conference on the conservation of earthen architecture (Adobe 90),* Las Cruces, New Mexico, U.S.A.

Ciancio, D., and Augarde, C. (2013). "Capacity of unreinforced rammed earth walls subject to lateral wind force: elastic analysis versus ultimate strength analysis." *Materials and Structures,* 46, 1569–1585.

Ciancio, D., and Beckett, C. (2013). "Rammed earth: an overview of a sustainable construction material." *3rd International conference on sustainable construction materials and technologies,* Kyoto Research Park, Kyoto, Japan.

Ciancio, D., and Gibbings, J. (2012). "Experimental investigation on the compressive strength of cored and molded cement stabilised rammed earth samples." *Construction and Building Materials*, 28, 294-304.

Ciancio, D., and Jaquin, P., and Walker, P. (2013). "Advances on the assessment of soil suitability for rammed earth." *Construction and Building Materials*, 42, 40-47.

Clark, D., and Walker, P. (2003). "The influence of soil properties on the behaviour of rammed earth", *Proceeding 9th International conference on study and conservation of earthen architecture Terra,* Yazd, Iran, 93 - 101.

Cusson D., and Paultre, P. (1994). "High-strength concrete columns confined by rectangular ties." *Journal of Structural Engineering,* 120 (3), 783-804.

Easton, D. (1982). "The rammed earth experience." 1st Ed., Blue Mountain Press, Wilseyville, CA.

EBAA. (2004). "Building with earth bricks and rammed earth in Australia." *Earth Building Association of Australia (EBAA),* Sydney, Australia.

Favhomedecors.FavoritesHomeDecorationsIdeas.http://www.favhome decors.com/wp-content/uploads/2014/earth_home_designs_rammed_earth_house_plansave_designs.jpg. Accessed on January 2015.

Gaind, K.J., and Char, A.N.R. (1983). "Reinforced soil beams." *Journal of Geotechnical Engineering*, 109 (7), 977 - 982.

Gao, Z., X. Yang, Z. Tao, Z. Chen, and C. Jiao. (2009). "Experimental study of rammed earth wall with bamboo cane under monotonic horizontal load." *Journal of Kunming University of Science and Technology*, 34 (2), 1–4.

Gardner, H.J., and Jacobson, E.R. (1967). "Structural behaviour of concrete filled steel tube." *Journal of American Concrete Institute*, 64(7), 404-413.

Ghavami, K. (2005). "Bamboo as reinforcement in structural concrete elements." *Cement and Concrete Composites*, 27 (6), 637–649.

Gomes, M.I., Lopes, M., and Brito, J. (2011). "Seismic resistance of earth construction in Portugal." *Engineering Structures*, 33, 932-941.

Greenleafdoors. http://www.greenleafdoors.com. Accessed on 27 March 2015.

Guettala, A., Abibsi, A., and Houari, H. (2006). "Durability study of stabilised earth concrete under both laboratory and climatic conditions exposure." *Construction and Building Materials*, 20(3), 119–127.

Gupta, R. (2014). "Characterizing material properties of cement stabilised rammed earth to construct sustainable insulated walls." *Journal of Case Studies in Construction Materials*, 1, 60-68.

Hall, M. (2002). "Rammed earth: Traditional methods, modern techniques, sustainable future." *Building Engineer*, 77(11), 22–24.

Hall, M., and Djerbib, Y. (2004). "Rammed earth sample production: Context, recommendations and consistency." *Construction and Building Materials*, 18(4), 281–286.

Han, L.H. (2000). "Test on concrete filled steel tubular columns with high slenderness ratios." *Advances in Structural Engineering-An International Journal*, 3(4), 337-344.

Heathcote, K. A. (1995). "Durability of earth wall buildings." *Construction and Building Materials*, 9 (3), 185–189.

Helfritz, H. (1937). "Land without shade." Central Asian Society, 24, 201–216.

Houben, H., and Guillaud, H. (1994). “Earth construction-A comprehensive guide.” Intermediate Technology Publications, London.

IS 1786. (1985). “Specification for high strength deformed steel bars and wires for concrete reinforcement.” Indian standard, New Delhi, India.

IS 1905. (2002). “Code of practice for structural use of unreinforced masonry.” Indian standard, New Delhi, India.

IS 2110. (2002). “Code of practice for in-situ construction of walls in buildings with soil-cement.” Indian standard, New Delhi, India.

IS 2720 (Part 4). (1995). “Specification for methods of test for soils-grain size analysis.” Indian standard, New Delhi, India.

IS 2720 (Part 5). (1995). “Determination of liquid and plastic limit.” Indian standard, New Delhi, India.

IS 2720 (Part 7). (2002). “Determination of water content-dry density relation using light compaction.” Indian standard, New Delhi, India.

IS 401. (2001). “Preservation of timber - code of practice.” Indian standard, New Delhi, India.

IS 4332 (Part 2). (2006a). “Determination of moisture content of stabilised soil mixture.” Indian standard, New Delhi, India.

IS 4332 (Part 5). (2006b). “Specification for determination of unconfined compressive strength of stabilised soils.” Indian standard, New Delhi, India.

IS 6874. (2008). “Method of tests for bamboo.” Indian standard, New Delhi, India.

IS 8112. (2005). “Specification for 43 grade ordinary Portland cement.” Indian standard, New Delhi, India.

IS 9096. (2006). “Preservation of bamboo for structural purposes - code of practice.” Indian standard, New Delhi, India.

Jaquin, P. A., Augarde, C. E., and Gerrard, C. M. (2006). “Analysis of historic rammed earth construction.” *Structural Analysis of Historical Constructions*, New Delhi 2006.

Jaquin, P.A. (2008). “Analysis of historic rammed earth construction.” Ph.D. thesis, School of Engineering, Durham University, UK.

Jaquin, P.A., Augarde, C.E., and Gerrard, C.M. (2008). "Chronological description of the spatial development of rammed earth techniques." *International Journal of Architectural Heritage,* 2(4), 377-400.

Jayasinghe, C. (1999). "Alternative building material and methods for Sri Lanka." Ph.D. thesis, Department of Civil Engineering, University of Moratuwa, Sri Lanka.

Jayasinghe, C., and Kamaladasa, N. (2007). "Compressive strength characteristics of cement stabilised rammed earth walls." *Construction and Building Materials*, 21(11), 1971–1976.

Jiyao, H., and Weitung, J. (1990). "The protection and development of rammed earth and adobe architecture in China." *6th International conference on the conservation of earthen architecture (Adobe 90),* Las Cruces, New Mexico, U.S.A.

Kandamby, T., and Jayasinghe C. (2011). "Cement stabilised rammed earth for wall junctions of two storey houses." *Civil Engineering Research for Industry – 2011,* Department of Civil Engineering – University of Moratuwa, Sri Lanka, 119-124.

Keable, J. (1996). "Rammed earth structures - A code of practice." IT publication, UK.

King, B. (1996). "Buildings of earth and straw: Structural design for rammed earth and straw bale architecture." Ecological Design Press, Sausalito, CA.

Kleespies, T. (2000). "The history of rammed earth buildings in Switzerland." *Proceeding of 8th International conference on study and conservation of earthen architecture Terra-2000*, Devon UK, 137 - 138.

Kotak, T. (2007). "Constructing cement stabilised rammed earth houses in Gujarat after 2001 Bhuj earthquake." *Proceedings of International symposium on earthen structures*, Interline Publishers, Bangalore, India, 62–71.

Kumar, P. P. (2009). "Stabilised rammed earth for walls: Materials, compressive strength and elastic properties." PhD thesis, Dept. of Civil Engineering, Indian Institute of Science, Bangalore, India.

Lehmbau Regeln. (2009). Dachverbandlehm, e.V., (Hrsg.), Begriffe-Baustoffe-Bauteile, and Auflage., PRAXIS, Germany.

Liang, R., Stanislawski, D., and Hota, G. (2011). "Structural responses of Hakka rammed earth buildings under earthquake loads." *International workshop on rammed Earth materials and sustainable structures & Hakka Tulou Forum 2011,* Civil Engineering Xiamen University, China.

Lilley, D. M., and Robinson, J. (1995). “Ultimate Strength of rammed earth walls with openings.” *Proceeding Institution Civil Engineers, Structures and Buildings*, 110, 278 – 287.

Lindsay, R. (2012). “Structural steel elements within stabilised rammed earth walling.”Modern earth building-materials, engineering, construction and applications,

Woodhead Publishing Series in Energy: Number 33, 461-480.

Maiti, S.K., and Mandal, J.N. (1985). “Rammed earth house construction.” *Journal of Geotechnical Engineering*, 111(11), 1323 - 1328.

Maniatidis, V., and Walker, P. (2003). *A review of rammed earth construction (project report)*, Natural Building Technology Group, Dept. of Architecture and Civil Engineering, Univ. of Bath, U.K.

Maniatidis, V., and Walker, P. (2008). “Structural capacity of rammed earth in compression.” *Journal of Materials in Civil Engineering*, 20(3), 230–238.

Maniatidis, V., Walker, P., Heath, A., and Hayward, S. (2007). “Mechanical and thermal characteristics of rammed earth.” *International symposium on earthen structures*, Bangalore, India.

Miccoli, L., Müller, U., and Fontana, P. (2014a). “Mechanical behaviour of earthen materials: A comparison between earth block masonry, rammed earth and cob.” *Construction and Building Materials* 61, 327–339.

Miccoli, L., Oliveira, D.V., Silva, R.A., Müller, U., and Schueremans, L. (2014b). “Static behaviour of rammed earth: experimental testing and finite element modeling.” *Materials and structures*, DOI 10.1617/s11527-014-0411-7.

Middleton, G. F. (1992). *Bulletin 5. Earth wall construction*, 4th Ed., CSIRO Division of Building, Construction and Engineering, North Ryde, Australia.

Milani, A.P.S., and Labaki, L.C. (2012) “Physical, mechanical and thermal performance of cement stabilised rammed earth–rice husk ash walls.” *Journal of Materials in Civil Engineering*, 24(6) 775-782.

Minke, G. (2000). *Earth construction handbook. The building material earth in modern architecture*, WIT Press, Southampton, U.K.

Ngowi, A.B. (1997). "Improving the traditional earth construction: a case study of Botswana." *Construction and Building Materials*, 11(1), 1–7.

Nowamooz, H., and Chazallon, C. (2011). "Finite element modelling of a rammed earth wall." *Construction and Building Materials*, 25, 2112–2121.

NZS 4297. (1998). "Engineering design of earth buildings." New Zealand Standard, Wellington, New Zealand.

NZS 4298. (1998). "Materials and workmanship for earth buildings." New Zealand Standard, Wellington, New Zealand.

Patriciagrayinc.http://patriciagrayinc.blogspot.in/2009/07/rammed-earth-walls.html. Accessed on February 2015.

Patton, M.L., and Singh, K.D. (2014). "Finite element modelling of concrete-filled lean duplex stainless steel tubular stub columns." *International Journal of Steel Structures*, 14, 619-632.

Patty, R. L. (1936). "Clay soil unfavourable for rammed earth walls." Bulletin 298, South Dakota State College Agricultural Experiment Station, South Dakota State College, Brookings, South Dakota, USA.

Patty, R.L., and Minium, L. W. (1945). "Rammed earth walls for farm buildings." Bulletin 277, (revised), Agricultural Engineering Department, Agricultural Experiment Station, South Dakota State College, Brookings, South Dakota, USA.

Pollock, S. (1999). "Ancient Mesopotamia." Cambridge University Press, Cambridge.

Rauch, M., and Kapfinger, O. (2001). "Rammed Earth." Birkhaeuser, Publisher for Architecture, Switzerland.

Reddy, B. V.V., and Kumar, P. P. (2009a). "Compressive strength and elastic properties of stabilised rammed earth and masonry."*Masonry International*, 22(2), 39–46.

Reddy, B.V.V. (2004). "Sustainable building technologies." *Current Science*, 87 (7), 899-907.

Reddy, B.V.V., and K.S. Jagadish. (2003). "Embodied energy of common and alternative building materials and technologies." *Energy and Buildings*, 35, 129–137.

Reddy, B.V.V., and Kumar, P. P. (2011). "Structural behaviour of story-high cement stabilised rammed earth wall under compression." *Journal of Materials in Civil Engineering*, 23 (3), 240 –247.

Reddy, B.V.V., and Kumar, P.P. (2010). "Embodied energy in cement stabilised rammed earth walls." *Energy and Buildings*, 42, 380–385.

Reddy, B.V.V., Leuzinger, G., and Sreeram, V.S. (2014). "Low embodied energy cement stabilised rammed earth building—A case study." *Energy and Buildings*, 68, 541–546.

Sahlin, S. (1971). *Structural masonry*. Prentice Hall, Upper Saddle River, NJ.

Schick, W. (1987). "Der Pise–Bau Zu Weilburg an der Lahn." Publisher: Burgerintiative, Alt Weilburg, Germany.

Sharma, P., Dhanwantri, K., and Mehta, S. (2014). " Bamboo as a building material." *International journal of Civil Engineering Research*, 3 (5), 249–254.

Taylor, P., and Fuller, R.J., and Luther, M.B. (2008). "Energy use and thermal comfort in a rammed earth office building." *Energy and Building*, 40, 793–800.

Taylor, P., and Luther, M.B. (2004). "Evaluating rammed earth walls: a case study." *Solar Energy*, 76, 79–84.

Tripura, D., and Sharma, R. (2014). "Bond behaviour of bamboo splints in cement stabilised rammed earth blocks." *International Journal of Sustainable Engineering*, 7(1), 24–33.

Verma, P. L., and Mehra, S. R. (1950). "Use of soil-cement in house construction in the Punjab." *Indian Concrete Journal*, 24(4), 91–96.

Walker, P. (1995). "Strength, durability and shrinkage characteristics of cement stabilised soil blocks." *Cement and Concrete Composites*, 17(4), 301–310.

Walker, P. J., and Dobson, S. (2001). "Pullout test on deformed and plain rebars in cement stabilised rammed earth." *Journal of Materials in Civil Engineering*, 13 (4), 291–297.

Walker, P., Keable, R., Martin, J., and Maniatidis, V. (2005). *Rammed earth design and construction guidelines*, BRE Press, Bracknell, UK.

Wikipedia.http://en.wikipedia.org/wiki/Church_of_the_Holy_Cross_%28Stateburg,_South_Carolina%29#mediaviewer/File:Stateburg_holy_cross_1419.JPG. Accessed on February 2015.

Yamin, L.E., Phillips, C.A., Reyes, J.C., and Ruiz, D.M. (2004). "Seismic behaviour and rehabilitation alternatives for adobe and rammed earth buildings." *13th World Conference on Earthquake Engineering*, Vancouver, B.C., Canada.

Appendix A

A.1 Compaction energy calculation for standard Proctor test

$$E_c = \frac{nNWH}{V} \tag{A.1}$$

where

E_c = compaction energy, kg.cm/ cm^3

V = volume of Proctor mould = 1000 cm^3

W = weight of Proctor rammer = 2.49 kg

H = rammer height of fall = 30 cm

N = number of blows per layer = 25

n = number of compacted layer = 3

Therefore,

$$E_c = \frac{n\,N\,W\,H}{V} = \frac{3\times 25\times 2.49\times 30}{1000} = 5.60 \approx 6.0 \quad \text{kg.cm/ cm}^3$$

Total number of blows, N_T = 3 x 25 = 75 for compaction of 10 cm (apprx.) thick layer compaction.

A.2 Compaction energy calculation for wooden cubic mould

Size of mould = 10 cm x 10 cm x 10 cm

Volume of mould, V = 1000 cm^3

Weight of rammer, W = 5.6 kg

Rammer height of fall, H = 30 cm

Total number of blows per layer of 10 cm thick, N_T =?

Number of compacted layer, n = 1

Compaction energy, E_c = 6.0 kg.cm/ cm^3

Note: *Here one layer of 10 cm thick is considered, which is equivalent to three layers of standard Proctor test.*

$N_T = \frac{E_c\,V}{n\,W\,H} = \frac{6\times 1000}{1\times 5.6\times 30} = 35.7 \sim 36$, for compaction of 10 cm thick layer.

From this experiment, the average mass of compacted soil is determined to be 2.1 kg.

A.3 Estimation of E_c in terms of N and mass of soil required for column of size 15 cm x 15 cm x 90 cm

Total volume of mould, V_T = 15 x 15 x 90 = 20250 cm^3

Volume of mould for 10 cm thick layer, V = 15 x 15 x 10 = 2250 cm^3

Weight of rammer, W = 5.6 kg

Rammer height of fall, H = 30 cm

Total number of blows per layer, N_T =?

Number of compacted layer, n = 1

Compaction energy, E_c = 6.0 kg.cm/cm^3

$$N_T = \frac{E_c V}{n W H} = \frac{6 \times 2250}{1 \times 5.6 \times 30} = 80.4 \quad \text{(A.3)}$$

Therefore, number of blows required for 90 cm high column or 9 such layers = 80.4 x 9 = 723 blows.

Mass of soil required for Volume of mould, V = 15 x 15 x 10 = 2250 cm^3 is determined as follows:

Mass of soil = (2250/1000) × 2.1 = 4.73 kg

Therefore, total mass of soil required for 90 cm high column or 9 such layer = 9 x 4.73 = 42.57 kg

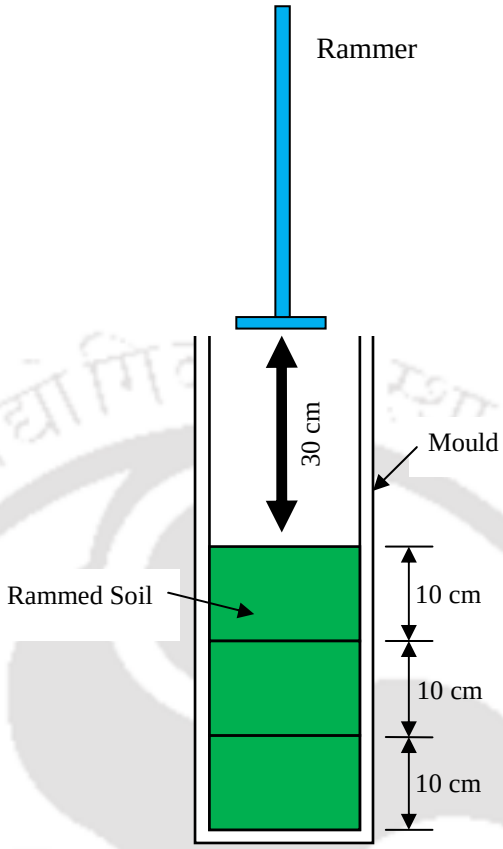

Fig. A.1. Schematic diagram of compaction process

Appendix B

B.1 Determination of tangent modulus for columns from the stress-strain curve of prism

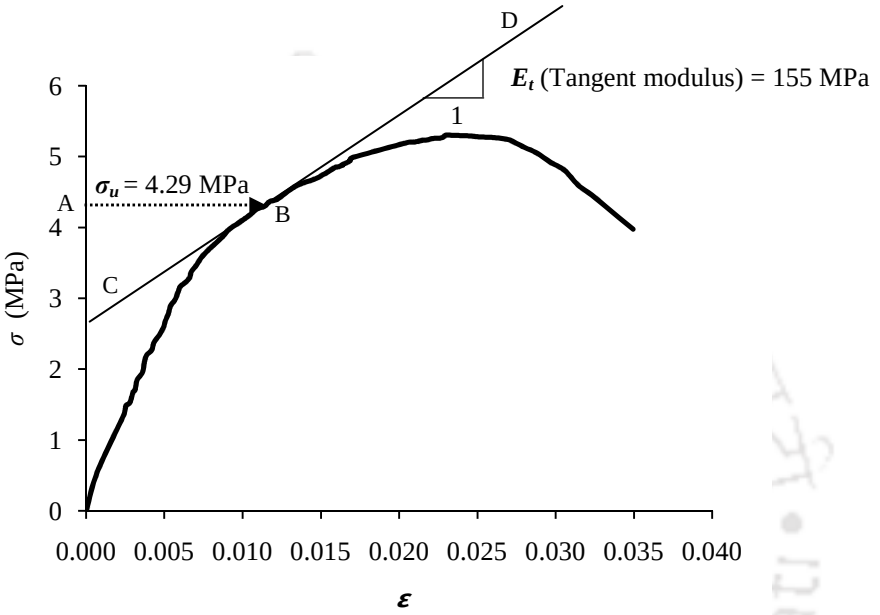

Fig. B.1. Stress-strain curve of prism

It is known that greater the slenderness ratio (λ) the lesser is the load-capacity of CSRE column. Therefore, CSRE prism of slenderness ratio equals to 2 possess the maximum load-capacity when compared to columns of greater slenderness ratios (λ>>2). Fig. B.1 shows the stress-strain curve of prism.

The tangent modulus for the corresponding values of ultimate stress (σ_u) of columns is determined from Fig. B.1.

Let us consider a square column (S-0.9) with the following data:

a) Height of column = 900 mm
b) Load-capacity = 96.5 kN
c) Ultimate stress (σ_u) = 4.29 MPa

At first, abscissa corresponding to stress value 4.29 MPa is drawn, which is marked by dotted line AB intercepting the stress-strain curve at B. Now, a tangent CD is drawn at point B as shown in Fig. B.1. The tangent modulus (E_t) of S-0.9 column is determined by finding the slope of the tangent, i.e., $E_t = \frac{3.41}{0.022} \approx 155$ MPa

B.2 Determination of stress/capacity reduction factor

The stress or capacity reduction factor (k) is determined by dividing the average compressive strength or load-capacity of respective column series by the average compressive strength or load-capacity of column series of slenderness ratio equal to 6. For example:

a) Compressive strength of S-0.9 column = 96.5 kN (SR = 6)
b) Compressive strength of S-1.2 column = 88.4 kN (SR = 8) and
c) Compressive strength of S-1.5 column = 81.0 kN (SR = 10)

The RF is calculated as:

a) RF for S-1.2 column = 88.4 ÷ 96.5 = 91.6 ~ 92
b) RF for S-1.5 column = 81.0 ÷ 96.5 = 83.9 ~ 84

B.3 Determination of factor of safety

Characteristic strength of column (f_k) = 3.58 MPa (Table 4.6)

Allowable stress (σ_a) = 0.1 MPa (BS 5628 part 1, 1992)

Therefore, factor of safety = f_k / σ_a = 3.58/0.1 = 35.8

Appendix C

Estimation of reinforcement details

C.1 Longitudinal reinforcement

Longitudinal reinforcement ratio is calculated using the following formula:

$$\rho_l = \frac{A_{sl}}{A_g} \tag{C.1}$$

where

ρ_l = longitudinal reinforcement ratio in percent

A_{sl} = total longitudinal reinforcement area = $A_{sl} = 4 \times \frac{\pi}{4} \times D^2$

Number longitudinal bars = 4

A_g = gross area of section

Example:

Diameter of steel bar, D = 8 mm

Cross-sectional area of steel bar, $A_s = \frac{\pi}{4} \times D^2 = 50.27 \text{ mm}^2$

Gross area of section, A_g = 150 x 150 = 22500 mm^2

Total longitudinal reinforcement area, A_{sl} = 4 x 50.27 = 201.08 mm^2

Longitudinal reinforcement ratio in percent, $\rho_l = (A_{sl} / A_g)$ x 100 = 0.89 %

C.2 Lateral reinforcement

Lateral reinforcement ratio is calculated using the following formula:

$$\rho_\omega = \frac{4 \times A_{st} \times c}{A \times s} \times 100 \tag{C.2}$$

where,

ρ_ω = lateral reinforcement ratio in percent

A_{st} = cross-sectional area of steel tie = $A_{st} = 4 \times \frac{\pi}{4} \times D^2$

A = cross-sectional area of CSRE core bounded by centerline of outer tie

s = center to center spacing between ties

c = side dimension of CSRE core

Example

Diameter of steel bar, D = 6 mm

Cross-sectional area of steel bar, $A_{st} = \frac{\pi}{4} \times D^2 = 28.27 \text{ mm}^2$

Side dimension of CSRE core, c = 90 mm

Center to center spacing between ties, s = 200 mm

Cross-sectional area of CSRE core bounded by centerline of outer tie, A = 90 x 90 = 8100 mm^2

Therefore,

Lateral reinforcement ratio in percent,

$$\rho_{\omega 200} = \frac{4 \times 28.27 \times 90}{8100 \times 200} \times 100 = 0.628 \sim 0.63\%$$

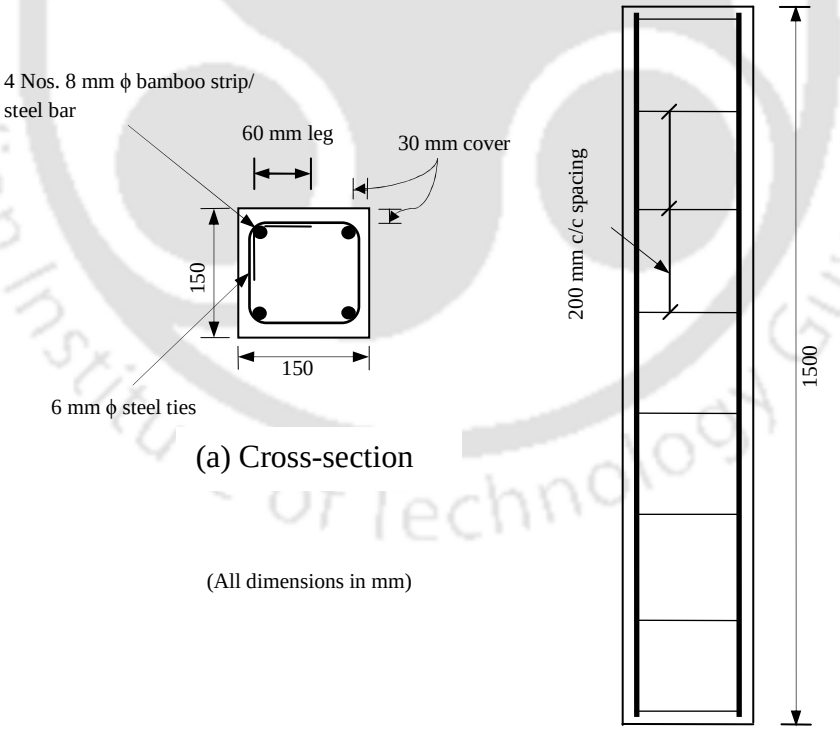

(a) Cross-section

(All dimensions in mm)

(b) Longitudinal-section

Fig. C.1. Reinforcement details of column

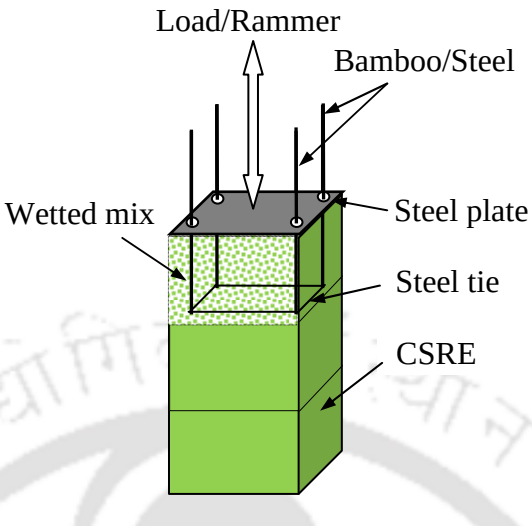

Fig. C.2. Schematic diagram of compaction technique

List of Publications

Journal

1. **Tripura, D.,** and Singh, K.D. (2014). "Characteristic properties of cement stabilised rammed earth blocks." *Journal of Materials in Civil Engineering* (ASCE) – DOI: 10.1061/ (ASCE) MT.1943-5533.0001170.

2. **Tripura, D.,** and Singh, K.D. (2014). "Behaviour of cement stabilised rammed earth circular column under axial loading." *Materials and Structures* (Springer) – DOI: 10.1617/s11527-014-0503-4.

3. **Tripura, D.,** and Singh, K.D. (2015). "Axial load capacity of rectangular cement-stabilised rammed earth column." *Engineering Structures* (Elsevier), 99, 402–412. – http://dx.doi.org/10.1016/j.engstruct.2015.05.014.

4. **Tripura, D.,** and Singh, K.D. (2015). "Structural behaviour of steel reinforced cement-stabilised rammed earth column." *European Journal of Environmental and Civil Engineering* (Taylor and Francis). (Under review)

5. **Tripura, D.,** and Singh, K.D. (2015). "Structural capacity of bamboo-steel reinforced cement-stabilised rammed earth column." *Structural Engineering International* (IABSE). (Under review)

Conference

1. **Tripura, D.,** and Singh, K.D. (2015). "Structural capacity of rammed earth square column in compression." *1st International conference on rammed earth construction: cutting-edge research on traditional and modern rammed earth*, University of Western Australia, Perth, Australia. 157-161, DOI: 10.1201/b18046-32; ISBN 978-1-13-802770-1 CRC Press.

2. **Tripura, D.,** and Singh, K.D. (2014) "Structural behaviour of rammed earth rectangular column under compression." *Structural Engineering Convention*, Indian Institute of Technology Delhi, India. 3, 2459-2469, DOI: 10.1007/978-81-322-2187-6_188.

3. **Tripura, D.,** and Singh, K.D. (2013). "Study on Characteristic properties of stabilised and unstabilised rammed earth blocks." *International Journal of Arts and Sciences (IJAS) Conference*, Harvard University, Boston, USA.